Comparative molecular and morphogenetic characterisation of larval body regions in the polychaete annelid *Platynereis dumerilii*

Dissertation

zur Erlangung des Doktorgrades der Naturwissenschaften

Doctor rerum naturalium

(Dr. rer. nat.)

dem Fachbereich der Biologie

der Philipps-Universität Marburg

vorgelegt von

Dipl.-Biol. Patrick R. H. Steinmetz

aus Luxemburg, Großherzogtum Luxemburg

Marburg/Lahn, März 2006

Vom Fachbereich Biologie
der Philipps-Universität Marburg als Dissertation am
angenommen.

Erstgutachterin: Prof. Dr. Monika Hassel
Zweitgutachterin: Prof. Dr. Renate Renkawitz-Pohl

Tag der mündlichen Prüfung:

Erklärung

Ich versichere hiermit, dass ich meine Dissertation

"Comparative molecular and morphogenetic characterisation of larval body regions in the polychaete annelid *Platynereis dumerilii*"

selbst und ohne unerlaubte Hilfe verfasst und mich dabei keiner anderen Hilfsmittel als der von mir ausdrücklich bezeichneten Quellen und Hilfen bedient habe und dass ich die Dissertation in der vorliegenden oder einer ähnlichen Form bei keiner anderen Hochschule zu Prüfungszwecken eingereicht habe.

Marburg, den 31.März 2006

Dipl.-Biol. Patrick Steinmetz

Comparative molecular and morphogenetic characterisation of larval body regions in the polychaete annelid *Platynereis dumerilii*

Acknowledgments

I am very thankful to Dr. Detlev Arendt for all his support that helped me to become a PhD student in his lab, for his supervision, help, and sharing his endless scientific knowledge. I would also like to thank Dr. Jochen Wittbrodt for his financial support during part of my time as a PhD student. I thank Prof. Dr. Monika Hassel for her support, help and for reviewing this thesis. I thank Dr. Jochen Wittbrodt, Prof. Dr. Monika Hassel and Dr. Elena Conti for helpful comments, criticism and discussions as members of my thesis advisory committee. I also thank Prof. Dr. Renkawitz-Pohl for accepting to review this thesis and all the other members of my defence committee at the University of Marburg.

I acknowledge the people from the Ministère de la Culture, de l'Enseignement Supérieur et de la Recherche, especially Pierre Decker and Josiane Entringer, for the allocation of a "bourse formation-recherche" that made this thesis possible.

I want to thank all past and present members of the Arendt team for their support, critical comments and help, especially Dr. Carola Burgtorf, Dr. Fabiola Zelada and Dr. Detlev Arendt for their previous work on the *Platynereis otx, gbx*, *hox1*, and *six3* genes, without which considerable parts of this thesis would not have been possible, Dr. Kristin Tessmar-Raible for technical help, helpful discussion and constructive criticism and Heidi Snyman for keeping the *Platynereis* worms happy and alive as well as for technical help and personal support. I thank Isabelle Philipp (Innsbruck) for a SP600125 protocol.

I also thank Jens Rietdorf, Timo Zimmermann and Stefan Terjung from the Advanced Light Microscopy Facility (ALMF) at EMBL for their initiation, help and support in confocal microscopy and Dr. Martina Rembold (Wittbrodt lab) for very helpful hints and comments on time-lapse analysis.

I would like to thank the librarians at the EMBL Szílard library, especially David Wesley for digging out ancient books and publications.

I express my thanks for materials to Prof. Dr. Michael Brandt (BODIPY dyes), Dr. Angel Nebreda (α-tubulin antibody) and Dr. Jochen Wittbrodt (medaka cDNA).

Last but not least, I am very thankful to my family for their support and the following people for the good moments I have shared with them outside the lab (in order of appearance): Tom Fleming, Solveig Frick, Inês Baptista, Heike Link, Christiane Jost, Will Norton and Corina Guder.

Table of contents

Index of figures

1 Introduction

1.1 Understanding the evolution of animals by studying their development

The development of extant animals is the product of their evolutionary history. Although the process of natural selection acts mainly on adult stages, the grounds for the variation of adult forms and structures that are subject to selection are often laid during animal development. In his famous biogenetic law, Ernst Haeckel claimed that ontogeny recapitulates phylogeny (Haeckel, 1874). He stated that the development of extant animals is a recapitulation of the evolutionary changes and of the stages their ancestors have undergone (Haeckel, 1874). In the hypothetical case where an animal's ontogeny fully recapitulates its phylogeny, all changes and stages of an animal's evolutionary history can be analysed by studying its development. As the development of an animal undergoes variations, losses and can also acquire novel characters – all driven by natural selection – the recapitulation of phylogeny can be substantially blurred during evolution. Therefore, if one wants to understand for example the evolutionary history of bilateral-symmetric animals (Bilateria) by studying the development of some of their representatives, it is most informative to choose animals that have undergone the least changes and conserved as many ancestral characters as possible.

1.2 Platynereis dumerilii as a model organism to study evolution and development

The polychaete worm *Platynereis dumerilii* has been chosen for the study of evolution and development for several reasons. As a polychaete, it belongs to the phylum Lophotrochozoa, the third branch of the bilaterian phylogenetic tree that comprises many marine animals so far widely underrepresented in molecular studies in comparison to Ecdysozoa (grouping the insect and nematode molecular model organisms) or Deuterostomia (grouping many model organisms of developmental biology as e.g. vertebrates, ascidians, lancelets, and sea urchins). *Platynereis dumerilii* therefore rep-

resents a third reference point to which data from ecdysozoans and deuterostomes can be compared to find evolutionary conserved characteristics in Bilateria (Aguinaldo et al., 1997; Philippe et al., 2005; Tessmar-Raible and Arendt, 2003).

As mentioned before, the evolutionary history of Bilateria can be best reconstructed by studying the development of an animal species that has undergone relatively few changes and has kept many ancestral characters since its evolution from the last common ancestor of Bilateria. Polychaete worms exhibit many ancestral characteristics for Bilateria. As marine animals, many polychaetes have not changed their habitat for hundreds of millions of years, suggesting that they did not accumulate many changes that would have occurred due to the adaptation to new ecological niches. There are very few, if any at all, synapomorphies of polychaete worms, meaning that almost all characters shared among polychaetes are not polychaete-specific but can also be found in other animal phyla (Westheide and Rieger, 1996). Therefore, it can be assumed that polychaetes show a very low level of evolutionary specialisation.

The polychaete *Platynereis dumerilii* (Nereididae) presents developmental characteristics that are proposed to be ancestral at least for Protostomia (Nielsen, 2001). For example, it shows an amphistome gastrulation mode and a primary ciliated larva with an apical organ (Nielsen, 2001), a character that has even been proposed to be ancestral for Bilateria (Arendt et al., 2001). Recently, *Platynereis dumerilii* has been found to share ancestral genomic features with vertebrates rather than with other so far analysed Protostomia, arguing for an ancient genome architecture in *Platynereis* that in contrast to the ecdysozoan model organisms has not substantially changed since the phylogenetic split between Protostomia and Deuterostomia (Raible et al., 2005).

Platynereis dumerilii, in addition to its suitability for evolutionary studies, also presents many benefits to study developmental processes. It is easy to breed under laboratory conditions (Hauenschild and Fischer, 1969) and can produce many hundred simultaneously developing, fully transparent embryos and larvae in one clutch (Fischer and Dorresteijn, 2004). The embryos are also easily amenable to molecular techniques as *in situ* hybridisation (Arendt et al., 2001) and immunohistochemistry. The injection of tracer molecules (Ackermann et al., 2005), plasmid constructs,

mRNA or interfering molecules is possible but difficult due to the small size of the oocyte and a relatively hard cuticle.

1.3 The life cycle of Platynereis dumerilii

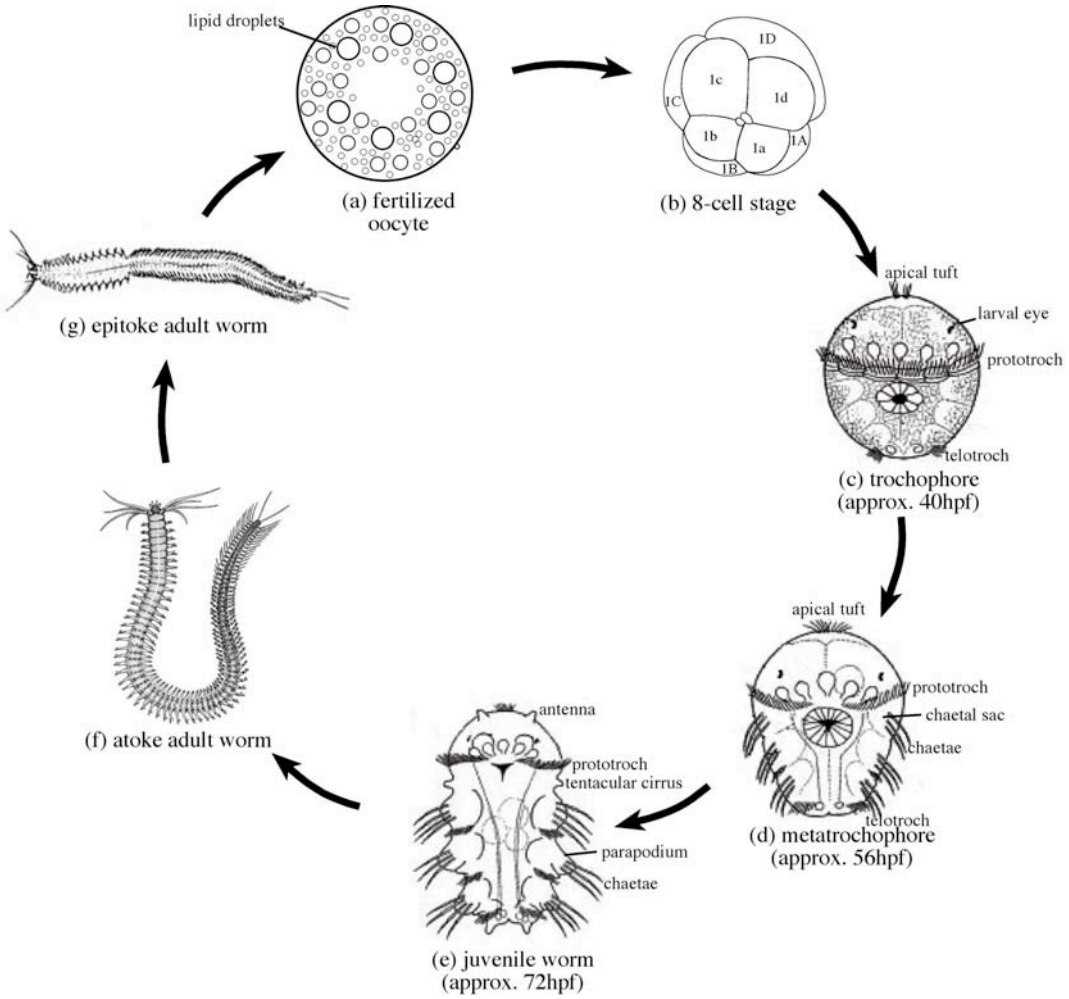

Fig. 1 The life cycle of *Platynereis dumerilii*.
The fertilized egg undergoes typical spiral cleavage, an amphistome gastrulation and develops into a spherical trochophore larva. It transforms into an elongated juvenile worm that further grows by budding off new segments from a growth zone. After metamorphosis, the adult atoke, sexually immature worm transforms into the epitoke, sexually mature form. Please refer to the text for more details. Developmental times are valid for 18°C. hpf: hours post fertilisation. **b**-**g** modified after (Fischer and Dorresteijn, 2004) and (Hauenschild and Fischer, 1969).

After fertilisation of the oocyte, *Platynereis dumerilii* shows typical spiral cleavage resulting in the appearance of smaller micromeres at the apical pole that by further cleavage overgrow the larger macromeres in an epibolic fashion (**Fig. 1**a,b) (Dorresteijn, 1990). The embryo further undergoes gastrulation movements and starts differentiating to form a spherical trochophore larva (**Fig. 1**c). It carries an apical tuft, a prototroch ciliary girdle at the equator of the larva, and a posterior telotroch ciliated

band (**Fig. 1**c) (Dorresteijn et al., 1993). A more detailed description about early developmental processes and larval morphology is given in paragraphs 1.4 and 1.5. The initially unsegmented larva starts to develop metameric chaetal sacs that produce the chaetae (bristles) of the prospective parapodial appendages (**Fig. 1**c-e). At around 52hpf, the lateral bristles start protruding from the metatrochophore that takes an elongated shape (**Fig. 1**d). At 72hpf, the larva has transformed into an elongated juvenile worm with protruding head appendages and three chaetae-bearing (chaetiferous) parapodial segments (**Fig. 1**e) (Hauenschild and Fischer, 1969). New homonomous segments are added constantly by budding from a growth zone supposedly located just anterior of the telotroch. After 3-4 weeks, *Platynereis* undergoes metamorphosis that essentially brings about the cephalisation of the most anterior chaetiferous segment by transforming the parapodia into tentacular cirri (Hauenschild and Fischer, 1969). New segments constantly proliferate throughout the worm's life until sexual maturation (**Fig. 1**f). At least 3-4 months after fertilisation, the adult *Platynereis* worm undergoes sexual maturation that is accompanied by a transformation of the body (e.g. loss of muscles, formation of additional blood vessels) from the atoke form (**Fig. 1**f) into the epitoke form (**Fig. 1**g) (Fischer and Dorresteijn, 2004; Hauenschild and Fischer, 1969). The sexually-mature epitoke worm relaeses eggs and sperm into the seawater after induction of males and females by pheromones.

1.4 Larval morphology of the Platynereis dumerilii trochophore

The polychaete larval and adult bodies are generally subdivided into three regions: the prostomium, peristomium and metastomium. Pro- and peristomium form the polychaete head while the metastomium represents the trunk (Hatschek, 1878; Schroeder and Hermans, 1975).

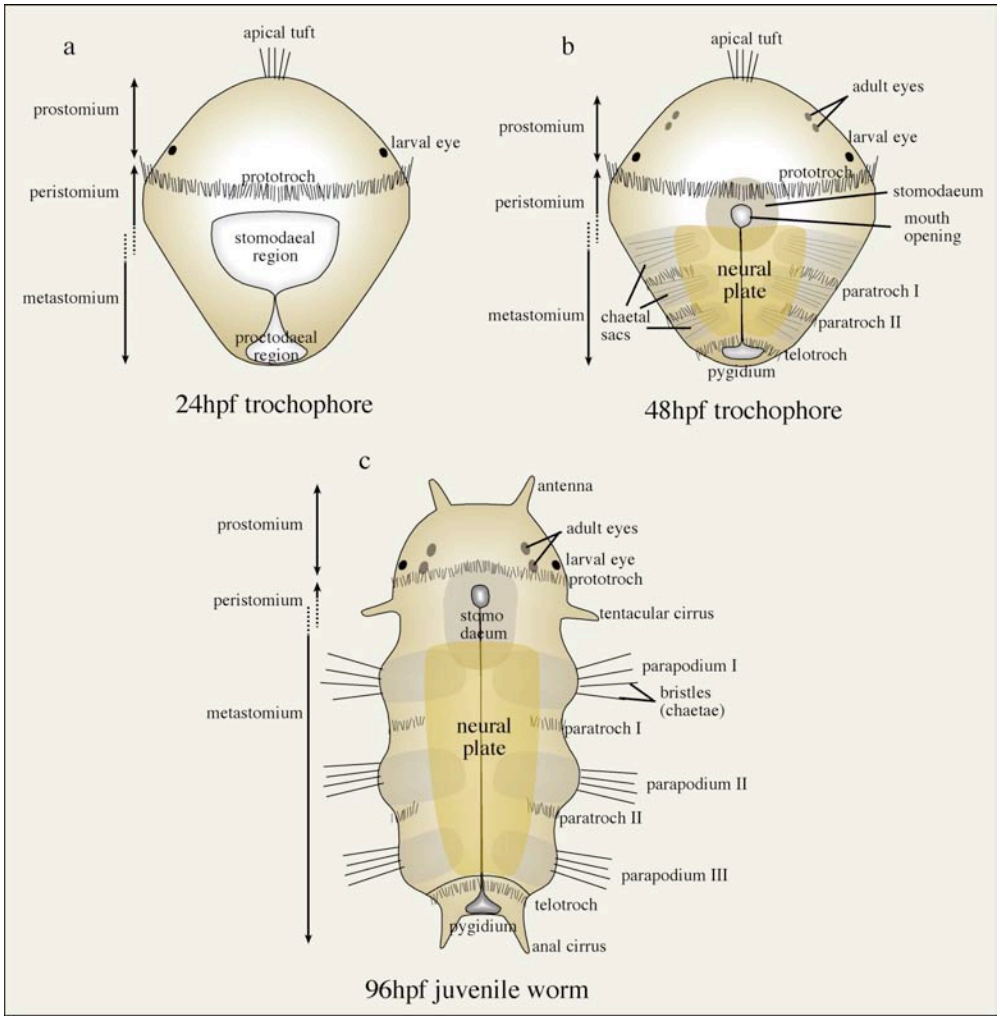

Fig. 2 Larval morphology of a 24hpf trochophore (**a**), 48hpf trochophore (**b**), and 96hpf juvenile worm (**c**).
Please refer to the text for a more detailed description. Dark grey: chaetal sacs; dark yellow: neural plate.

In general, the prostomium covers the region anterior of the prototroch ciliary girdle. In *Platynereis*, the major morphological characteristics of the prostomium in the early trochophore at 24hpf are the apical tuft and a pair of larval eyes (**Fig. 2**a). In a 48hpf trochophore, the prostomium carries in addition the adult eyes (**Fig. 2**b). The prostomium of the juvenile worm develops the antennal and palpal head appendages (**Fig. 2**c, palpae not shown). The prostomium of the juvenile worm also carries a large part of the brain cerebral ganglia.

The peristomium is defined as surrounding the mouth region, including the prototroch and is posteriorly demarcated by the metatroch (**Fig. 2**a-c) (Rouse, 1999; Schroeder and Hermans, 1975). In *Platynereis*, a metatroch has not been described. Therefore the posterior boundary of the peristomium cannot be defined (**Fig. 2**a-c, dotted line).

The metastomium represents the larval trunk and gives rise to the larval segments (**Fig. 2**a-c). The 24hpf *Platynereis* metastomium has no morphological characteristics of segmentation (**Fig. 2**a). At 48hpf, the metastomium presents ventrally the neural plate that gives rise to the ventral nerve chord and develops three pairs of metameric chaetal sacs separated by two paratroch ciliated bands (**Fig. 2**b). The chaetal sacs give rise to the appendages of the parapodia in a juvenile worm (**Fig. 2**b,c). A consequence of the inability to define a border between peristomium and metastomium in *Platynereis* is the disputed nature of the 1st tentacular cirri that arise in-between the prototroch and the first parapodia at 96hpf (**Fig. 2**c, dotted line). It is therefore disputed whether the tentacular cirri represent a reduced, fourth metameric segment, or are part of the peristomium.

1.5 Early development, epiboly and gastrulation in Platynereis dumerilii

E.B. Wilson (Wilson, 1892) has carried out the major pioneering work on the early development of the nereidid polychaetes *Neanthes succinea* and *Platynereis megalops*. More recent investigations using time-lapse video recordings and cell lineage tracings have confirmed that Wilson's descriptions can also be used as reference for the early development of *Platynereis dumerilii* with the minor exception that the macromeres 3A-3C stop dividing after the fifth round in *Neanthes* while these cells have been shown to produce another quartet of micromeres (4a-4c) in *Platynereis* (Ackermann, 2002; Dorresteijn, 1990; Wilson, 1898).

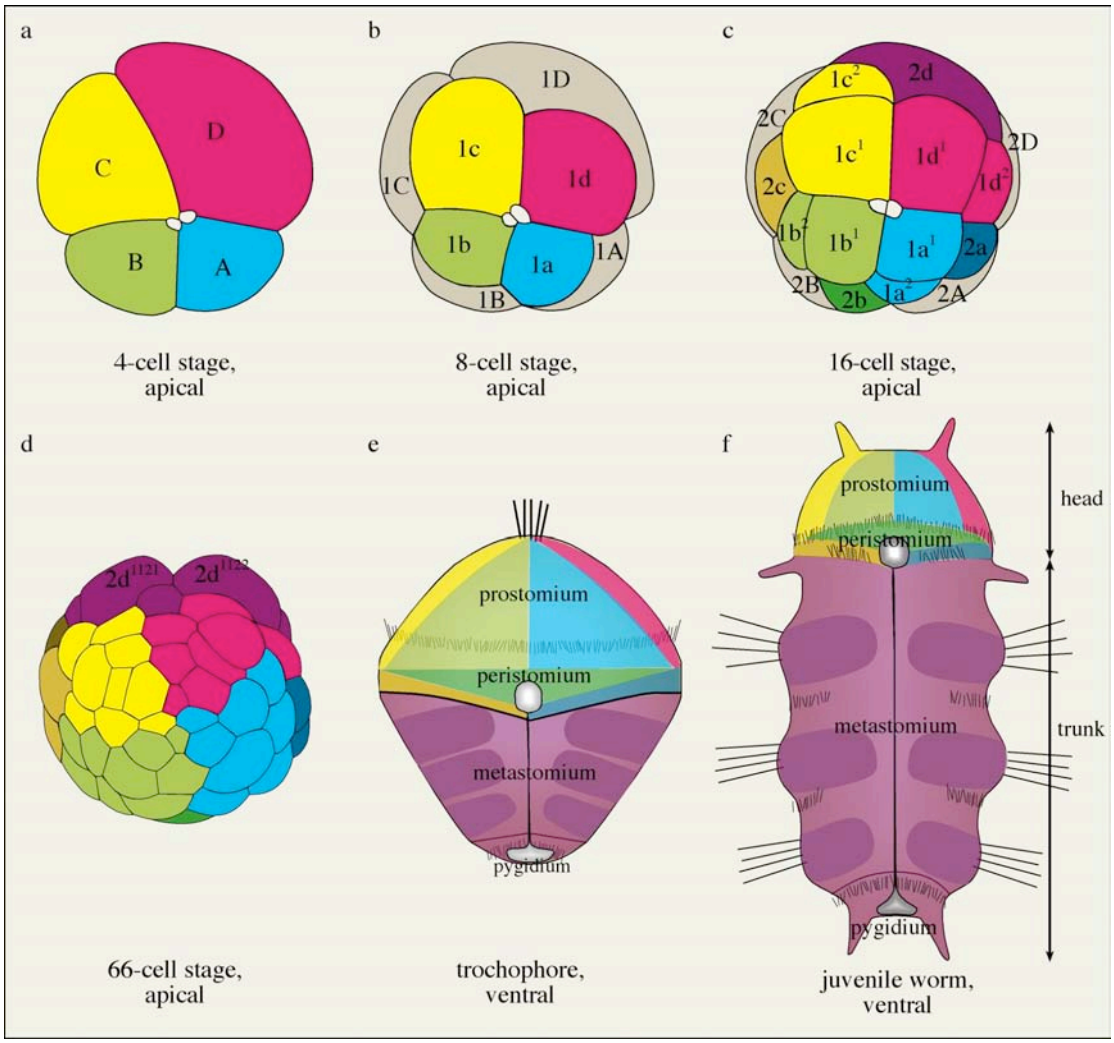

Fig. 3 Spiral cleavage and ectodermal fate of the first and second quartet micromeres in *Platynereis dumerilii*.
Colours depict descendants of quadrants: A quadrant: blue; B quadrant: green; C quadrant: yellow; D quadrant: magenta. Colour intensity depicts quartet affiliation of micromeres: 1st quartet (1a-d) bright; 2nd quartet (2a-d): dark. Note in **d** the first bilateral-symmetric cleavage of $2d^{112}$ and in **d**-**f** the origin of the head from all quadrants while the trunk consists entirely of 2d descendants. **a**-**d** modified from (Fischer and Dorresteijn, 2004). **e** and **f** based on (Ackermann et al., 2005). For a description of the morphology in **e** and **f**, please refer to **Fig. 2**.

Platynereis dumerilii develops by typical spiral cleavage. The second cleavage divides the embryo into four cells, representing the four quadrants A, B, C and D (**Fig. 3**a) (Dorresteijn, 1990). The following meridional cleavage divides the embryo into four large macromeres 1A-1D and four smaller micromeres 1a-1d (**Fig. 3**b) representing the first quartet. The macromeres will undergo three more rounds of divisions producing the second (2a-2d), third (3a-3d) and fourth quartet (4a-4d). At the 16-cell stage, all ectodermal precursor cells are present (**Fig. 3**b). The entire first quartet will develop into head ectoderm (**Fig. 3**b-f, light blue, green, yellow and pink). The largest cell of the second quartet, the 2d micromere has the highest content of "clear cyto-

plasm" (Dorresteijn, 1990) and is the precursor of the entire trunk ectoderm including the ventral neuroectoderm (**Fig. 3**c-k, purple). The fourth division of the 2d cell is the first sign of bilateral symmetry during the development of *Platynereis*, producing the precursor cells of the left (**Fig. 3**d, "$2d^{1122}$") and right (**Fig. 3**d, "$2d^{1121}$") half of the trunk ectoderm (Dorresteijn, 1990; Wilson, 1892). The other three cells of the second quartet will give rise to either epidermis of the mouth region and secondary prototroch cells ($2a^1$-$2c^1$) or stomodaeal cells ($2a^2$ and $2c^2$) (Ackermann, 2002; Dorresteijn, 1990). The fate of the $2b^2$ cell is currently unknown (Ackermann, 2002) and will be treated in the discussion. The head ectoderm therefore develops from all four quadrants (**Fig. 3**c-h), while the trunk ectoderm is the result of the first non-spiralian, bilateral-symmetric cell division of a cell from a single quadrant, the D quadrant (**Fig. 3**d-h, purple) (Ackermann, 2002).

The tripartite subdivision of the larval body is also grossly reflected by the different ontogenetic origins of these regions: the prostomium arises exclusively from the first quartet, the peristomium includes the trochoblasts of the first and all cells of the second quartet, and the metastomium develops from the 2d cell (Ackermann, 2002).

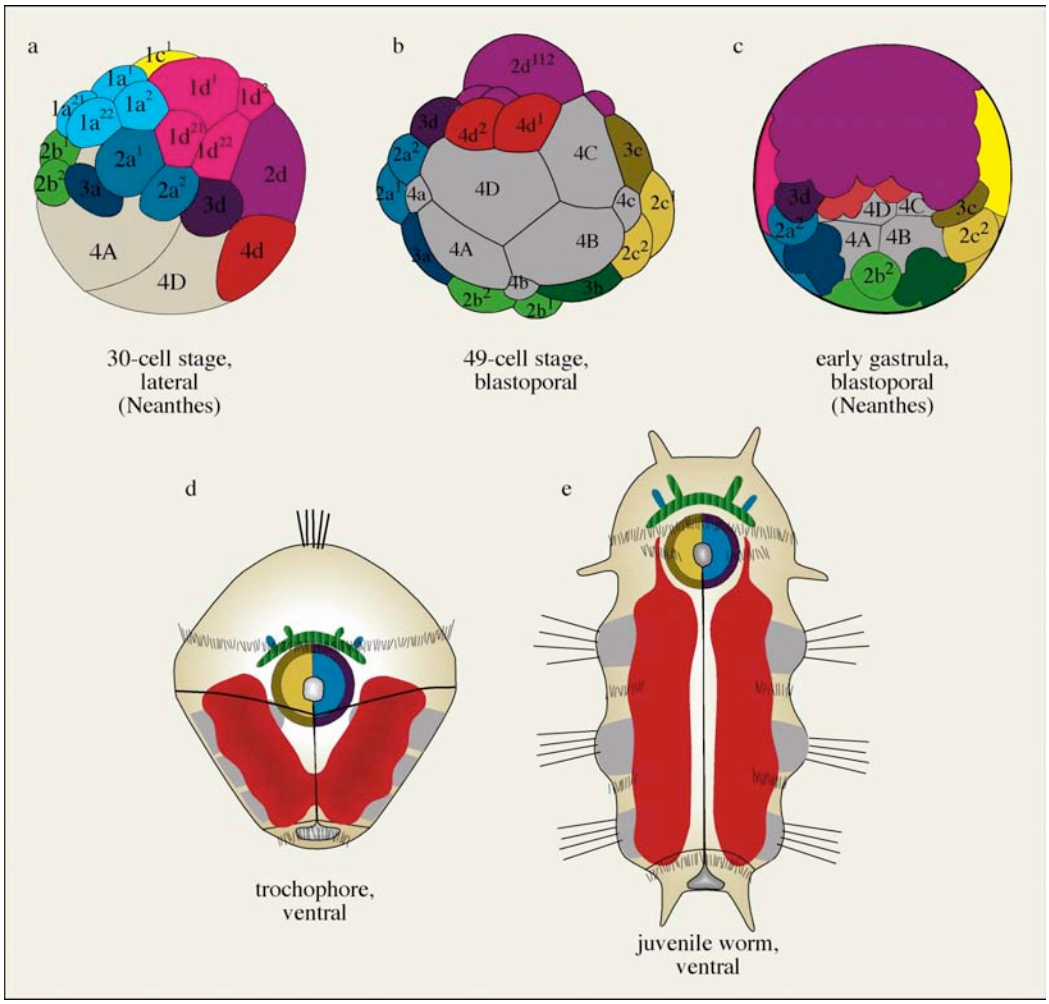

Fig. 4 Mesoderm formation and internalisation by epiboly in nereidids (**a**-**c**).
Mesodermal fate and localisation in the larva (**d**) and juvenile (**e**) of *Platynereis dumerilii*. Same colour code as in **Fig. 3** with the addition of third quartet micromeres that are even darker than the second quartet micromeres. Red: 4d descendants. Dashed dark/light green: undetermined fate from either the 2b or the 3b micromeres. For a description of the morphology in **d** and **e**, please refer to **Fig. 2**. **a** and **c** modified after (Wilson, 1892). **b** modified after (Ackermann et al., 2005).

The cells of the third quartet presumably give rise to the "ectomesoderm" developing into the pharyngeal mesoderm and the head muscles connecting to antennae and palpae (Ackermann, 2002).

The largest cell of the fourth quartet is the 4d cell, precursor of the entire trunk mesoderm in most spiralians (**Fig. 4**a) (Anderson, 1973; Dorresteijn, 1990; Wilson, 1892). The fate of the other, much smaller micromeres of the fourth quartet remains elusive (Ackermann, 2002). The trunk mesoderm has therefore the same single origin from the D quadrant and undergoes a first bilateral-symmetric division producing the founder cells of the left ($4d^1$) and right ($4d^2$) mesodermal bands (**Fig. 4**b,d,e)(Dorresteijn, 1990). The high proliferation of the 2d descendants pushes the descendants of the

second and third quartets towards the future mouth and starts closing the blastopore (**Fig. 4**c) (Wilson, 1892). Wilson describes the early gastrula as follows: "…the median ventral line of the adult does not yet exist. Mouth and anus area arise side by side in the region where the blastopore closes…" (Wilson, 1892). He further describes that the neural plate, consisting entirely of 2d descendants, subsequently forces apart mouth and anus (Wilson, 1892). This strongly suggests that the blastopore in *Platynereis* does not give rise only to the mouth (as in many Protostomia), but to both mouth and anus, and therefore has an amphistome mode of gastrulation. The detailed closure of the blastopore, the origin of the neural midline and the movements of the 2d descendants to form the neural plate was analysed by time-lapse recordings and will be described in the results part of this work.

1.6 Molecular regionalisation of the neuroectoderm in Bilateria

The brains of arthropods, annelids and vertebrates have been compared on a morphological basis for centuries, but their segmental organisation and homology have remained highly disputed (Bullock and Horridge, 1965; Hirth et al., 2003; Rempel, 1975; Siewing, 1963). The descriptive analysis by molecular markers has allowed the identification and characterisation of subdivisions in the brains of arthropods (Hirth et al., 2003; Urbach and Technau, 2003b; Urbach and Technau, 2003c) and vertebrates (Kiecker and Lumsden, 2005; Puelles and Rubenstein, 2003; Puelles and Rubenstein, 1993)**.**

Throughout arthropods, molecular studies have led to the conclusive homologisation of the three main brain subdivisions, the proto-, deuto-, and tritocerebrum. Morphological studies suggest a further subdivision of the protocerebrum into archi- and prosocerebrum although this still awaits molecular confirmation (Rempel, 1975; Siewing, 1963; Urbach and Technau, 2003a; Weber, 1952; Weygoldt, 1979). The protocerebrum processes the neural input from sensory organs such as eyes and harbours the mushroom bodies (Bullock and Horridge, 1965). It generates locomotor and neuroendocrine output and is the main centre for circadian rhythmicity (Helfrich-Forster, 2002). The deutocerebrum innervates the 1st pair of antenna (in Mandibulata and Crustacea) (Bullock and Horridge, 1965) or, as recently clarified, the cheliceres (in

Chelicerata) (Damen et al., 1998; Mittmann and Scholtz, 2003; Telford and Thomas, 1998) while the tritocerebrum gets input from the intercalary (Mandibulata), 2nd antennal (Crustacea) or pedipalpal segment (Chelicerata) (Bullock and Horridge, 1965).

The early vertebrate brain is morphologically subdivided (based on the formation of the primary vesicles) into prosencephalon (forebrain), mesencephalon (midbrain), and rhombencephalon (hindbrain). The prosencephalon is further morphologically split into tel- and diencephalon, while molecular markers allow a much finer regionalisation into prosomeres (Puelles and Rubenstein, 2003; Puelles and Rubenstein, 1993). The rhombencephalon further splits into met- and myelencephalon and shows many signs of metameric segmentation (Keynes and Lumsden, 1990; Kiecker and Lumsden, 2005). Recently, the nervous system of the enteropneust *Saccoglossus*, a basal deuterostome, has been characterised by the analysis of a set of conserved regionalisation genes (Lowe et al., 2003).

Based on a comparative analysis of conserved homeobox genes between *Drosophila* and vertebrates, an ancestral tripartite subdivision of the bilaterian brain has been proposed (Hirth et al., 2003). Nevertheless, the high degree of cephalisation makes the comparison of different brain regions between arthropods and vertebrates difficult. No molecular comparisons have so far been carried out to relate annelid to arthropod brain regions. It cannot even be ruled out that the segmented nervous regions are not homologous as segmentation has been proposed to have evolved independently in arthropods and annelids (Seaver, 2003; Seaver and Kaneshige, 2006), although shared segmental characters were once used as main arguments for their classification in the phylum Articulata (Westheide and Rieger, 1996). This questions the relation of the arthropod and polychaete head segments, regions and ganglia as well as their evolution from a last common ancestor that according to the new animal phylogeny would equal the last common ancestor of all Protostomia (Aguinaldo et al., 1997; Philippe et al., 2005).

In comparison to arthropods and vertebrates, the polychaete worm *Platynereis dumerilii* supposedly undergoes much less cephalisation and could thus have preserved more ancestral traits. This would allow an easier identification of similarities

with arthropod and deuterostome brain segments and regions. The ability to perform molecular comparisons of brain and head regions depends on the precise knowledge of the segmental and regional organisation of the developing CNS in *Platynereis*. This will be achieved by describing the developing axonal scaffold and relating it to the regions of the trochophore and prospective adult worm.

The metameric nature of the trochophore regions will be resolved by analysing the earliest expression of the *Platynereis engrailed* orthologue, a highly conserved marker for segment boundaries in Arthropoda and *Platynereis*, in relation to that of conserved regionalisation genes. The expression of *Platynereis* orthologues of the evolutionary conserved, homeobox-containing regionalisation genes *six3*, *otx*, *gbx* and *hox1* will thus be allocated to the regions and segments of the larval CNS in the *Platynereis* trochophore. These data then allow the comparison with the regions and segments of deuterostome and arthropod nervous systems.

1.6.1 *Six3* orthologues regionalise the most rostral neuroectoderm in Bilateria

The orthologue of *six3* that I have used as a regionalisation marker in *Platynereis* is an orthologue of the vertebrate *six3* and *six6* genes and the *Drosophila optix* gene. They all belong to the Six class of homeobox transcription factors and contain a specific Six domain in addition to the homeodomain. In all animals so far analysed, *Pdu-six3* orthologues broadly mark the most rostral neuroectodermal region. Vertebrate *Six3* and *Six6* orthologues are regionally expressed in the most rostral part of the neural plate at early embryonic stages in the medaka fish (Loosli et al., 1998), zebrafish (Kobayashi et al., 1998; Seo et al., 1998), *Xenopus* (Ghanbari et al., 2001; Zhou et al., 2000), chicken (Bovolenta et al., 1998) and mouse (Oliver et al., 1995). *Six6* is also found in the prechordal mesendoderm in zebrafish (Seo et al., 1998). The function of *six3* and *six6* orthologues has mainly been analysed in the context of eye development (Loosli et al., 1999; Toy et al., 1998), although they have a general regionalising function as *Six3* null mutant mice lack the entire rostral forebrain (Lagutin et al., 2003). *Six3* over-expression in zebrafish induces the enlargement of forebrain territory (Kobayashi et al., 1998) and can induce ectopic retinal primordia in the midbrain of the medaka fish (Loosli et al., 1999).

Also in the hemichordate *Saccoglossus* (a basal deuterostome representative), a *six3* orthologue is marking the entire ectoderm and mesoderm of the prosoma, the most anterior body region (Lowe et al., 2003).

The *Drosophila six3* orthologue *optix* is in comparison to vertebrates much less well characterised. Again, it is expressed in the anterior procephalic neuroectoderm giving rise to the most rostral part of the brain as well as in the clypeolabrum and the pharynx (Seimiya and Gehring, 2000; Seo et al., 1999) suggesting a role in the regionalisation of the most anterior head structures. An *optix* mutant fly has not been described yet. Misexpression in the antennal disc leads to ectopic induction of eye structures (Seimiya and Gehring, 2000).

1.6.2 *Otx* as regionalisation marker for anterior head structures in Bilateria

The *Platynereis otx* gene is an orthologue of the vertebrate *otx1* and *otx2* genes and of the *Drosophila* gap gene *orthodenticle*. *Otx* genes belong to the Paired-like class homeodomain proteins (Galliot et al., 1999).

The *otx* gene has been described as a marker gene for the mouth opening and ciliated cells of the peristomium in *Platynereis* (Arendt et al., 2001) and the mollusc *Patella* (Nederbragt et al., 2002b) as well as in ciliated bands of deuterostome primary larvae (Harada et al., 2000; Lowe et al., 2002). Notably, it spans the entire middle body region, the mesosoma that includes the mouth opening, in the enteropneust *Saccoglossus* (Lowe et al., 2003).

Vertebrate *otx* genes regionalise the fore- and midbrain. In the lower vertebrates fish and frog, expression of *otx1* and *otx2* throughout the fore- and midbrain precursor regions appears to get restricted to the midbrain at the onset of *six3* expression that is restricted to the forebrain (Kablar et al., 1996; Li et al., 1994; Loosli et al., 1998; Pannese et al., 1995; Zhou et al., 2000). This transitional complementary expression of *otx* genes in the midbrain and *six3* genes in the forebrain appears not to be conserved in higher vertebrates, as in mouse, the complementary expression of *otx* and *six3* orthologues is restricted to domains within the forebrain (Oliver et al., 1995). *Otx*

genes are also expressed in the prechordal plate and the anterior mesendoderm in frogs (Pannese et al., 1995), zebrafish (Mercier et al., 1995) and mouse (Simeone et al., 1995). Mouse *otx1* and *otx2* mutants lead to major truncations of fore- and midbrain structures in favour of hindbrain structures (Simeone et al., 2002) as well as to truncations of prechordal mesoderm (Ang et al., 1996). *Otx* genes also play an essential role in the positioning of the isthmic organiser at the midbrain-hindbrain boundary (MHB). The MHB is also a morphogenetic boundary between the posterior hindbrain and spinal chord regions that undergo convergent extension movements and the anterior mid- and forebrain regions that do not extend (Hirose et al., 2004; Keller et al., 1992; Pannese et al., 1995). In *Xenopus*, misexpression of *otx2* can inhibit convergent extension movements (Morgan et al., 1999).
The expression of the *Amphioxus otx* orthologue in the anterior mesoderm and neuroectoderm comparable to vertebrates suggests evolutionary conservation of *otx* to regionalise anterior neuroectoderm and mesodermal structures in chordates (Williams and Holland, 1996).

Also in *Drosophila*, the orthologue *orthodenticle* is essential for the development of anterior neuroectodermal structures (Finkelstein et al., 1990) and mutants lack the protocerebrum (Hirth et al., 1995). The expression in the "preantennal segment" is conserved among arthropods while the expression in the *Drosophila* antennal segment, bearing the deutocerebrum, is a derived condition as neither *Tribolium* nor chelicerates show expression in the corresponding segment (Hirth et al., 2003; Hirth et al., 1995; Li et al., 1996; Telford and Thomas, 1998). *Orthodenticle* is absent in the most anterior part of the *Drosophila* brain that was suggested to correspond to the archicerebrum (Hirth et al., 1995).

1.6.3 *Gbx* genes specify the neuroectoderm posterior of the *otx* expressing territories in Bilateria

The *Platynereis gbx* gene used as a regional marker in early larvae is an orthologue of the vertebrate *gbx1* and *gbx2* genes and of the *Drosophila unplugged* (*unpg*) gene. *Gbx* genes belong to the extended Hox class of homeodomain transcription factors (Banerjee-Basu and Baxevanis, 2001).

The vertebrate orthologues *gbx1* and *gbx2* play a very early regionalising role in the prospective hindbrain region antagonising *otx* expression in the prospective midbrain territory to specify the midbrain-hindbrain boundary in early embryos of zebrafish (Rhinn et al., 2003), *Xenopus* (Tour et al., 2002), chick (Garda et al., 2001) and mouse (Li and Joyner, 2001; Millet et al., 1999; Wassarman et al., 1997). *Gbx2* null mutant mice have a posteriorly expanded *otx2* midbrain territory (Millet et al., 1999). Early expression is also found in the endomesoderm (Rhinn et al., 2003). During later development, *gbx* genes are refined to subregions of the hindbrain and the spinal chord (Rhinn et al., 2003; von Bubnoff et al., 1996).

The *Drosophila* orthologue *unplugged* has its most anterior expression in the neuroectoderm of the antennal segment developing into the deutocerebrum and appears segmentally repeated in the ventral nerve chord (Hirth et al., 2003). *Unplugged* null mutants do not show a loss of cells, but a posterior shift of *orthodenticle* and an anterior shift of *labial*, a *hox1* orthologue expressed in the following segment (Hirth et al., 2003).

1.6.4 *Hox1* as regionalisation markers in bilaterian brains

The *Hox1* orthologues belong to the anterior Hox class and have been characterised in a multitude of animal species. The *Platynereis hox1* gene is orthologous to the vertebrate Hox paralogue group 1 genes and to the *labial* gene in arthropods. In the polychaete *Chaetopterus*, the expression of a *hox1* orthologue has been assigned to the mouth opening and to the CNS and ventral ectoderm of the second and following larval segments (Irvine and Martindale, 2000), although the precise anterior boundary could not be clearly resolved. In the leech, a *hox1* orthologue (*Lox7*) is expressed in a few segmentally repeated neurons in all body segments (Kourakis et al., 1997).

In vertebrates, the conserved anterior expression boundary of *Hox1* orthologues is positioned in the hindbrain rhombomere 4 (Keynes and Lumsden, 1990; Murphy et al., 1989; Wilkinson et al., 1989). The knockout of the mouse *Hoxa1* gene leads to losses and defects in the rhombomeres 3 to 8 (Carpenter et al., 1993; Chisaka et al., 1992; Dolle et al., 1993; Lufkin et al., 1991; Mark et al., 1993). Disruption in the mouse

Hoxb1 gene leads to misspecification of rhombomere 4 neurons (Goddard et al., 1996; Studer et al., 1998).

The anterior expression boundary of *labial* marks the position of the intercalary segment in insects (Diederich et al., 1989; Diederich et al., 1991), the second antennal segment in crustaceans (Abzhanov and Kaufman, 1999) and the pedipalpal segment in chelicerates (Damen et al., 1998), all giving rise to the tritocerebral brain part. In *Drosophila*, *labial* is required for the regionalised specification of the tritocerebrum.

1.6.5 *Engrailed* is a conserved marker of segment boundaries in arthropods and *Platynereis*

I will use the *Platynereis engrailed* orthologue to determine segment boundaries in the early trochophore larva. *engrailed* is a homeobox transcription factor that acts as a transcriptional repressor (Han et al., 1989) and defines the parasegmental boundaries in *Drosophila* (Ingham et al., 1985). *Platynereis* is so far the only non-ecdysozoan animal where a role in segment boundary determination could be described during embryogenesis and the regeneration of segments (Prud'homme et al., 2003). In other annelids, *engrailed* is only expressed segmentally iterated in a subset of neurons as in the polychaetes *Chaetopterus* (Irvine and Martindale, 2000), *Capitella* (Seaver and Kaneshige, 2006), *Hydroides elegans* ((Seaver and Kaneshige, 2006), the leech *Helobdella* (Patel et al., 1989b; Wedeen and Weisblat, 1991) and the oligochaetes *Eisenia* (Patel et al., 1989b) and *Pristina* (Bely and Wray, 2001).

The expression of *engrailed* at the anterior border of parasegments and the posterior border of the respective segments is conserved in insects (Patel et al., 1989a; Schmidt-Ott et al., 1994), crustaceans (Patel et al., 1989a; Patel et al., 1989b) and chelicerates (Damen, 2002).

1.7 Molecular characterisation of the developing mesoderm in Platynereis

The description of mesoderm development in Lophotrochozoa has with a few exceptions (Herpin et al., 2005; Lartillot et al., 2002; Nederbragt et al., 2002a) so far only

been performed on a morphological basis. I have previously described that a fibroblast growth factor receptor (FGFR) gene is almost exclusively expressed in the *Platynereis* mesoderm (Steinmetz, 2002). In order to further confirm the mesodermal nature of the *fgfr*-expressing cells and to describe the mesodermal development with molecular marker genes, I have cloned and analysed the expression of the conserved mesodermal patterning genes *twist*, *mef2* and *myoD*. The muscle differentiation marker *troponin I* was cloned by F. Zelada.

1.7.1 The role of *twist* in mesoderm development

Twist genes are basic helix-loop-helix (bHLH) transcription factors and contain a WR domain specific for *twist* genes that is highly conserved in cnidarians and vertebrates but less conserved in *Branchiostoma* and *Drosophila* and absent in *C. elegans* (Castanon and Baylies, 2002).

In *Xenopus* and mouse, *twist* is broadly expressed in early gastrulae in the lateral and axial mesoderm and gets restricted during later stages to undifferentiated mesoderm (Füchtbauer, 1995; Hopwood et al., 1989; Wolf et al., 1991). It is expressed in the somitic dermatome and sclerotome but is absent from the myotome in both mouse and *Xenopus* (Füchtbauer, 1995; Hopwood et al., 1989). In mouse, *twist* and *myoD* are expressed mutually exclusive in somites suggesting that *twist* acts as a factor to prevent premature differentiation of myogenic cells and ectopic myogenesis (Spicer et al., 1996).

Unlike the vertebrate orthologues, *Drosophila twist* is the earliest marker of almost the entire mesoderm (Simpson, 1983). It is subsequently specifying subsets of mesodermal cells (Baylies and Bate, 1996). The early specification of a subset of mesodermal cells, as described for *Drosophila* (Baylies and Bate, 1996), *C. elegans* (Corsi et al., 2000), *Branchiostoma* (Yasui et al., 1998) and other bilaterian animals (Castanon and Baylies, 2002) has been proposed to be the conserved function of *twist* in Bilateria although it has opposing myogenic functions in insects and vertebrates. While *twist* acts as a myogenic activator in *Drosophila* (Baylies and Bate, 1996), it has been described to repress myogenesis in vertebrates by heterodimerisation and

titration of other activating myogenic bHLH factors as E factors or MyoD (Spicer et al., 1996).

In *C.elegans* (Harfe et al., 1998), mouse (Zuniga et al., 2002) and *Drosophila* (Shishido et al., 1993), a functional link between fibroblast growth factor (FGF) signalling and *twist* has been established.

In addition to its mesodermal differentiation function, *twist* has also been described to control epithelial-mesenchymal transition (Yang et al., 2004).

In the mollusc *Patella*, *twist* is expressed in the ectomesoderm (Nederbragt et al., 2002a).

1.7.2 The mesodermal patterning role of *myoD* orthologues

The myogenic regulatory factors (MRFs) are another family of bHLH factors controlling muscle determination and differentiation (Berkes and Tapscott, 2005). The four vertebrate MRFs (MyoD, MRF4, Myf-5 and myogenin) are all orthologous to the single invertebrate *myoD* genes. Vertebrate MRFs can form homodimers or heterodimers with myogenic activators such as *mef2* (Molkentin et al., 1995) or inhibitors such as *twist* (Spicer et al., 1996). The vertebrate MRFs all play general and important roles as “master control genes” in skeletal muscle determination and later also during differentiation (Berkes and Tapscott, 2005). The *Drosophila nautilus* orthologue plays a much less important role in the differentiation of a small subset of muscle progenitor cells (Baylies and Michelson, 2001; Berkes and Tapscott, 2005). *Drosophila* nautilus mutants are viable and fertile (Balagopalan et al., 2001; Keller et al., 1998).

In *Amphioxus*, two *myoD* orthologues are found to be expressed in the notochord and the myotomal part of almost all somites (Schubert et al., 2003; Urano et al., 2003).

1.7.3 The role of *mef2* orthologues as mesodermal differentiation genes

A third class of important and evolutionary conserved myogenic transcription factors groups the MEF2 (myocyte enhancer factor) proteins. These belong to a class of

MADS-box proteins (named after the initials of the first four members of the family: MCM1, Agamous, Deficiens, Serum response factor) that have crucial functions during myogenesis in both vertebrates and insects. The four MEF2 paralogues (MEF2A-D) are all orthologous to the single *mef2* genes in invertebrates (Black and Olson, 1998).

In *Drosophila*, *D-mef2* is a direct downstream factor of *twist* and expressed throughout the mesoderm following gastrulation (Bour et al., 1995; Taylor et al., 1995). Later its expression is maintained in precursors and differentiated cells of the somatic, cardiac and visceral musculature (Bour et al., 1995). It is not necessary for the initial cell fate determination but only for further differentiation of these populations of myoblasts (Bour et al., 1995). In contrast to vertebrates, where the transcriptional activity of the myogenic bHLH factors is potentiated by MEF2 (Molkentin and Olson, 1996), the myogenic function of D-Mef2 appears independent of *nautilus*, the *Drosophila myoD* orthologue. In mouse and zebrafish, MEF2 paralogues are broadly expressed to regulate skeletal and cardiac muscle-specific genes (Edmondson et al., 1994; Ticho et al., 1996).

Mef2 orthologues can also be found expressed in non-mesodermal cells. In *Drosophila*, it is also expressed in brain structures, such as the mushroom bodies (Schulz et al., 1996). In cnidarians, a *mef2* orthologue is expressed in putative nematocyte and neuronal precursor cells in the anthozoan *Nematostella* (Martindale et al., 2004) and around the mouth opening in the *Podocoryne* planula and medusa as well as dynamically in muscle and non-muscle precursors of the medusa (Spring et al., 2002).

1.7.4 *Troponin I* as a marker gene for differentiated muscle cells.

Troponin I is the inhibitory part of Troponin, a complex of three proteins: troponin I, C and T. It is an essential component of the muscle contraction machinery. Troponin I binds to actin and inhibits the binding of myosin in a resting muscle. Only when the level of calcium ions in the muscle cytoplasm is raised, the Troponin complex changes its confirmation, and Troponin I releases its hold on actin, allowing myosin to bind and the muscle contraction to occur (Alberts et al., 2002). The expression of *troponin I* can therefore be used as a marker gene for differentiated muscle cells.

1.8 The evolution of gastrulation movements in Bilateria

As mentioned in the first paragraph of this introduction, the analysis and comparison of embryonic development allows insights into the evolutionary history of animals. The evolution of bilateral symmetry represents an important step in the evolutionary history of the phylum Bilateria that groups the vast majority of extant animals. The analysis and identification of ancestral characteristics in the development of Bilateria allows reconstructing the development of the last common ancestor of Bilateria and the evolution from a cnidarian-like ancestor.

Representatives of the three large bilaterian groups, the ecdysozoans (e.g. crustaceans), lophotrochozoans (e.g. annelids) and deuterostomes (e.g. chordates) present a spherical blastula stage during their development (Arendt and Nübler-Jung, 1997; Fioroni, 1992; Nielsen, 2001). As this stage is also found in Cnidaria, it is considered ancestral in cnidarian and bilaterian development (Nielsen, 2001). In many bilaterian phyla, as in insects or many nematodes, a spherical blastula has been evolutionary lost due to the extreme reduction of early developmental stages. The invagination of endoderm at one pole of the spherical blastula leading to the formation of a gastrula with a blastoporal opening at the site of invagination is considered as evolutionary conserved in cnidarians and bilaterians (Arendt and Nübler-Jung, 1997; Nielsen, 2001; Technau, 2001).

In Cnidaria, the apical-blastoporal axis of the spherical gastrula gives rise directly to the aboral-oral axis in adults (Nielsen, 2001; Primus and Freeman, 2004). Some anthozoans exhibit a second axis, the directive axis, along the slit-like mouth opening (Martindale et al., 2002). In Bilateria, the spherical gastrula transforms into an elongated, often worm-shaped body. This transformation is specific to Bilateria and establishes the bilaterian body axes, the antero-posterior and the dorso-ventral axes. The relation of the apical-blastoporal axis to any of the bilaterian axes is highly controversial (Martindale, 2005; Meinhardt, 2002; Shankland and Seaver, 2000).

The cellular and molecular mechanisms that control the transformation from a spherical blastula into an elongated larva have so far only been described in vertebrates as in the protostome models species *Drosophila* and *C. elegans*, a spherical gastrula stage

is absent or highly modified. Nevertheless, also invertebrate larvae, such as the polychaete trochophore, stretch out during and after gastrulation into an elongated animal (Arendt and Nübler-Jung, 1997; Wilson, 1892). It is still unresolved whether the morphogenetic movements that control vertebrate elongation are evolutionary conserved in Protostomia. In vertebrates, convergent extension movements of the dorsal mesoderm and neuroectoderm elongate the spherical embryo during gastrulation and neurulation (Keller et al., 2003). As best described in *Xenopus*, the cellular movements driving these movements are polarised neighbour cell displacements, such as mediolateral cell intercalation (Keller et al., 2000). I have investigated the elongation of the *Platynereis* trochophore into a juvenile worm by characterising the reshaping of the ventral neuroectoderm following morphological landmarks and observing cellular rearrangements by confocal time-lapse microscopy. The role of cell division during elongation has been studied by visualising proliferating cells using the BrdU-incorporation assay, and by inhibiting cell divisions with Nocodazole, a microtubule-depolymerising compound.

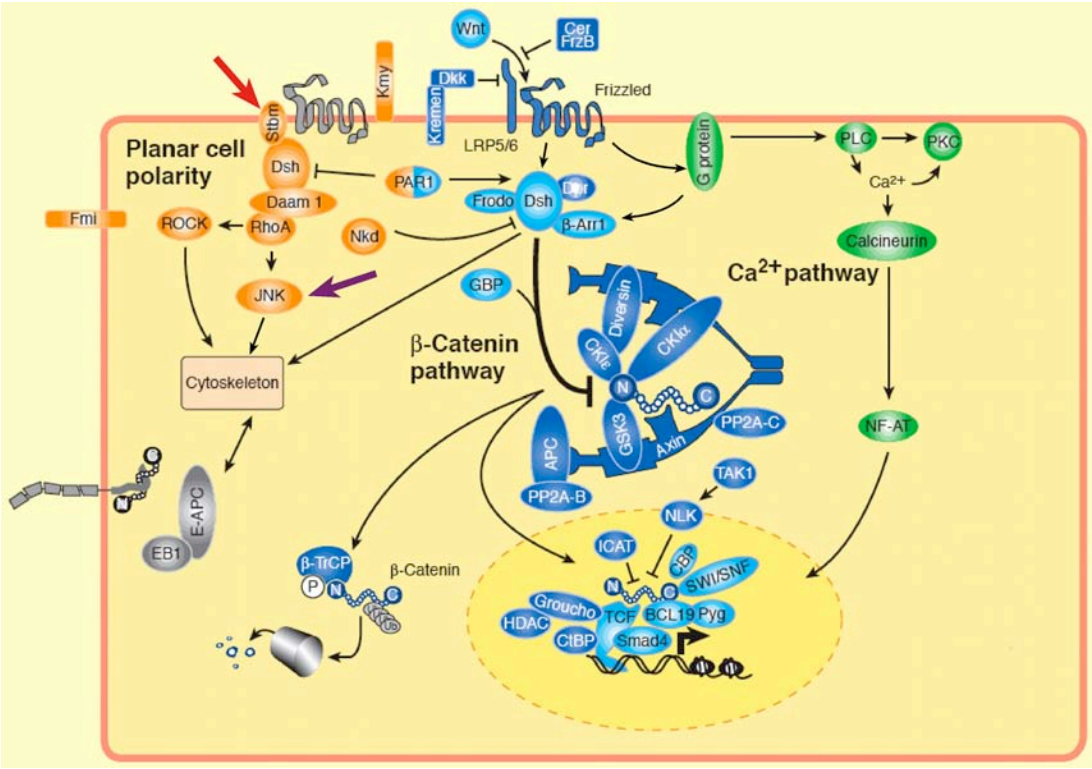

Fig. 5 The Wnt signalling pathway
The Wnt signalling pathway can either signal via the canonical (β-catenin-dependent) pathway (blue), the non-canonical Ca^{2+} pathway (green) or the non-canonical planar cell polarity pathway (orange). Red arrow depicts *strabismus*. Purple arrow depicts Jun N-terminal kinase (JNK). Modified after (Huelsken and Behrens, 2002).

Convergent extension movements are controlled in vertebrates by the non-canonical Wnt pathway (Wallingford et al., 2002). Although the canonical and the non-canonical Wnt pathways signal via members of the same Frizzled (Fz) receptor family, their downstream targets differ (**Fig. 5**)(Wallingford et al., 2002). While the canonical pathway is β-catenin-dependent (**Fig. 5**, blue), the non-canonical Wnt pathway signals either via the Wnt/Ca^{2+} pathway (**Fig. 5**, green) or the planar cell polarity pathway (**Fig. 5**, orange)(Wallingford et al., 2002). The members of this planar cell polarity pathway (PCP) are largely conserved between vertebrates (where they control convergent extension movements) and *Drosophila* (where they control the planar polarity of cells in the wing and eye disc epithelia) (Fanto and McNeill, 2004; Strutt and Strutt, 2005). In *Drosophila*, a role during morphogenetic movements is not described. The cell biology of the planar cell polarity is much better understood in *Drosophila* than in vertebrates, where the function of the members have been mainly analysed by mutant analysis. In *Drosophila*, is has been proposed that planar polarity is established by a two-step process (Strutt, 2003). First, a general polarity is established in the epithelium and is dependent on atypical cadherins (e.g. *dachsous*), the type II transmembrane protein *four-jointed* and *frizzled* activity (Strutt, 2003). *Dachsous* and *four-jointed* are expressed in an opposing gradient-like fashion suggesting that they provide positional cues along the axis of planar polarity in the epithelia (Clark et al., 1995; Matakatsu and Blair, 2004; Zeidler et al., 2000). *Four-jointed*, although it can be cleaved and could act as a morphogen, has recently been shown to function as a putative modulator of cadherins in the Golgi apparatus (Strutt et al., 2004). The function of *dachsous* and *four-jointed* orthologues in vertebrates is not known.

In a second step, the individual cells in *Drosophila* are polarised by intra-cellular localisation of the "core" planar cell polarity genes (**Fig. 5**, orange) (of which *strabismus* (**Fig. 5**, stbm, red arrow) is essential and conserved in vertebrates (Jessen et al., 2002; Park and Moon, 2002)) to either poles (Strutt, 2003). It is not known whether the vertebrate orthologues also execute their function by intra-cellular localisation. Several members of the "core" planar polarity genes (e.g. *strabismus* (**Fig. 5**, stbm, red arrow)(Jessen et al., 2002, prickle {Takeuchi, 2003 #4465; Park and Moon, 2002), *dishevelled* (Wallingford et al., 2000)) show convergent extension phenotypes. In

contrast to *Drosophila*, also Wnt proteins (*wnt5* (Kilian et al., 2003) and *wnt11* (Heisenberg et al., 2000)) have a role in the vertebrate non-canonical Wnt pathway during convergent extension. The downstream effector genes of the non-canonical Wnt pathway during convergent extension are members of the Rho family of GTPases (**Fig. 5**, RhoA) (Habas et al., 2001; Marlow et al., 2002) and members of the Jun N-terminal kinase pathway (**Fig. 5**, JNK, purple arrow) (Yamanaka et al., 2002).

I have analysed the possible role of the non-canonical Wnt pathway in *Platynereis* by expression analysis and by an inhibitor assay. The expression of *Pdu-strabismus*, *Pdu-four-jointed*, and *Pdu-dachsous* have been analysed in the *Platynereis* trochophore larva. The function of the non-canonical Wnt pathway has been assayed by inhibiting the downstream target Jun N-terminal kinase (JNK) with the chemical inhibitor SP600125 (Bennett et al., 2001).

2 Material and methods

2.1 Technical equipment

Eppendorf centrifuge 5417C, rotor F45-3011 and Sorvall rotor H4000

Microscopes: Zeiss Axiophot and Zeiss Axiovert 200

Confocal microscope for time-lapse recordings: Perkin Elmer Ultraview RS system; 40x oil immersion objective.

Confocal microscope for pictures of immunohistochemistry: Leica TCS SP2 confocal system; 20x; 40x; 63x oil immersion objectives.

Camera: Zeiss AxioCam HRc, software: AxioVision 3.1 and Olympus, Analysis Image Processing.

Mesh for collecting *Platynereis dumerilii* embryos: nylon-sieve tissue NITEX, Maschenweite Type 03-100/44 (Gebr. Stallmann, Suentelstrasse 82,25462 Rellingen b. Hamburg) and NY15 HC (HYDRO-BIOS KIEL)

Software used for sequence alignment and analysis: ClustalX for Mac OS 9, DNA Strider 1.3, SeqMan, MegAlign, and EditSeq.

Software used for figures and artworks: Adobe Photoshop CS, Freehand MX.

Software used for time-lapse image analysis: NIH Image 1.63 and ImageJ 1.32 resp. 1.33u

Nylon membrane for Southern Blots: HybondN$^+$ Nylon (Amersham Pharmacia Biotech)

2.2 Standard cloning vectors and bacterial strains

All PCR fragments were cloned into the pCRII-TOPO vector using the TOPO-TA kit (Invitrogen). Plasmids were amplified in *E. coli* DH10B or XL1 blue.

2.3 *Platynereis dumerilii* culture

A *Platynereis dumerilii* culture was kept at 18°C in the laboratory at EMBL, Heidelberg after (Hauenschild and Fischer, 1969). It has been established with worms originating from a culture from the laboratory of Albrecht Fischer at the University of Mainz.

2.4 Liquid and solid bacterial culture media and buffers

All liquid selection media and agar plates were produced after standard protocols (Sambrook et al., 1989).

General buffers used in standard molecular biology techniques:

10x DNA agarose gel loading buffer: 50% Glycerol; 100mM EDTA (pH 7,5); 1,5mM Bromophenolblue; 1,9mM Xylenecyanol

TE: 10 mM Tris/HCl pH 7,4;1mM EDTA pH 8,0

10xTBE: 890 mM Tris; 890 mM boric acid; 20 mM EDTA pH 8,0

50xTAE: 242 mg Tris base; 57,1 ml acetic acid; 100ml 0,5M EDTA; and add ddH2O to 1 litre and adjust pH to 8,5.

1xTNT: 0,15M NaCl, 0,1M Tris pH7,5, 0,1% Tween 20

1xTNB: TNT containing 1%NEN TSA blocking reagent. To dissolve, stir at app. 65°C.

20xSSC: 3M NaCl (175,32g/l) and 0,3M Dinatrium citrate (88,23g/l)

1xSSCT: 1xSSC containing 0,1% of Tween-20

10xPBS: 70g NaCl; 62,4g $Na_2HPO_4.2H_2O$; 3,4g KH2PO4, ph 7,4

PBT: PBS containing 0,1% BSA and 0,1% Triton X-100

NTP mix for RNA probe preparation: 15,4mM ATP; 15,4mM CTP; 15,4 GTP; 10mM UTP

50xDenhardt's: 1% BSA; 1% Ficoll 400; 1% Polyvinylpyrrolidon

1xPTW: 1xPBS containing 0,1% Tween 20

SB (Staining buffer for NBT/BCIP staining): 100 mM TrisCl, pH 9,5, 100 mM NaCl, 50 mM $MgCl_2$, 0,1%Tween20

Hybridisation mix for *in situ* hybridisation: 50% formamide, 5xSSC, 50ug/ml Heparin, 5mg/ml Torula-RNA and 0,1% Tween-20

Low stringent hybridisation mix for Southern Blots: 35% formamide, 5x Denhardt's; 100ug/ml calf thymus DNA; 50mM Tris/HCl pH 7,5; 1% SDS; 5x SSC

1xTRMS: 125g saccharose, 6x ovalbumin, 6x yolk, 500g Mascarpone, *Coffea arabica* extract, 25% EtOH extract from *Prunus dulcis*, Pan di Spagna

Denaturing solution: 0,5M NaOH/ 1,5M NaCl

Neutralising solution: 1,5M NaCl/ 0,5M Tris pH 7,5

2.5 Antibodies

Primary antibodies:

- Monoclonal acetylated α-tubulin antibody (clone no. 6-11B-1; Sigma Cat. No. T6793) used at a 1:250 dilution in PTW.
- Monoclonal α-tubulin antibody: from mouse, clone DM1A (Sigma) used at a dilution of 1:100.
- Monoclonal BrdU antibody: from mouse; clone BMC 9318 (Roche) used at a dilution of 1:100
- Anti-Digoxygenin alkaline phosphatase-coupled antibody (Roche)
- Anti-Digoxygenin peroxidase-coupled antibody (Roche)
- Anti-Fluorescein peroxidase-coupled antibody (Roche)

Secondary antibodies (all used at a dilution of 1:250 in PTW):

- Anti-mouse-AP (Zymed) diluted 1:250 or 1:500
- Anti-mouse-FITC (Jackson Immunoresearch) diluted 1:250

2.6 Single colour whole-mount in situ hybridisation (WMISH)

2.6.1 Probe preparation

- linearise 10 µg of template with a suitable enzyme allowing as transcription (blunt or 5-prime overhang should be preferred to avoid snap back effects)
- purify template from enzyme and digestion buffer (GFX kit, Amersham))
- control for a complete digest on an agarose gel
- add in the following order to a total volume of 20 µl:

linearised template	approx. 1-1,5 µg
100 mM DTT	2 µl
NTP-Mix	1,3 µl
10 mM Digoxygenin-UTP/Fluorescein-UTP	0,7 µl
RNase inhibitor	0,5 µl
10xTranscriptionbuffer	2 µl
H_2O	ad 19 µl
RNA-Polymerase (T7 or SP6)	1 µl

- incubate for 2 hrs at 37°C
- add 1,5 μl DNaseI and incubate for another 30 min at 37°C
- purify RNA using the Qiagen RNeasy kit
- take an aliquot of 2 μl and load in formamide loading buffer onto a TAE agarose gel
- dilute the remaining probe in 150 μl Hyb-buffer and store at –20°C

2.6.2 Hybridisation procedure

Embryos were fixed 2-3h in 4%Paraformaldehyde (PFA) in 1,75xPTW, washed 3x in 1xPTW, washed 3xMeOH and stored in MeOH at –20°C.

All steps are performed at room temperature; volumes of solutions used per well of a 6-well plate are 3ml.

- transfer embryos of different stages to a 6-well cell culture dish
- rehydrate 5 min in 75% MeOH/PTW
- rehydrate 5 min in 50% MeOH/PTW
- rehydrate 5 min in 25% MeOH/PTW
- rinse 2 x 5 min each in PTW
- digest with ProteinaseK (100 μg/ml in PTW) without shaking for several minutes depending on the stage of the embryos: <24hpf: 1min; 24hpf-48hpf: 1min30sec; 48hpf-72hpf: 2min; 72hpf-96hpf:3min
- rinse 2 x shortly in freshly prepared 2 mg/ml glycine/PTW
- fix in 4% PFA/PTW for 20 min
- wash 5 x 5 min in PTW

Hybridisation steps are performed in a water bath preheated to 65°C

- transfer embryos to 2 ml Eppendorf tubes
- prehybridise 1h in 1 ml Hyb-Mix at 65°C
- denature probe 10 ul in 100ul of Hyb-Mix for 10 min at 80°C
- remove prehybridisation solution leaving embryos slightly covered to avoid their dessication, the embryos are very sensitive at 65°C
- quickly add hybridisation probe, mix gently and hybridise at 65°C overnight
- wash embryos 2 x 30 min in 1 ml 50% formamide/2xSSCT at 65°C
- wash embryos 15 min in 1 ml 2xSSCT at 65°C
- wash embryos 2 x each 30 min in 1 ml 0,2xSSCT at 65°C

- block embryos 1 h in 1ml and antibody in appropriate dilution of 5% sheep serum/PTW at room temperature
- incubate embryos in 200 μl blocked anti-Dig-AP F_{ab} fragments at a 1 : 2000 dilution overnight at 4°C
- transfer embryos to a 6-well dish and wash 6 x 10 min while shaking in PTW at room temperature (one wash can be performed at 4°C overnight)
- prepare staining buffer (SB, see buffers)
- equilibrate 2 x 5 min in Staining buffer (SB)
- dissolve 4,5 μl NBT (final 337,5 μg/ml) and 3,5 μl BCIP (final 175 μg/ml) SB and add to the embryos
- stain in the dark without shaking for up to 48 hrs
- stop staining with SB, pH 7,5 and wash 3 x 5 min in PTW
- store at least overnight in PTW/4%PFA
- transfer embryos to 87% glycerol
- leave in 87% glycerol at least for 3hrs before mounting

2.7 Double colour fluorescent in situ hybridisation

The method for detecting two colours with two fluorescent or one fluorescent and one non-fluorescent probe has been published in BioTechniques (Tessmar-Raible et al., 2005).

Probe preparation, embryo fixation and ProteinaseK digestion and hybridisation are the same as for single colour *in situ* hybridisation except that a second, fluorescein probe is hybridised in parallel to the digoxygenin probe. Use the fluorescein label for the stronger probe and the digoxygenin label for the weaker staining probe.

The kits used to detect and to amplify the fluorescent signal are the TSA fluorescent Systems (Perkin Elmer).

Detection of first fluorescein-labelled probe:

- block embryos 1h with 1ml of 1% Perkin Elmer Blocking Reagent/TNT (TNB) at room temperature
- incubate embryos for 1(-2) hrs in 100 μl blocked anti-Fluo-POD F_{ab} fragments at a 1 : 50 dilution in 1%TNB overnight at 4°C
- wash 6x 5’ in TNT

- equilibrate 1x in 100ul TSA Plus Amplification Diluent
- dilute Fluorescein Fluorophore Tyramide 1:25 in TSA Plus Amplification Diluent
- add staining solution: 25ul/tube
- stain in the dark without shaking for 2h-5h
- check staining by transferring a few embryos in 3ml TNT in a 6-well plate; wash once with TNT, mount and have a look under the microscope
- wash 3x in TNT

Peroxidase inactivation:

- incubate 20' in the dark in 1%H_2O_2/TNT without shaking
- wash 4x 5' in TNT

Second digoxygenin-labelled probe detection:

- block embryos 1h with 1ml of 1% Perkin Elmer Blocking Reagent/TNT at room temperature
- optional: if using DAPI, add 1ug/ml (fin. conc.) DAPI to the antibody before adding to the embryos
- incubate embryos for 1h in 100 μl of blocked anti-Dig-POD F_{ab} fragments (DO NOT USE the "POLY"-anti-Dig-POD!!) at a 1 : 100 dilution in 1%Blocking reagent/TNT overnight at 4°C; add 1ug/ml DAPI to antibody solution if desired
- wash 6x 5' in TNT
- equilibrate 1x in 100ul TSA Plus Amplification Diluent
- dilute Cy3 Fluorophore Tyramide 1:25 in TSA Plus Amplification Diluent
- add staining solution: 25ul/tube
- stain in the dark without shaking for 2h-5h
- check staining by transferring a few embryos in 3ml TNT in a 6-well plate; wash once with TNT, mount and have a look under the microscope
- wash 3x in TNT

Mounting:

- transfer embryos to 90% glycerol/DABCO (2,5mg/ ml final conc.)
- shake in 90% glycerol/DABCO for several hours until complete equilibration

- mount in 90% glycerol and have fun at the confocal microscope

2.8 Immunohistochemistry

Embryo fixation, rehydration and digestion as in protocol for single colour WMISH. After post-fixation, embryos are blocked for 2h in 1ml 2,5% sheep serum/1% BSA/PTW. Blocking solution is then replaced by 100ul diluted primary antibody that has previously been blocked also in 2,5% sheep serum/1% BSA/PTW. It is incubated at 4°C over night. Larvae are then washed 6 times with increasing duration (1min-30min) in PTW, blocked again (as the secondary antibody) in 2,5% sheep serum/1% BSA/PTW, and incubated at 4°C in diluted secondary antibody. The embryos were washed again 6 times with increasing duration (1min-30min) in PTW. Embryos incubated with a secondary antibody coupled to alkaline phosphatase were washed twice in SB (staining buffer) and stained in NBT/BCIP (following the WMISH protocol). If the antibody was coupled to a fluorophore, the embryos were mounted in DABCO (1,4-diazabicyclo([2,2,2])octane) /Glycerol (25mg DABCO, Sigma in 1ml PTW and 9ml glycerol).

2.9 BrdU assay

Incubate embryos in 2h pulses in BrdU at 10mM BrdU final concentration in natural seawater. Fix embryos in 4%PFA/1,75xPTW for 2h. Wash 3x in PTW, 2x in MeOH and transfer to MeOH for storage at –20°C.

Detection:

- rehydrate in 75%, 50%, 25% MeOH/PTW as for WMISH
- wash 2x PTW
- digest 1min in 100ug/ml ProteinaseK (for embryos 48-72h)
- wash 2x glycine
- fix 20’ 4%PFA/PTW
- wash 3x PTW
- rinse 1x in ddH_2O / 0,1%Tween20
- incubate 1h in 2N HCl / 0,1% Tween20
- rinse 4xPTW
- Block embryos 15min at RT in 2,5% sheep serum/1%BSA/PTW

- Block α-BrdU antibody 1:100 in same blocking buffer for 15min
- Remove blocking buffer from embryos and add α-BrdU antibody
- Incubate 6x5min shaking at RT
- Wash 6x5min in PTW
- Block antibodies: α-mouse-Alexa (fluo) 1:500 or α-mouse-AP 1:500 in 2,5%sheep serum / 1%BSA / PTW for 1h at RT
- If necessary, add DAPI to the α-mouse antibody
- Incubate in α-mouse antibody over night
- Wash 6x5' PTW (If using fluorescein antibody, keep in dark)
- For AP-coupled antibody: wash 2x in staining buffer and proceed to NBT/BCIP staining. Beware: immediate staining!!
- Fix 20' in 4% PFA/PTW

2.10 Visualising F-actin by phalloidin staining

Protocol modified after (Jacobsohn, 1999)

- Fix embryos 1h in 4xPFA/PBS
- Wash 4x in 1xPBS
- Incubate 1h in 400mM Glycine
- Wash 2x in 1xPBS
- Incubate 1h in 100ul of 25ul/mlAlexa488-Phalloidin
- Wash 2x in PBS
- Mount in 87% Glycerol

2.11 In vivo staining of cellular outlines by BODIPY564/570

Embryos were incubated for 15min in 5uM BODIPY564/570 coupled to propionic acid (Molecular Probes) in natural seawater, then rinsed twice in natural seawater and mounted in a 1:1 mixture of natural seawater and 7,5% $MgCl_2$ to prevent muscular contractions.

2.12 Time-lapse recordings

Embryos were kept during recordings at a constant temperature of 25°C in natural seawater between slide and cover slip separated by two layers of adhesive tape and a

very thin layer of silicone paste. This chamber was sealed with mineral oil (Sigma). 12 frames were taken per hour, the resolution on the z-axis was 2um between two focal planes.

2.13 Morphometric measurements

Lengths and widths measurements have been taken between the centers of two tracked cells. The cellular length/width ratio was taken by dividing the maximal cell length (parallel to the neural midline) and the maximal cell width (perpendicular to the midline). The change in surface area has been measured by averaging the surface area changes between 5 tracked cells along the mediolateral axis and 20 tracked cells along the antero-posterior axis. Elongation index and mediolateral intercalation index measured as in (Shih and Keller, 1992).

2.14 Incubations in Nocodazole, Cytochalasin B and SP600125

Embryos were incubated between 48hpf and 72hpf and immediately fixed upon treatment in 4%PFA/1,75xPBSTween20. All drug stocks dissolved in DMSO. Nocodazole (Sigma) was applied at 0,2ug/ml and 20ug/ml in natural seawater. Nocodazole controls were incubated in 0,20% DMSO/natural seawater. Cytochalasin B (Sigma) was applied at 0,1ug/ml and 2,5ug/ml in natural seawater. Cytochalasin B controls were treated with 0,25% DMSO/natural seawater. SP600125 (A.G. Scientific) was applied at 2,5uM and 25uM in natural seawater. SP600125 controls were treated with 0,25% DMSO/natural seawater.

2.15 General gene cloning strategy

2.15.1 Cloning of novel fragments

Novel gene fragments of *Platynereis dumerilii* were cloned by designing degenerated primers (Buck and Axel, 1991) in conserved regions, based on the amino acid sequence alignment of bilaterian and if possible cnidarian orthologues of the gene of interest. The primers were designed with the help of the Oligo 6.44 software for Mac OS 9. Primers were synthesised by MWG Biotech AG, Invitrogen and Qiagen. These

primers were used in a degenerated PCR using either a phage- or single stranded cDNA library in a 50ul reaction. 5ul of the PCR reaction were analysed on a 1,5% agarose/TAE gel. For some clonings, the DNA was transferred to a nylon membrane and hybridised under low stringent hybridisation conditions with a ^{32}P labelled DNA fragment of an orthologous gene of another species (Southern Blot). The band that gave a positive signal after Southern Blotting, or was located at the expected size in the case in which no Southern Blot was performed, was gel-eluted from a preparative gel with GFX™ Gel Band Purification Kit (Amersham Pharmacia Biotech) and cloned into the pCR II®-TOPO vector using the TopoTA kit (Invitrogen) and amplified in electrocompetent *E.coli* DH10B. After, in some cases, the identification of positive clones by colony lifting and low stringent hybridisation, colonies were picked and mini-prepped using Plasmid Purification Kit (QIAGEN). Alternatively, the presence of positive inserts was in some cases confirmed by insert-PCR directly onto bacterial cultures. The resulting plasmids were independently digested with EcoRI and HinfI to analyse the presence and diversity of inserts. Plasmids that differed in their insert sizes and HinfI digest patterns were sequenced by the Genomics Core Facility at EMBL, Heidelberg.

2.15.2 Rapid amplification of cDNA-ends (RACE) of existing fragments

Specific primers were designed based on the sequence of the cloned fragments using Oligo 6.44 program. In general, two primers on the 5'end, referred to as "upper primers", and two primers on the 3'end, referred to as lower primers were designed in a way that none of them overlaps with the sequence of the degenerated primers used for the initial cloning and that the most inner primers would still be at least 100bp apart. RACE PCRs were preformed using a specific primer for the gene of interest and a specific primer for the library used. Libraries that have been used for RACE are:
48hpf cDNA library in a pCMV-Sport6 plasmid (constructed for a random EST sequencing screen by K. Tessmar-Raible), 24hpf, 48hpf and 72hpf single-stranded cDNA libraries, SMART RACE libraries (constructed with the SMART RACE cDNA amplification kit, Clontech), or a λ-Zap phage library (Stratagene) constructed by C. Heiman and A. Dorresteijn. Specific primers for libraries are:

- For pCMVSport6: pCMVSport6-623; pCMVSport6-804; pCMVSport6-896

- For first strand single-stranded cDNA synthesis: RaceAda
- For SMART RACE libraries: UPM long&short mix, NUP (for nested reactions)
- For λ-Zap phage library: T7(70); T3(70):

In a first PCR reaction, the outer primers were used. From this reaction, 1ul was used in a "nested" PCR reaction to re-amplify extended fragments. This increases the chances of amplifying the desired cDNA fragment. All the products were separated by gel electrophoresis (1-1,5% agarose/TAE gels), then transferred according to the Southern blot technique and hybridised with highly stringent conditions, using the existing fragment of the gene as a template to synthesise a ^{32}P-labeled probe. Positive bands were then cut out from a preparative gel, eluted with GFX™ Gel Band Purification Kit (Amersham Pharmacia Biotech) and subcloned using the TopoTA Cloning Kit (Invitrogen). Following steps remain the same as for the cloning of novel gene fragments.

2.16 Synthesis of ^{32}P-labeled probes

Probe templates were either existing *Platynereis* gene fragments or fragments from orthologues of different species. The fragment was digested out of the plasmid and gel eluted with GFX™ PCR DNA and Gel Band Purification Kit (Amersham Bioscience). Then it was labelled with Megaprime DNA Labelling Kit (Amersham Bioscience, #RPN 1604) and P^{32}dCTP radioactive nucleotide.

2.17 Southern Blots and colony-lifts from bacterial plates

2.17.1 High stringency Southern Blots and colony-lifts

After transfer of the DNA to nylon filters as described in a protocol of (Sambrook et al., 1989), the filters were shortly rinsed with 1xSSC and prehybridised for 15 min at 65°C in RapidHyb Buffer (Amersham Bioscience, #RPN 1636). Then 25ul of the synthesised probe was added after denaturing for 5min at 95°C. After hybridising for 1,5h at 65°C, the blot was rinsed twice with 2xSSC containing 0.1%SDS, followed by a 30min wash in 0.1xSSC containing 0.1% SDS at 65°C. The blot was then exposed with an intensifier screen at -80°C until a clear signal was detected.

2.17.2 Low stringency Southern Blots with heterologous probes

After transfer of the DNA to nylon filters as described in a protocol of (Sambrook et al., 1989), the filters were prehybridised for 1-2h in 35% formamide hybridisation mix. Then 25ul of the synthesised probe was added after denaturing for 5min at 95°C. After hybridising over night at 42°C, the blot was rinsed twice shortly, followed by two 30min washes in 5xSSC/0,1%SDS at 42°C. The blot was then exposed with an intensifier screen at -80°C until a clear signal was detected.

2.18 Polymerase chain reactions

2.18.1 Reaction mixtures for cloning of novel fragments for *twist*, *strabismus* and *dachsous*

From first strand cDNA:
1-1,5 µl of ss cDNA; 2,5 µl of dNTPs (5mM); 1,5 µl of degenerated forward primer (100mM); 1,5 µl of degenerated reverse primer (100mM);5 µl of PCR Buffer (10x, Qiagen); 0,2-0,3 µl of Taq DNA polymerase (Qiagen); add deionised water to 50ul

From λ-Zap phage library:
4 µl of cDNA library; 2,5 µl of dNTPs (5mM); 1,5 µl of degenerated forward primer (100mM); 1,5 µl of degenerated reverse primer (100mM);5 µl of PCR Buffer (10x, Qiagen); 0,3 µl of Taq DNA polymerase (Qiagen); 35,2 µl of deionised water

For nested reactions, 1ul of the first reaction was added instead of cDNA library and the volume of water adjusted accordingly.

2.18.2 Reaction mixtures for RACE of *twist, strabismus, myoD, mef2*

From first strand cDNA:

2 µl of single-stranded cDNA; 2,5 µl of dNTPs (5mM); 1 µl of specific forward primer (100mM); 1µl of Race Ada primer (100mM); 5 µl of PCR Buffer (10x, Qiagen)
0,2 µl of Taq DNA polymerase (Qiagen); 38,2ul deionised water.
From SMART RACE library:
3 µl of Smart Race cDNA library; 2,5 µl of dNTPs (5mM); 2,5 µl of specific primer (5mM); 5 µl of UPM primer mix (see kit); 5 µl of PCR Buffer (10x,Qiagen); 0,3 µl of Taq DNA polymerase (Qiagen); 31,7 µl of deionised water

From λ-Zap phage library:
4 µl of λ-Zap library; 2,5 µl of dNTPs (5mM); 1,5 µl of specific primer (100mM); 1,5 µl of T3/T7 primer (100mM); 5 µl of PCR Buffer (10x, Qiagen); 0,3 ul of Taq DNA polymerase (Qiagen); 37,2 µl of deionised water

For nested reactions, 1ul of the first reaction was added instead of cDNA RACE library and the volume of water adjusted accordingly. For the SMART RACE, the UPM mix is replaced by 1ul of NUP primer and the volume of deionised water adjusted accordingly.

Cloning of a medaka *strabismus* fragment used as hybridisation probe in Southern Blots:
3 µl of cDNA library; 2,5 µl of dNTPs (5mM); 1,5 µl of primer Ol-stbm-U1 (100mM); 1,5 µl of primer Ol-stbm-L1 (100mM); 5 µl of PCR Buffer (10x, Qiagen); 0,2 ul of Taq DNA polymerase (Qiagen); 36,3 µl of deionised water

Insert PCRs:
As template, pick colony and inoculate PCR mix with bacteria before inoculating liquid culture medium; 0,5 µl of dNTPs (5mM); 0,5 µl of forward primer (100mM); 0,5 µl of reverse primer (100mM); 3 µl of PCR Buffer (10x, Qiagen); 0,5 ul of "home-made" Taq DNA polymerase (Protein purification facility, EMBL); 24,85 µl of deionised water

2.18.3 Cycle programs

Novel gene clonings:
95°C hot start. 1min 95°C; 2min 42°C-45°C (depending on primer annealing temperatures); 4min 72°C; repeat 5x. 1min 95°C; 2min 47°C-50°C; 4min 72°C; repeat 35x. 10min 72°C; end with 10°C.

RACE clonings:
For most reactions, the plasmid- or library-specific primers have been added only after the first 5 cycles.

95°C hot start. 1min 95°C; 2min 60°C (depending on primer annealing temperatures); 4min 72°C; repeat 5x. add primers. 1min 95°C; 2min 60°C; 4min 72°C; repeat 35x. 10min 72°C; end with 10°C.

Cloning of a medaka *strabismus* fragment used as hybridisation probe in Southern Blots:
95°C hot start. 20sec 95°C; 20sec 62°C (depending on primer annealing temperatures); 1min 72°C; repeat 25x. 10min 72°C; end with 10°C

Insert PCRs:
95°C hot start. 30sec 95°C; 30sec 55°C (depending on primer annealing temperatures); 72°C according to expected length (1min/1kb); repeat 25x. 10min 72°C; end with 10°C

2.19 Primer sequences

MyoD:

MyodSpecU1: `AGGAGACGCCTCAAGAAAGTGAACG`
MyoDSpecU2: `AGTGCTCAAGAGAAGAACCTGCTCC`
MyoDSpecU3: `CCCCAACCAAAGACTCCCCAAAGTG`

Mef2:

Mef2specU1: `TTCTGTGTGATTGCGAGATAGCCTTG`

Mef2specU2: GATCATCTTCAACTCTGCCAACAAGC

Mef2specU3: GCTATTCCAGTATGCCAGCACAGACA

Twist:

TwiSpecU1: TCGTGAACGGCAAAGGACGCAATCG

TwiSpecU2: GAAAGATCATCCCCACCCTCCCATC

TwiSpecL1: GTAACTGCAGGACGGGGGAATGAGC

TwiSpecL2: TGCCACTAAAGAAGCGTCGTCGGTC

Oryzias latipes (medaka) strabismus:

Ol-stbm-U1: TAAGGTGGTCCGGAGCGCAGATG

Ol-stbm-L1: GGGCGTCATGTTGTGCGTGATG

Platynereis strabismus

Stbm-degU1: ATHCARMGNGCNGCIGTITGGRT

Stbm-degU2: MMNGAYTTYCCNRTITAYAAYCC

Stbm-degL1: NGSRAADATNGCYTGIGCIGCYTC

Stbm-degL2: YTTDATRTGNGTRAAIGCYTCYTC

Pd-stbm-U1: TGCCGTGAACAATCTCGCCTTCC

Pd-stbm-U2: CGACTGGTCACGCCGCCTAGC

Pd-stbm-L1: ACTCTCGGGATTTAAAGTTTACGACA

Pd-stbm-L2: GATGGAGTGCAAGGATCTCAAACG

Pd-stbm-RACEII-L1: CCTTCACACTCAGGTCCACAGGG

Pd-stbm-RACEII-L2: TCCTGCTCCCATTCCTCTAAG

Dachsous:

Dsdeg-U1: NGARGAYGANGARATHMGIATGA

Dsdeg-U2: GAYGAYGARATHMGNATGATHAAYGA

Dsdeg-L1: NGCNARNGGYTGRWAYTGIGG

Dsdeg-L2: ARRTARTCCCARTTRTAISWICC

RACE primers:

T7(70): GTGAATTGTAATACGACTCACTATAG

T3(70): AGCTCGAAATTAACCCTCACTAAAG

RaceAda: ACTCGAGTCGACATCG

UPM long: CTAATACGACTCACTATAGGGCAAGCAGTGGTAACA

UPM short: CTAATACGACTCACTATAGGGC

NUP: AAGCAGTGGTATCAACGCAGAGT

PCMVSport6-623: CACAAAGATCCCAAGCTAGCAGTTTTCCCAGTC

PCMVSport6-804: CCGGTCCGGAATTCCCGGGA

PCMVSport6-896: GCGGAGCGGATAACAATTTCACACAG

PCMVSport6-662lowTm: TTGTAAAACGACGGCCAGTGC

2.20 Sequence analysis

Sequencing reactions were performed with SP6, T7; M13forward, M13reverse or insert-specific primers and processed on an automated sequencer at Genomics Core Facility (EMBL, Heidelberg). The orthology of the sequences were tested with BLASTX and BLASTN (http://www.ncbi.nlm.nih.gov/BLAST/) to check for closest likely orthologues and to rule out that the gene was cloned by mistake from other organism than *Platynereis* dumerilii. DNA sequences were aligned by using SeqMan II and checked by eye for ambiguities. Protein sequences of a selected number of species were obtained from the NCBI database and aligned using CLUSTALX (Thompson et al., 1997). These alignments were used to calculate a 1000fold bootstrapped phylogenetic tree using the neighbour-joining method, and all positions with gaps in the alignment were excluded, and corrected for multiple substitutions, with the program CLUSTALX (Thompson et al., 1997). Parts of the alignments were transferred to MegAlign, where protein identities were graphically highlighted.

2.21 Accession numbers of sequences in multiple sequence alignments

Gbx alignment:

Dme-unpg, U35427; *Mmu-gbx2*, U74300; *Dre-gbx2*, AF288762; *Dre-gbx1*, AF288763; *Mmu-gbx1*, AY319256

Hox1 alignment:

Cva-hox1, AF163856; *Tca-hox1*, AF231104; *Csa-hox1*, AJ007431; *Bfl-hox1*, AB028206; *Mmu-hoxb1*, NM 008266; *Gga-hoxb1*, P31259; *Hsa-hoxa1*, NM 005522, *Mmu-hoxa1*, NM 010449.

Twist alignment:

Pv-twist: AAL15167; *Mm-twist*: BAB27885; *Bb-twist*: AAD10038; *Dr-twist*: NP_001005956; *Ec-twist*: CAD47857; *Am-twist*: CAH60991; *Hr-twist*: AAL05567; *Io-twist*: AAG25636; *Tt-twist*: AAN03868; *Ha-twist*: AAN03867; *Dm-twist*: CAA31024; *Am-twist*: CAH60991; *Tc-twist*: CAH25640; *At-twist*: BAD51393; *Pc-twist*: CAC12667; *Nv-twist*: AAR24458; *Mm-dHand*: 2203455B; *Mm-NeuroD*: NP_035024; *Mm-MyoD1*: NP_034996.

MyoD alignment:

Mm-myf5: AAG42686; *Mm-myogenin*: NP_112466; *Dr-myf5*: AAG42686; *Lv-SUM1*: Q00492; *Bf-mrf1*: AAN87801; *Dm-nau*: CAA39629.

Mef2 alignment:

Bm-mef2: BAE06225; *Dm-mef2*: AAA20463; *Hr-mef2*: BAA08722; *Mm-Mef2c*: AAH57650; *Mm-Mef2a*: AAH96598; *Dr-mef2c*: AAH70007; *Dr-mef2a*: ABC55064; *Dr-mef2d*: NP_571392; *Nv-mef2*: AAR24454; *Pc-mef2*: CAD21522; *At-mef2*: BAD01493; *At-AGL15*: NP_196883; *At-RlmA*: EAL92725; *Dm-blistered*: Q24535; *Mm-SRF*: NP_065239.

strabismus alignment:

Dme-stbm: AF044208; *Dre-stbm*: AF428249; *Hsa-stbm*: NP_065068; *Xla-stbm*: AY069979.

Dachsous alignment:

Am-dachsous: XP_392300; *Dm-dachsous*: NP_523446; *Hs-dachsous*: NP_003728; *Dr-dachsous*: XP_682805.

2.22 Additional molecular biology techniques

Standard techniques as DNA restriction digests, DNA ligations, bacterial mini preparations (‘mini preps’), electro-transformation of *E. coli*, gel electrophoresis (agarose gel: 1-2% in TAE buffer) were done after (Sambrook et al., 1989). Gels were stained with for 15min in ethidiumbromide in TAE (1:10000 dilution) and used for gel extraction, southern blots, and/or photographic documentation. DNA was gel eluted from agarose gel by cutting the desired band with a razor blade under long-wave UV

light (λ=366nm) and using the GFX™ Gel Band Purification Kit (Amersham Pharmacia Bioscience) according to the manufacturer's instructions. DNA solutions were cleared form enzymes, primers or buffers with GFX™ Gel Band Purification Kit (Amersham Pharmacia Bioscience) according to the manufacturer's instructions; bacterial maxi preparations were done using Maxi prep Kit (Qiagen) according to the manufacturer's protocol.

3 Results

3.1 The regionalisation of the trochophore prostomium

3.1.1 The development of the prostomial CNS

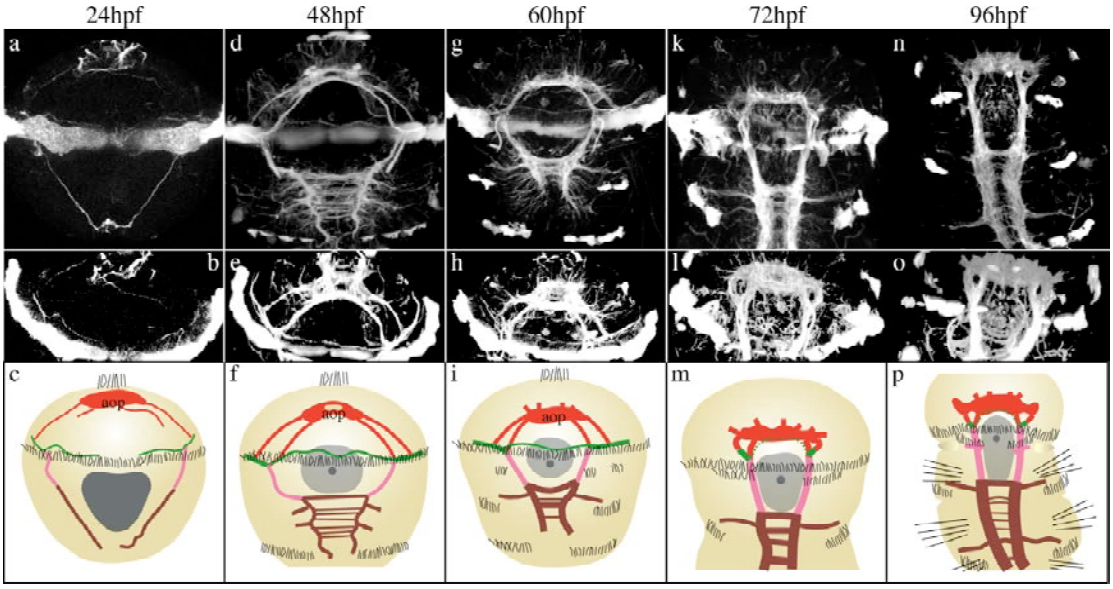

Fig. 6 Reconstructions of confocal sections (**a**, **d**, **g**, **k**, **n**), artificial rotations towards the apical pole of the reconstructions (**b**, **e**, **h**, **l**, **o**) and schematics (**c**, **f**, **i**, **m**, **p**) of the *Platynereis dumerilii* axonal scaffold by acetylated α-tubulin immunostainings at different developmental stages.
Red: prostomial neuropil. Green: Peristomial neuropil. Pink: Circumoesophageal connectives belonging to either peri- or metastomial neuropil. Brown: metastomial neuropil. Grey: stomodaeum. aop: apical organ plexus.

The developing central nervous system of the prostomium has been characterised by acetylated α-tubulin immunohistochemistry (**Fig. 6**a-p, red). The most conspicuous structure stained in the 24hpf trochophore larva is the apical organ, where axons form an apical neuropil and plexus from 24hpf onwards (**Fig. 6**a-c, "aop"). The number of axons that form the apical organ plexus increases consistently during development. At 48hpf and 60hpf, four connectives link the apical organ plexus (**Fig. 6**d-i, red) to the prototroch nerve ring of the peristomium (**Fig. 6**d-i, green) (Arendt et al., 2002) and transform into the four polychaete-characteristic roots entering the juvenile cerebral ganglion (**Fig. 6**k-p, red) (Orrhage, 1995). The major part of the juvenile cerebral ganglion is developing from the apical organ region.

3.1.2 Pdu-six3 regionalises the prostomial ectoderm

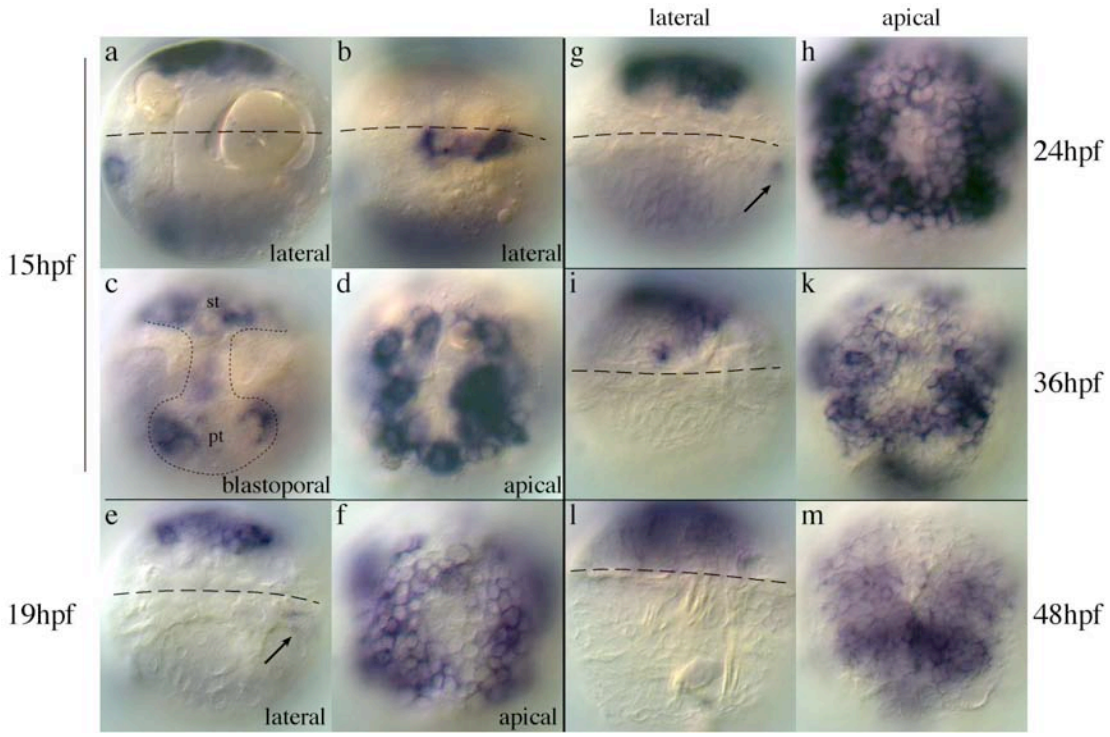

Fig. 7 Expression of *Pdu-six3* with emphasis on the prostomium at different developmental stages of *Platynereis dumerilii*.
Arrow: expression in dorsal patches of cells. Stippled line: blastopore rim. Dashed line: prototroch. pt: proctodaeal region; st: stomodaeal region. Orientation of embryos (applies to all following figures if not further specified) Lateral views: ventral oriented to the left; anterior to top. Apical views: ventral oriented to the bottom. Ventral views: anterior to the top.

Pdu-six3 was cloned by D. Arendt in the laboratory of J. Wittbrodt, and I have analysed the expression of *Pdu-six3* as a regionalisation marker from 15hpf onwards. While in all later stages, *Pdu-six3* ectodermal expression is almost entirely restricted to prostomial cells, its expression is broader at 15hpf. In addition to the strong expression in most cells of the prostomium (**Fig. 7**a,d) omitting the most apical cells, it is also expressed in a few cells on the lateral side possibly corresponding to prototroch cells (**Fig. 7**b) and in most non-ectodermal cells located within the blastopore (**Fig. 7**c, also compare to **Fig. 26**a,g). The only blastoporal cells that keep expressing *Pdu-six3* beyond 15hpf are the stomodaeal precursor cells (stomatoblasts) that will be analysed in the following paragraph 3.1.3.

At 19hpf and 24hpf, *Pdu-six3* shows strong expression in the prostomium omitting only a few cells in the apical organ region (**Fig. 7**e-h) and is still weakly expressed in a few dorsal cells just posterior of the prototroch (**Fig. 7**e,g, arrows). *Pdu-six3* expres-

sion in the prostomium gets patchier at 36hpf (**Fig. 7**i-k), while at 48hpf it covers the prostomium omitting a wedge-shaped dorsal area (**Fig. 7**l-m).

3.1.3 *Pdu-six3* as a marker for the mesodermal part of the prostomium?

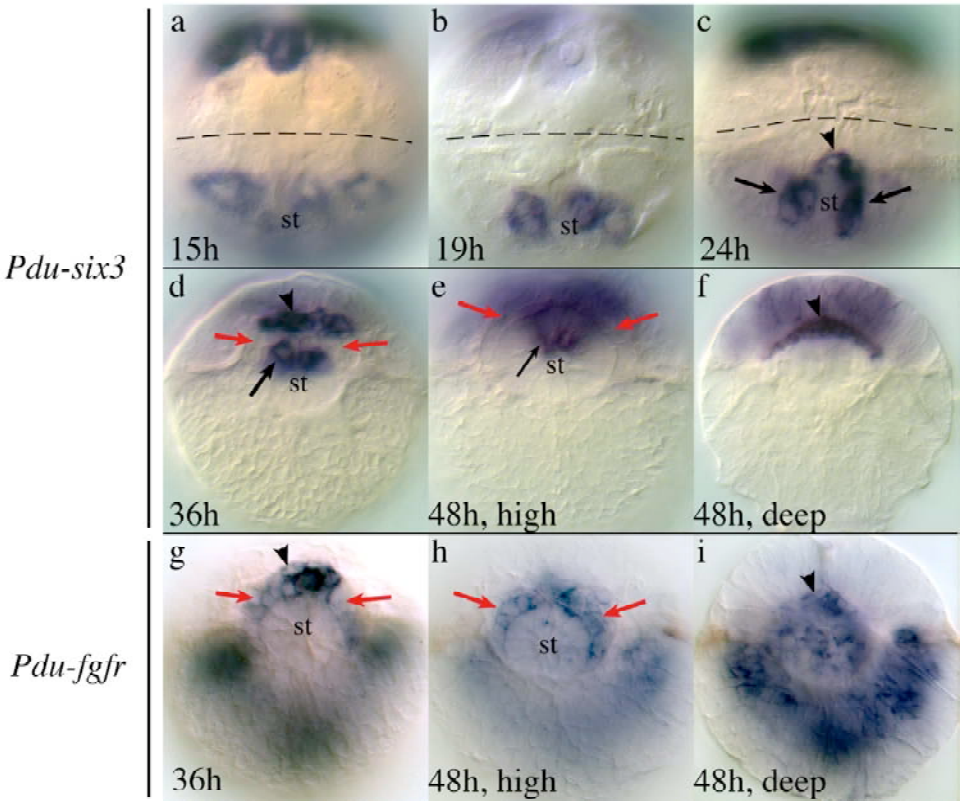

Fig. 8 Expression of *Pdu-six3* (**a-f**) and the mesodermal marker *Pdu-fgfr* (**g-i**) with emphasis on the stomodaeum and prospective head mesoderm at different developmental stages.
Black arrows: stomodaeal cells. Red arrows: mesodermal envelope surrounding the stomodaeum. Arrowheads: prospective "brain mesoderm" between the stomodaeal envelope and the brain neuropil. st: stomodaeum. Dashed line: prototroch.

In polychaetes, there is very few morphological and almost no molecular data describing the development of the head mesoderm (Anderson, 1973). The analysis of *Pdu-six3* expression revealed some interesting features that could relate its expression to the development of the most rostral head mesoderm in *Platynereis*. The expression of *Pdu-six3* in blastoporal cells at 15hpf (**Fig. 7**c) gets restricted to cells in the prospective stomodaeal area at 19hpf and 24hpf (**Fig. 8**a-c). From 24hpf to 48hpf, *Pdu-six3* is expressed in very anterior cells of the developing stomodaeum (**Fig. 8**c-e, black arrows). After 24hpf, the most anterior *Pdu-six3* expressing cells in the stomodaeal area appear to undergo peculiar movements, assuming that *Pdu-six3* keeps being expressed in the same cells. They appear to bulge out anterior of the stomodaeal

region (**Fig. 8**c, arrowhead) and get localised at 36hpf just below the developing brain (**Fig. 8**d, arrowhead). The localisation of the *Pdu-six3* expression in relation to the mesoderm can be visualised using *Pdu-fgfr* as a mesodermal marker in *Platynereis* (Steinmetz, 2002). Comparison at 36hpf shows that a subpopulation of the *Pdu-six3* expressing cells is probably co-expressing *Pdu-fgfr* (compare **Fig. 8**d with g, black arrowhead) and *Pdu-twist* (compare **Fig. 8**d with **Fig. 12**b and e, black arrowheads) leaving the mesodermal envelope surrounding the stomodaeum free of *Pdu-six3* expression (**Fig. 8**d and g, red arrows) (also see section 3.2.4 about mesoderm formation in the peristomium). At 48hpf, the *Pdu-six3*-expressing cells localise very close to the neuropil of the apical organ plexus of which some could still co-express *Pdu-fgfr* (compare **Fig. 8**f with i, black arrowhead), while the mesodermal cells surrounding the stomodaeum stay free of *Pdu-six3* expression (compare **Fig. 8**e with h, red arrow; the picture might wrongly infer staining because of the strong prostomial staining out of the focus). The probable co-expression of the mesodermal markers *Pdu-fgfr* and *Pdu-twist* in some of the *Pdu-six3* expressing cells suggests that these cells give rise to mesodermal structures.

3.2 The regionalisation of the trochophore peristomium

3.2.1 The development of the peristomial CNS

The *Platynereis* peristomium harbours the prototroch ciliary girdle and mouth field. The prototroch nerve ring lies in the peristomium, is still incomplete at 24hpf (**Fig. 6**a-c, green) and forms a complete ring at 48hpf and 60hpf (**Fig. 6**d-i, green). Beyond 60hpf, its major part cannot be followed by anti-acetylated α-tubulin immunostaining. It gets either integrated into the cerebral ganglion or disintegrates (**Fig. 6**k-p, green stippled line). Notably, the part of the nerve ring in-between the two connectives running on each side into the prostomium gets integrated into the juvenile dorsal root of the cerebral ganglion (**Fig. 6**k-p, green line).

3.2.2 *Pdu-otx* regionalises the peristomial ectoderm

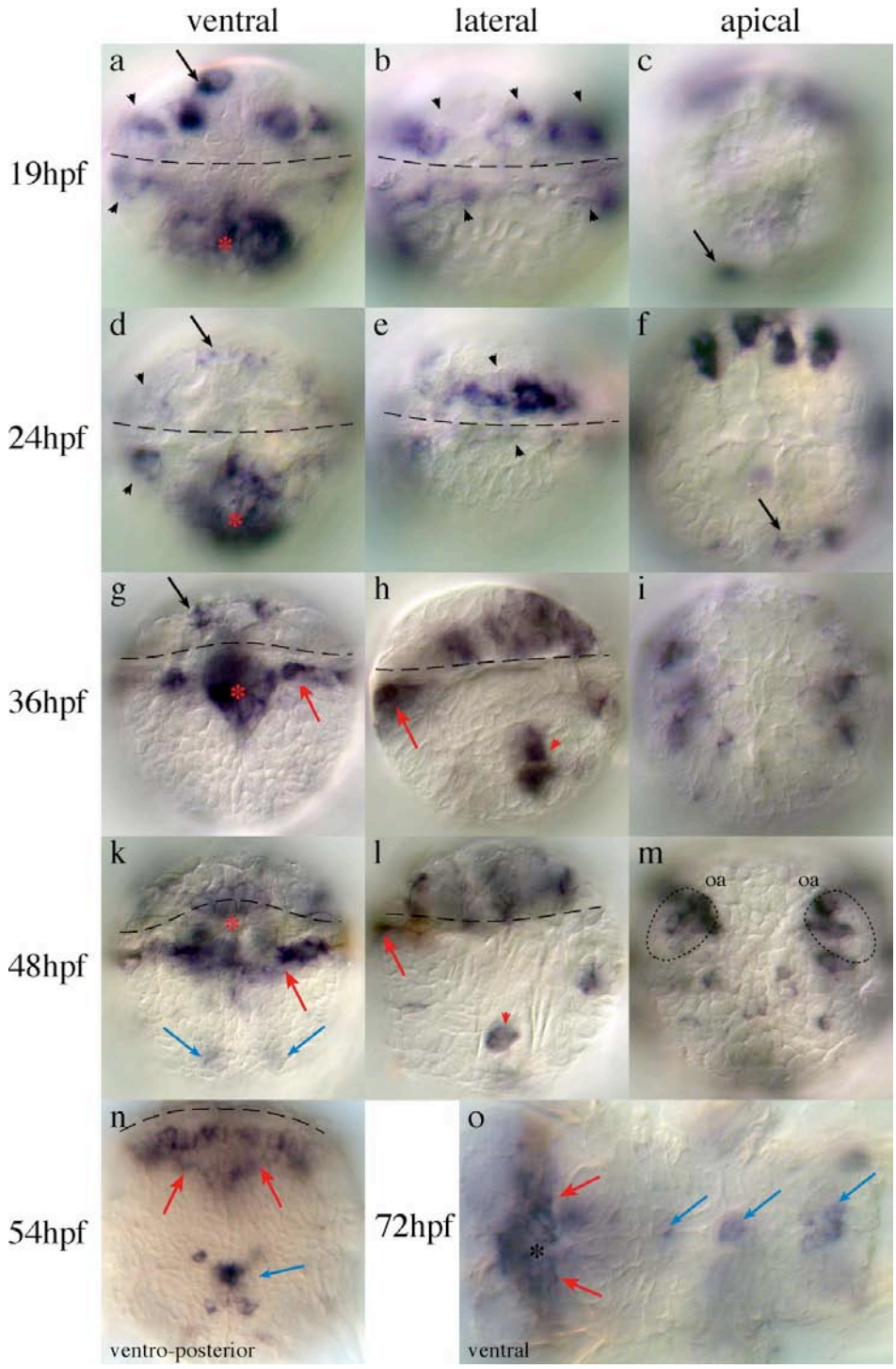

Fig. 9 Expression of *Pdu-otx* at different developmental stages of *Platynereis dumerilii*.
Black arrows: Ring of *otx*-expressing cells bend towards the apical organ. Blue arrows: Neural plate expression. Black arrowheads: Expression in primary or accessory trochoblasts. Red arrowheads: Expression in spinning glands. Red asterisk: Stomodaeal expression. Dashed line: prototroch. Stippled line, "oa": optical anlagen. Orientation in **o**: anterior to the left.

Pdu-otx expression has been shown in the primary and accessory prototroch cells in the peristomium (Arendt et al., 2001). I have analysed *Pdu-otx* in more detail and with

the aim to compare it with other marker genes of the prostomium (*Pdu-six3*) and trunk (*Pdu-engrailed*, *Pdu-gbx*). At 19hpf and 24hpf, *Pdu-otx* expression forms two rings anterior and posterior of the differentiated primary prototroch cells delimiting the peristomium (**Fig. 9** a,b,d,e, arrowheads). The anterior ring in the region of the prospective gland cells above the stomodaeum bends towards the apical organ region (**Fig. 9**a,d,g, arrow). The prostomium is almost free of expression at 19hpf and 24hpf (**Fig. 9**c,f) but shows *Pdu-otx* expression mainly in the optical anlagen at 36hpf and 48hpf (**Fig. 9**i,m, "oa") (Arendt et al., 2002). The majority of the stomodaeal cells also strongly express *Pdu-otx* throughout larval development (**Fig. 9**a,d,g,k, red asterisk). From 36hpf until 72hpf, *Pdu-otx* is expressed in cells surrounding and lateral of the mouth opening that are located at the anterior border of the neural plate (**Fig. 9**g,h,k,l,n,o, red arrows). At 36hpf, the spinning glands start to express *Pdu*-otx (**Fig. 9**h,l, red arrowheads) followed at 48hpf by a few cells in the neural plate (**Fig. 9**k,n,o, blue arrowhead).

3.2.3 Delimitating the boundaries of the peristomium by double fluorescent *in situ* hybridisation

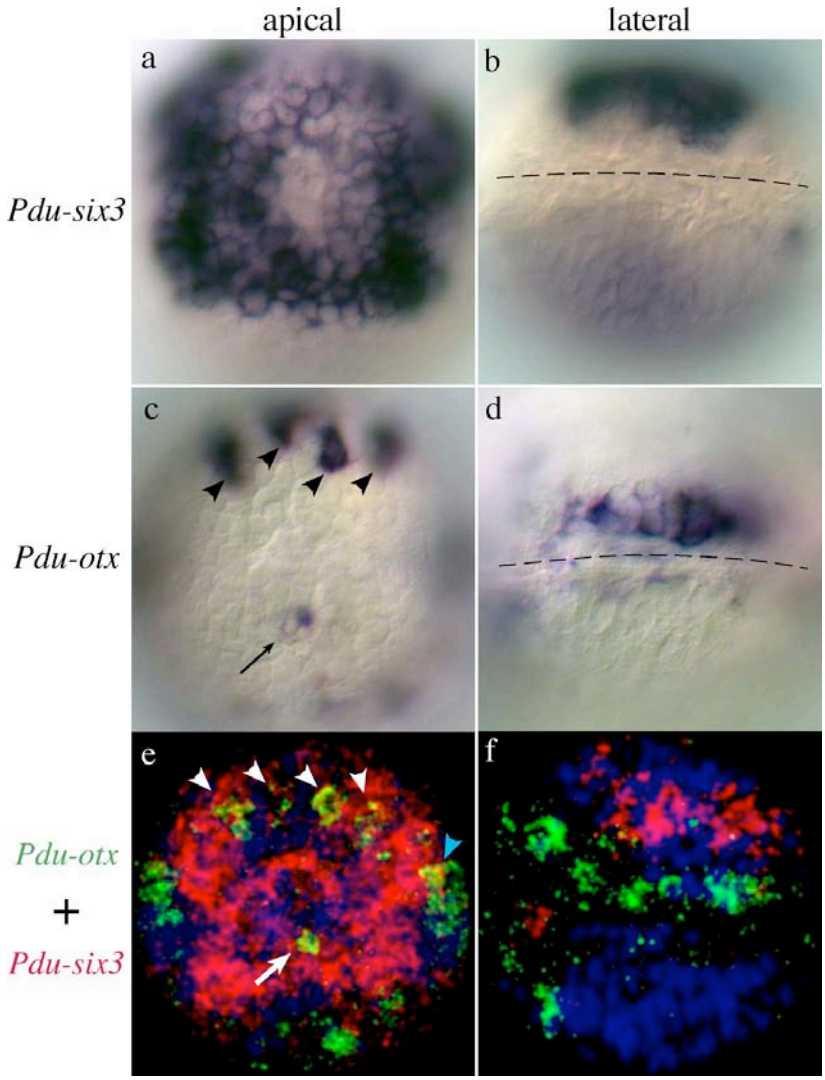

Fig. 10 Single (**a**-**d**) and double (**e**, **f**) detection of *Pdu-six3* (**a**, **b**, **e-f**) and *Pdu-otx* (**c**, **d**, **e-f**) at 24hpf.
e and **f**: reconstructions of confocal sections. Arrow: Co-expressing cells ventral of the apical organ region. White arrowheads: Four co-expressing cells in the dorsal episphere. Blue arrowhead: yellow colour (implying co-expression) is an artefact of the reconstruction of the confocal sections. Dashed line: prototroch.

The expression patterns of *Pdu-six3* covering most part of the prostomium and *Pdu-otx* in the peristomium suggest that the expression of both genes is mutually exclusive at 24hpf. Double fluorescent *in situ* hybridisation simultaneously detecting *Pdu-otx* and *Pdu-six3* shows that almost no co-expressing cells exist in the prostomium (**Fig. 10**). Exceptions are 2-3 co-expressing cells ventral of the apical organ region (**Fig. 10**a,c,e, arrow) that is free of *Pdu-otx* and *Pdu-six3* expression, and 4 co-expressing cells at the dorsal border of the prostomium (**Fig. 10**c,e, arrowheads). The lateral view

shows that the ring-like *Pdu-otx* expressing region surrounds the *Pdu-six3* cap posteriorly without any overlap on the lateral side (**Fig. 10**b,d,f).

The posterior boundary of the peristomium is morphologically defined by the position of the metatroch ciliary band (Rouse, 1999; Schroeder and Hermans, 1975). I tested whether *Pdu-otx*, proposed as a peristomial regionalisation marker (Arendt et al., 2001), fulfils this assumption and correlated its expression at 48hpf, to the localisation of the appearing metatroch (**Fig. 11**).

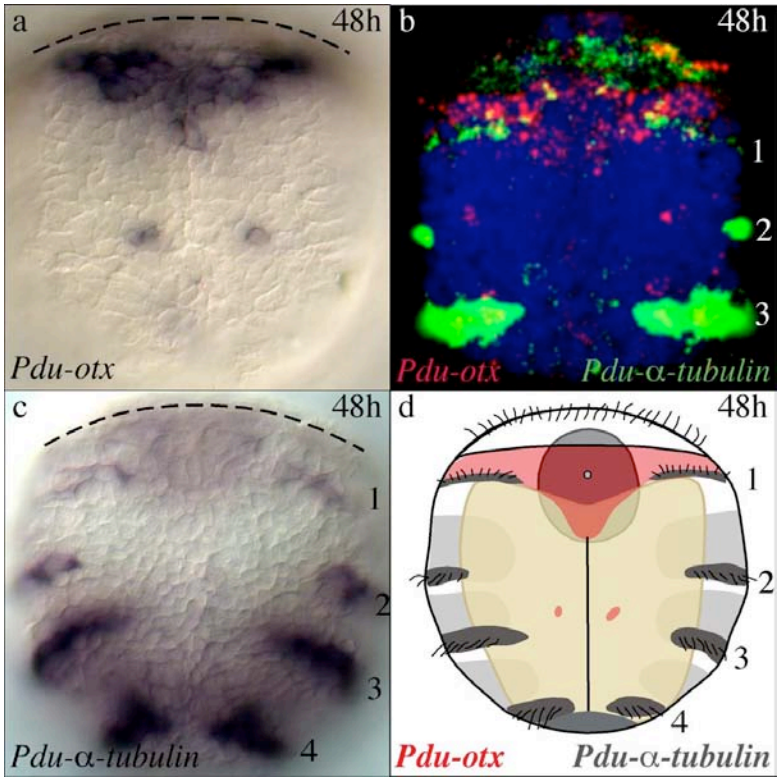

Fig. 11 Single detection (**a**, **c**), double detection (**b**) and schematics (**d**) of *Pdu-otx* (**a**, **b**) and *Pdu-α-tubulin* (**b**, **c**) expression at 48hpf.
1: metatroch; 2: paratroch I; 3: paratroch II; 4: telotroch. **b**: reconstruction of confocal sections. Dashed line: prototroch. All posterior-ventral views.

Double detection of *Pdu-otx* and *Pdu-α-tubulin*, a marker for ciliated bands, shows that the triangular-shaped *Pdu-otx* region around the mouth opening (**Fig. 11** a) is posteriorly abutted by the metatroch, the 1st ciliary band below the prototroch (**Fig. 11**b,c,d, at the level of "1"). This shows that *Pdu-otx* expression covers specifically the peristomium and assuming that *Pdu-otx* also marks the peristomial precursor cells, it can be used to delimitate the extent of the peristomium before the appearance of a detectable metatroch.

3.2.4 Mesodermal marker genes for the peristomium

Cell lineage tracings in *Platynereis* have shown that the pharyngeal muscles around the stomodaeum originate from "ectomesodermal" precursor cells located anterior of the trunk mesoderm precursor cell 4d (Ackermann et al., 2005). Despite their conspicuous origin, the affiliation of the pharyngeal mesoderm to the peristomium is still very speculative and its evolutionary origin from a putative peristomial coelomic pouch will be discussed later.

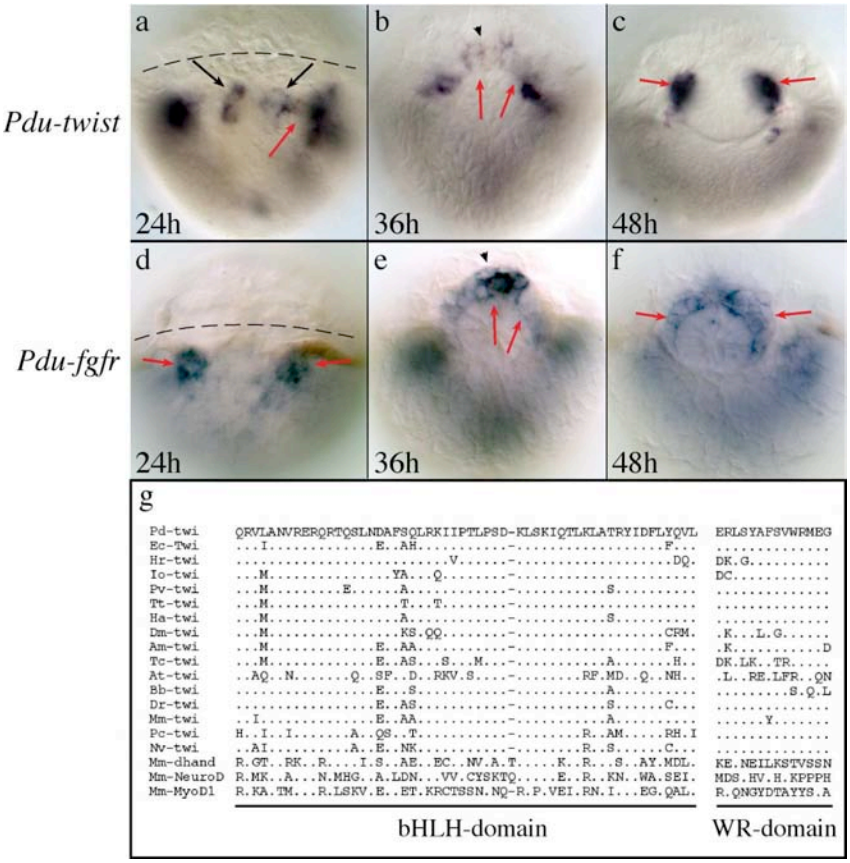

Fig. 12 Expression (**a-f**) and multiple sequence alignment of characteristic protein domains (**g**) of *Pdu-twist* (**a-c**, **g**) and the mesodermal marker *Pdu-fgfr* (**d**-**f**).
Black arrows: Medial stomodaeal expression domain. Red arrows: mesodermal envelope around stomodaeum. Black arrowheads: Putative "head mesoderm" expression domain. Dashed line: prototroch. All ventral views. In **g**: Dots represent amino acid identity; dashes represent gaps in the alignment. Species abbreviations: At: *Achaearanea tepidariorum*; Am: *Apis mellifera*; Bb: *Branchiostoma belcheri*; Dm: *Drosophila melanogaster*; Dr: *Danio rerio*; Ec: *Enchytraeus coronatus*; Ha: *Helix aspersa*; Hr: *Helobdella robusta*; Io: *Ilyanassa obsoleta*; Mm: *Mus musculus*; Nv: *Nematostella vectensis*; Pc: *Podocoryne carnea*; Pd: *Platynereis dumerilii*; Pv: *Patella vulgata*; Tc: *Tribolium castaneum*; Tt: *Transennella tantilla*. Accession numbers can be found in the materials and methods section.

I have identified *Pdu-fgfr* (Steinmetz, 2002) and *Pdu-twist* as mesodermal marker genes that can be used to characterise the stomodaeal mesoderm and study its development (**Fig. 12**). Multiple protein sequence alignments show that the *twist* basic he-

lix-loop-helix (bHLH) domain (Castanon and Baylies, 2002) shows very high protein identity with the bHLH domain of oligochaete, mollusc and chordate *twist* proteins, while it presents much less homology with other bHLH-domain proteins (**Fig. 12**g). A second domain characteristic to *twist* proteins, the WR-domain (Castanon and Baylies, 2002), is identical in *Platynereis*, *Enchytraeus*, some molluscs, zebrafish and two cnidarians (*Podocoryne* and *Nematostella*), but not recognisable in members of other bHLH-domain proteins (**Fig. 12**g).

The *Pdu-fgfr* has already been cloned and described as a mesodermal marker in *Platynereis* that also marks the mesodermal envelope surrounding the stomodaeum (**Fig. 12**d-f, red arrows, (Steinmetz, 2002)). The mesodermal envelope around the stomodaeum is located posterior of the putative *six3*-expressing "brain mesoderm" that probably also expresses *Pdu-twist* and *Pdu-fgfr* temporarily.

At 24hpf, a cell cluster in the antero-lateral corner of the stomodaeal region shows high expression of *Pdu-fgfr* (**Fig. 12**a, red arrows). I suspect these cells to be the precursors of the mesodermal sheath surrounding the stomodaeum as suggested by their position at the left and right border of the stomodaeal region and as the stomodaeum itself does not express *Pdu-fgfr* at later stages. Although *Pdu-twist* and *Pdu-fgfr* are expressed in cells of the stomodaeal mesoderm at later stages (compare **Fig. 12** b,c with e,f, red arrows), their expression differs at 24hpf. At this stage, *Pdu-twist* (**Fig. 12**a, black arrows) is expressed more medially than *Pdu-fgfr*, but at least one of the *Pdu-twist* expressing cells could also express *Pdu-fgfr* (compare **Fig. 12**a with d, red arrows). Other marker genes for the stomodaeal mesoderm support their identity as visceral and/or heart precursor cells: they also express *Pdu-tinman* and *Pdu-bagpipe*, two NK2-class homeobox genes expressed in the visceral and/or heart mesoderm in *Drosophila* (Azpiazu and Frasch, 1993; Bodmer, 1993)(not shown and G. Balavoine, personal communication).

3.3 The regionalisation of the trochophore trunk ectoderm

3.3.1 The development of the trunk CNS

The larval trunk CNS in the metastomium (Gilpin-Brown, 1958; Hempelmann, 1911) connects to the prototroch nerve ring in the peristomium (**Fig. 6**, green) by two ventral axon tracts running left and right of the developing stomodaeum (**Fig. 6**, pink & brown). Their anterior components form the circumoesophageal connectives (**Fig. 6**, pink) left and right of the mouth opening and run into the peristomium. A morphological boundary between the peri- and metastomial parts of the connectives cannot be discerned. Anteriorly, they are in direct connection with the ventral connectives running into the apical organ plexus (later the ventral roots of the cerebral ganglia). The first commissure below the stomodaeum (substomodaeal commissure) belongs to the first chaetiferous (chaetae-bearing) segment and is localised at the border between the circumoesophageal connectives (**Fig. 6** pink) and the metamerically segmented trunk CNS (**Fig. 6** brown). Laterally, a metamerically iterated pattern of axons innervating the parapodia is formed beyond 72hpf (**Fig. 6**k-p). In contrast, the commissures connecting the longitudinal axon tracts from 48hpf onwards are not segmentally iterated and remain thin in the analysed stages (**Fig. 6**k-p).

Pdu-engrailed patterns the larval metameric segments

It has been shown that *Pdu-engrailed* is expressed in metameric stripes at larval stages in *Platynereis* and marks the anterior segment boundaries in regenerating *Platynereis* terminal ends (Prud'homme et al., 2003). I have analysed *Pdu-engrailed* expression in detail during larval stages to solve several issues: a) determine the boundary between the peristomium and the first larval trunk segment; b) determine the position of segment boundaries before the morphological appearance of segmental properties (ciliated bands, parapodia); c) correlate regionalisation genes with the position of the developing trunk segments.

In order to correlate larval *Pdu-engrailed* expression and developing segment boundaries, I simultaneously detected *Pdu-engrailed* and *Pdu-α-tubulin*, a marker for ciliated bands localised at the posterior segment boundaries, by double fluorescent *in situ* hybridisation (**Fig. 13**).

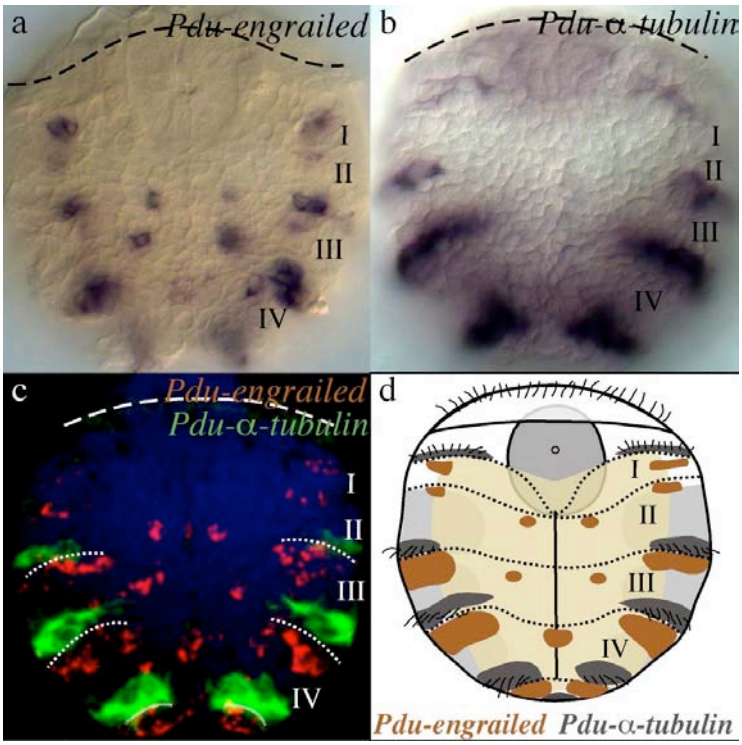

Fig. 13 Single detection (**a**, **b**), double detection (**c**) and schematics (**d**) of *Pdu-engrailed* (**a**, **c**) and *Pdu-α-tubulin* (**b**, **c**) expression at 48hpf.
I-IV: position of larval segments. **c**: reconstruction of confocal sections. Stippled lines: segment boundaries. Dashed line: prototroch. Light brown: neural plate. All posterior-ventral views.

The 48hpf stage is the earliest time-point when morphological boundaries can be clearly discerned by the position of the ciliated bands at the posterior segment boundary (**Fig. 13**b). Double stainings show that the *Pdu-engrailed* lateral cell clusters localise directly posterior of the ciliated bands (**Fig. 13**c,d). Therefore, *Pdu-engrailed* is a marker for the larval anterior segment boundary (as in adult regenerates) (Prud'homme et al., 2003), before any morphological manifestation of segmentation.

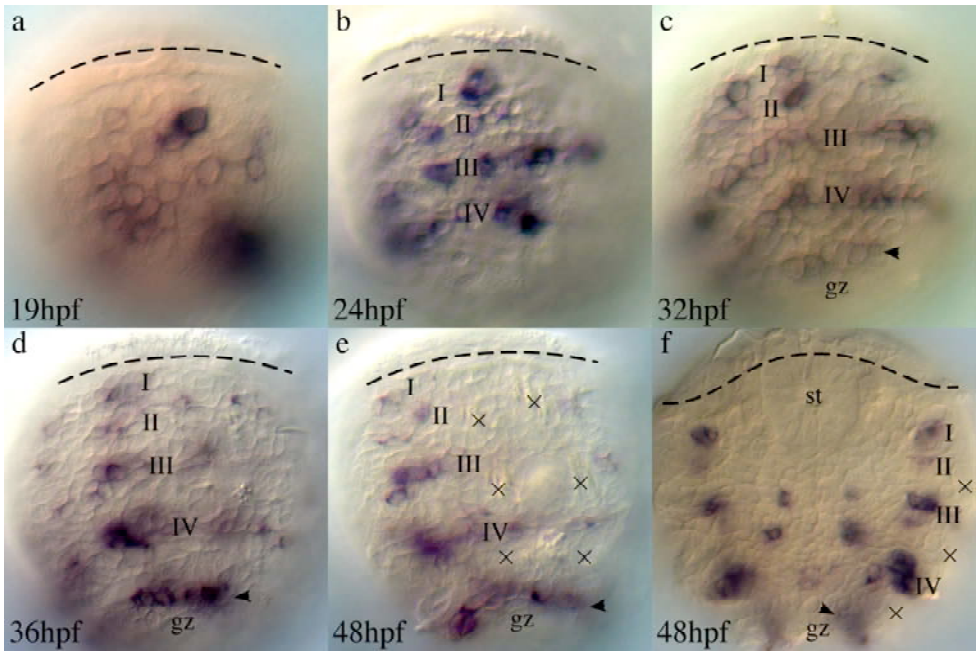

Fig. 14 Expression of *Pdu-engrailed* at different developmental stages of *Platynereis dumerilii*. I-IV: First to fourth *Pdu-engrailed* stripes at the anterior boundary of the first to fourth larval segments. Arrowhead: Fifth stripe of expression appearing in the growth zone. gz: growth zone. st: stomodaeum. "x": Position of chaetal sacs. Dashed line: Prototroch.

Metamerically iterated *Pdu-engrailed* expression starts between 19hpf and 24hpf (**Fig. 14**a,b). I find four *Pdu-engrailed*-expressing stripes of cells at 24hpf (**Fig. 14**b, I-IV) of which the most anterior one appears ventrally merged with the 2nd stripe. In addition to the four stripes present at 24hpf, a fifth band appears in the region of the posterior growth zone at 32hpf marking the anterior border of the next segment that will bud off from the growth zone (**Fig. 14**c, arrowhead). Beyond 36hpf, expression of *Pdu-engrailed* persists but a disintegration of the stripes is probably due to the proliferation in the neural plate without an increase of the number of expressing cells (**Fig. 14**d-f). Nevertheless, the remnants of the stripes are still apparent by the position of cell clusters at the lateral border of the ventral plate (**Fig. 14**d-f, I-IV).

The number of four stripes anterior of the growth zone is unexpected as only three metameric pairs of parapodial appendages develop in the *Platynereis* larva. The position of the protruding parapodial bristles at 48hpf (**Fig. 14**e, crosses) and the fact that *Pdu-engrailed* cells mark the anterior segment boundaries allow me to correlate the *engrailed* stripes with the position of the parapodial appendages (**Fig. 14**e,f). It becomes clear that an incomplete (without any parapodia and bristles), *Pdu-engrailed* expressing segment exists anterior of the first chaetiferous segment (**Fig. 14**b-f, at the level of "I"). Its characteristics will be analysed in the following section 3.3.3.

In order to correlate the position of this “segment I” to the peristomium, I co-stained for *Pdu-engrailed* and *Pdu-otx* in early larvae by double fluorescent *in situ* hybridisation.

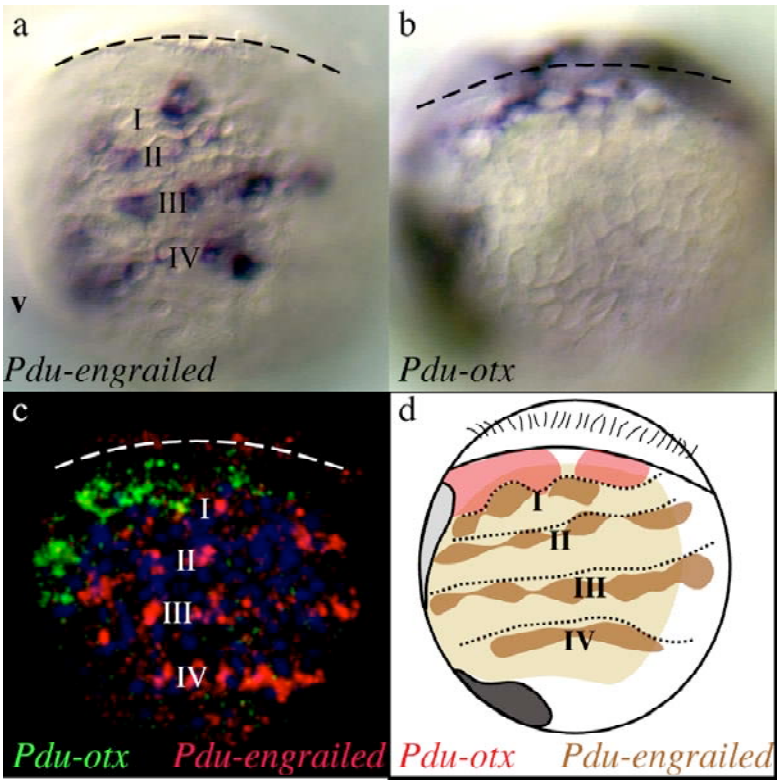

Fig. 15 Single detection (**a**, **b**), double detection (**c**) and schematics (**d**) of *Pdu-engrailed* (**a**, **c**) and *Pdu-otx* (**b**, **c**) expression at 48hpf.
I-IV: First to fourth *Pdu-engrailed* stripes at the anterior boundary of the first to fourth larval segments. **b**: reconstruction of confocal sections. Stippled lines: segment boundaries. Dashed line: prototroch. Light brown: neural plate. Light grey: stomodaeal region. Dark grey: proctodaeal region. All posterior-lateral views.

At 24hpf, the first *Pdu-engrailed* stripe is directly posteriorly abutting *Pdu-otx*-expressing cells (**Fig. 15** a-d). Its position and the lack of *engrailed* expression infers that the peristomium is a non-metameric region located directly anterior of the first metameric segment.

3.3.2 *Pdu-gbx* regionalises the first larval segment bearing the first tentacular cirri

The first larval segment, as described in the previous section, does not develop complete parapodia with chaetae as all other metameric segments in *Platynereis*.

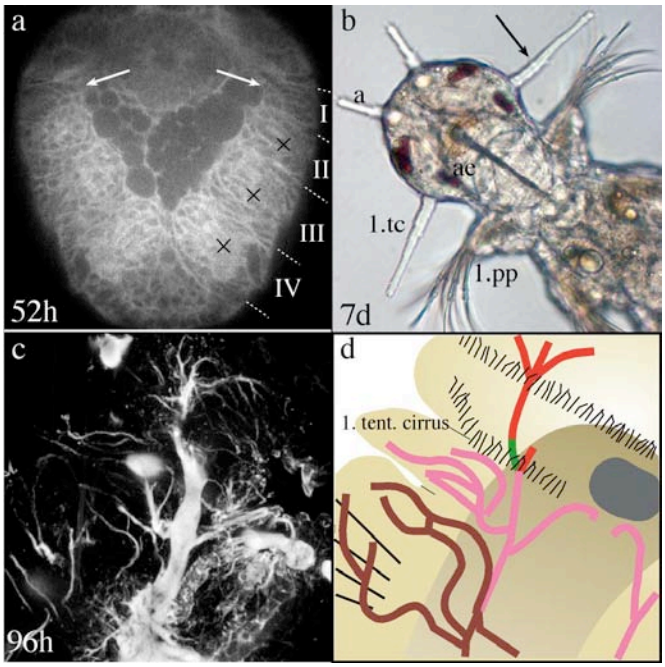

Fig. 16 The origin, position and innervation of the first tentacular cirri at different developmental stages in *Platynereis dumerilii*.
(**a**) Confocal section of a BODIPY564/570-propionic acid stained living embryo at 52hpf. White arrows: position of the chaetal-sac like structures in the first larval segment. Stippled lines: Segment boundaries. I-IV: larval segments. Posterior-ventral view. (**b**) Seven day old juvenile worm. a: antenna; ae: adult eyes; Arrow & 1.tc: first tentacular cirri. 1.pp: first pair of parapodia. Dorsal view. (**c**, **d**) Reconstruction of confocal sections of the axonal scaffold by acetylated α-tubulin immunostainings (**c**) and schematics (**d**) showing the innervation of the tentacular cirri at 96hpf. Colour coding as in **Fig. 6**.

Nevertheless, a confocal section of a living embryo stained with a membrane dye shows the presence of a small cup-like structure (**Fig. 16**a, arrow) very reminiscent of the parapodial sacs in the three following segments (**Fig. 16**, crosses). This lies exactly at the position where the first tentacular cirri protrude from 72hpf onwards (**Fig. 16**b, arrow). I analysed the connection of the tentacular cirri to the axonal scaffold by anti-acetylated α-tubulin immunohistochemistry (**Fig. 16**c,d). In 96h old worms, the tentacular cirri project axons onto the circumoesophageal connectives left and right of the mouth opening (**Fig. 16**c,d).

As described before, the 1st larval segment immediately abuts the *otx*-expressing peristomium. In vertebrates and insects, the larval regions regionalised by *otx* orthologues are posteriorly delimited by the expression of *gbx* orthologues. I have analysed whether the *Platynereis gbx* orthologue (cloned by C. Burgtorf in the lab of J. Wittbrodt, and F. Zelada, unpublished) is an early regionalisation marker for the 1st larval segment. A multiple sequence alignment performed by F. Zelada shows the al-

most identical similarity of the homeobox and the gbx domain with other *gbx* orthologues (**Fig. 17**o).

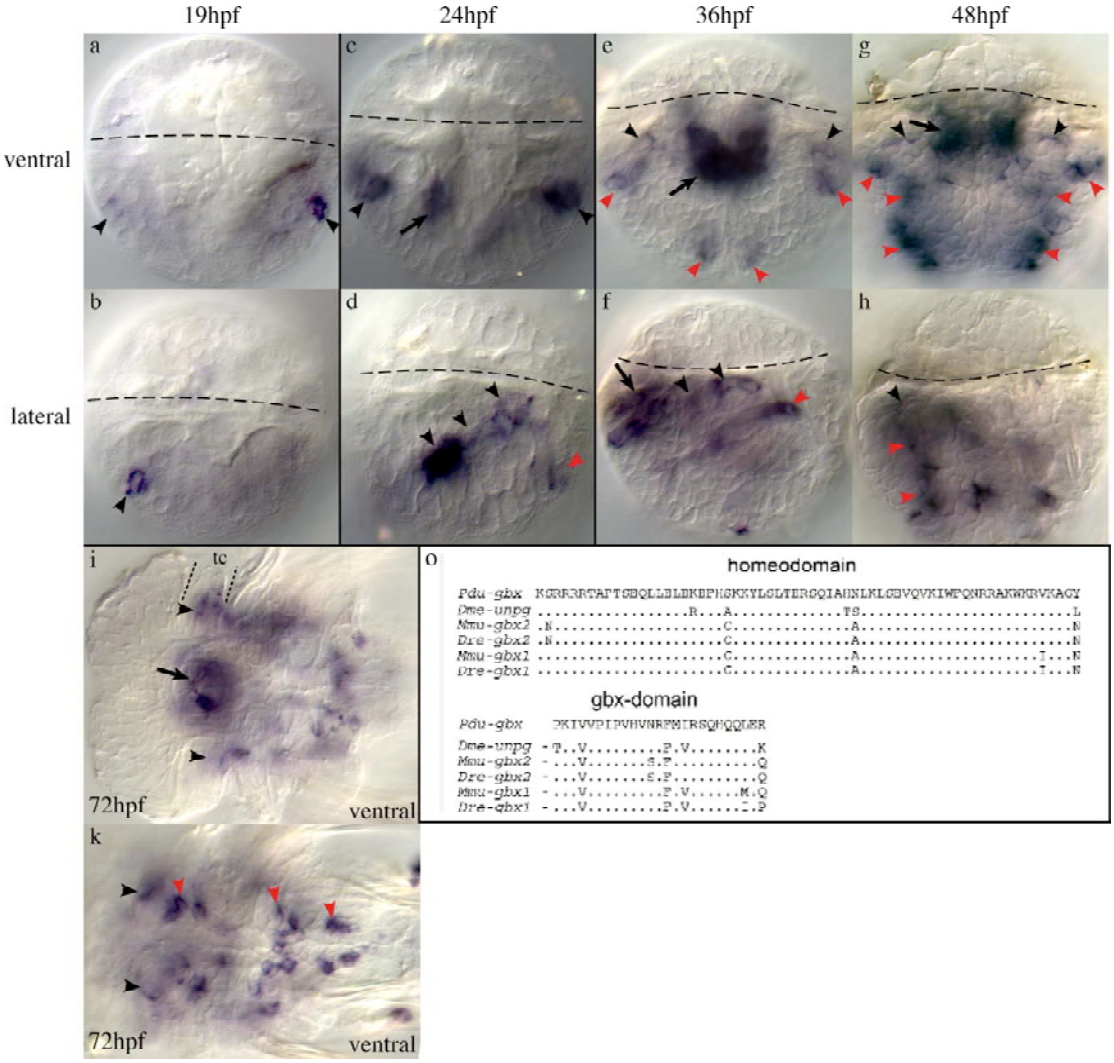

Fig. 17 Expression at different developmental stages (a-k) and multiple sequence alignment of the homeobox and gbx domains (o) of Pdu-gbx.
a-**k**: Black arrows: *Pdu-gbx* expression in stomodaeal cells. Black arrowheads: Anterior expression boundary. Red arrowheads: Expression in the neural plate and chaetal sacs. Dashed line: prototroch. Stippled line: boundaries of the developing 1st tentacular cirri in the first larval segment. tc: 1st tentacular cirri. Orientation in **i** and **k**: anterior to the left. **o**: species abbreviations: Dre: *Danio rerio*; Dme: *Drosophila melanogaster*; Mmu: *Mus musculus*; Pdu: *Platynereis dumerilii*. Alignment was done by F. Zelada. Accession numbers can be found in the materials and methods section.

At 19hpf, *Pdu-gbx* is expressed in two cells in the lateral hyposphere (**Fig. 17**a,b black arrowheads). At a similar position at 24hpf, *Pdu-gbx* is expressed in two bilateral-symmetric stripes that are possibly positioned directly posterior of the peristomium (**Fig. 17**c,d, black arrowheads). It also appears in a small cluster of cells lateral-posterior of the stripe (**Fig. 17**d, red arrowhead) and in cells of the developing stomodaeum (**Fig. 17**c, arrow). At later stages, the clear stripe-like expression is blurred due to the appearance of *Pdu-gbx*-expressing cell patches in the developing

nervous system and appendages of the developing trunk (**Fig. 17**e-k, red arrowheads). Nevertheless, the anterior boundary of *Pdu-gbx* expression is always localised posterior of the prototroch (**Fig. 17**e-k, black arrowheads) between 36hpf and 72hpf. At 72hpf, the most anterior expression can be correlated to the developing first tentacular cirri (**Fig. 17**i, black arrowhead and "tc"). The expression in the posterior half of the stomodaeum persists until 72hpf (**Fig. 17**e,g,i, arrow).

The stripe-like expression at 24hpf is suggestive of a regionalising role of *Pdu-gbx* and could, as in vertebrates and *Drosophila*, abut the *Pdu-otx* expression in the peristomium. I tested the precise position of *Pdu-gbx* in relation to the peristomium and the 1st larval segment by double *in situ* hybridisation co-detecting *Pdu-otx* and *Pdu-engrailed*.

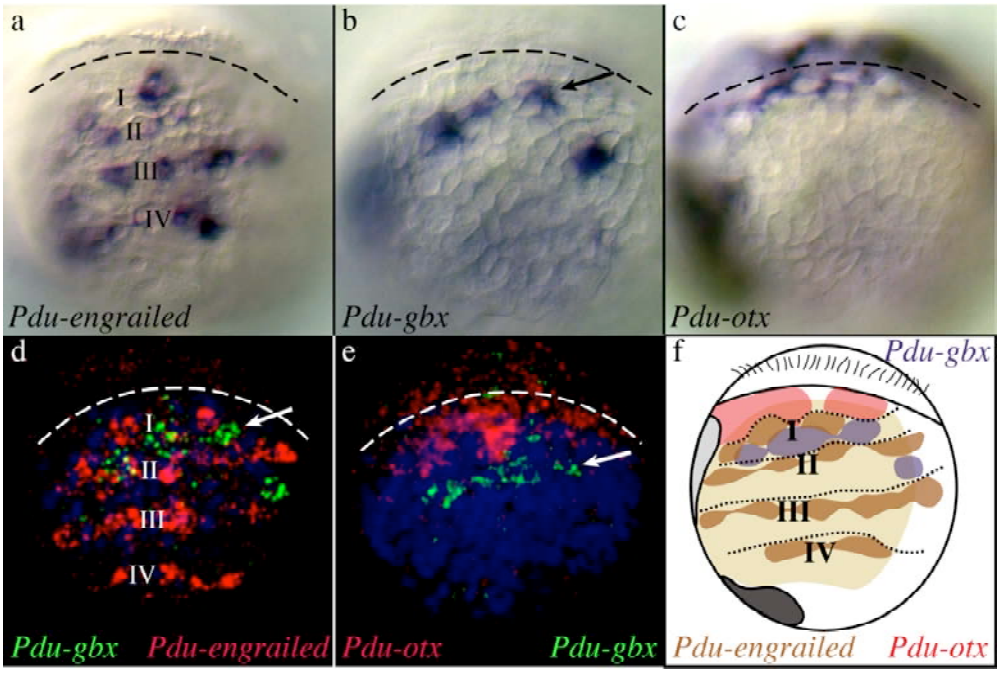

Fig. 18 Single detection (**a**-**c**), double detection (**d**, **e**) and schematics (**f**) of *Pdu-engrailed* (**a**, **d**, **f**), *Pdu-gbx* (**b**, **d**, **e**, **f**) and *Pdu-otx* (**c**, **e**, **f**) expression at 48hpf.
I-IV: First to fourth *Pdu-engrailed* stripes at the anterior boundary of the first to fourth larval segments. **d**, **e**: reconstruction of confocal sections. Dashed lines: prototroch. Stippled lines: segment boundaries. Arrow depicts stripe of *Pdu-gbx*-expressing cells. Light brown: neural plate. Light grey: stomodaeal region. Dark grey: proctodaeal region. All posterior-lateral views.

I found that at 24hpf, the stripe of *Pdu-gbx*-expressing cells (**Fig. 17**d, black arrowheads and **Fig. 18**b,d,e, arrow) is located exactly in-between the first and second stripe of *Pdu-engrailed* expressing cells (**Fig. 18**a,b,d,f). Double detection with *Pdu-otx* confirms that almost none of the *Pdu-gbx*-expressing cells abut *Pdu-otx*-expressing cells in the peristomium (**Fig. 18**b,c,e,f). The gap between both cell populations is most probably filled by *Pdu-engrailed*-expressing cells (compare **Fig. 18**e

with d). The data shows that the 1st larval segment expresses *Pdu-engrailed* in the most anterior cells and *Pdu-gbx* as a regionalisation marker in the more posterior cells.

3.3.3 *Pdu-hox1* regionalises the second larval segment bearing the first pair of parapodia

The correlation of *Pdu-engrailed* stripes with protruding chaetae has shown that the 2nd larval segment represents the first chaetiferous segment with complete larval parapodia (**Fig. 19**a, "1.pp"). During metamorphosis, this segment loses the chaetae and transforms into the second quartet of tentacular cirri (**Fig. 19**b, "2.tc").

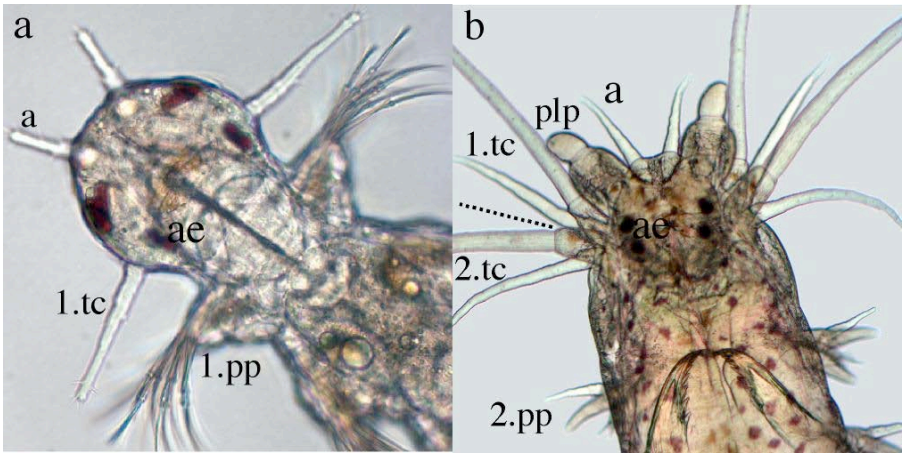

Fig. 19 The head region and appendages before (**a**) and after metamorphosis (**b**).
a: antenna; ae: adult eyes; plp: palpae; 1.tc: first tentacular cirri; 1.pp: first parapodia; 2.tc: second tentacular cirri (=metamorphosed 1.pp); 2.pp: second parapodia; Stippled line: boundary between first and second segment.

I have shown in paragraph 3.3.1. that the first chaetiferous segment bears the first substomodaeal commissure. In vertebrates and insects, *gbx* orthologues fill the gap between the *otx* expressing regions and the anterior boundary of *hox1* orthologues. Preliminary results from F. Zelada suggested that a similar situation could be present in *Platynereis* with *Pdu-hox1* expressed in the first chaetiferous segment. The *Platynereis hox1* gene was cloned by C. Burgtorf in the lab of J. Wittbrodt, and by F. Zelada. A multiple sequence alignment of the homeobox of *hox1* genes performed by F. Zelada has confirmed the identity of the cloned homeobox gene (**Fig. 20**k). I have analysed *Pdu-hox1* expression with emphasis on the precise localisation of its anterior boundary (**Fig. 20**a-i).

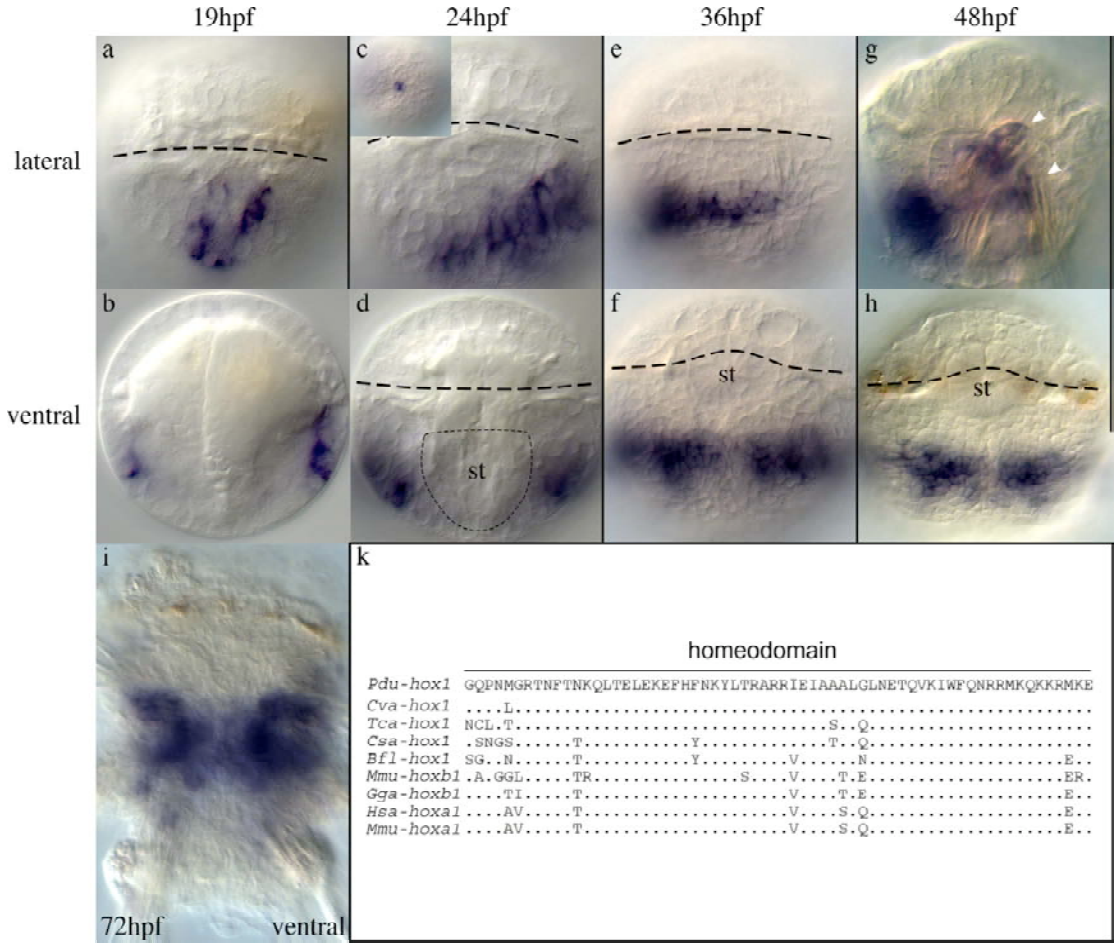

Fig. 20 Expression at different developmental stages (**a**-**i**) and multiple sequence alignment of the homeodomain (**k**) of *Pdu-hox1*.
a-**i**: Dashed line: prototroch. White arrowheads: Expression in the first and second chaetal sacs. st: stomodaeal region. Stippled line: approximate border of the stomodaeal region that separates the lateral *Pdu-hox1*-expressing domains. Inlet in **c**: Expression in the apical organ region; apical view. **k**: Species abbreviations: Bfl: *Branchiostoma floridae*; Csa: *Cupiennius salei* ; Cva: *Chaetopterus variopedatus*; Gga: *Gallus gallus*; Hsa: *Homo sapiens*; Mmu: *Mus musculus*; Pdu: *Platynereis dumerilii*; Tca: *Tribolium castaneum*. Multiple sequence alignment was performed by F. Zelada. Accession numbers can be found in the materials and methods section.

At 19hpf, *Pdu-hox1* is expressed in a lateral cluster of cells reaching from the prototroch to almost the posterior pole of the embryo and forming almost at a 90° angle to the prototroch (**Fig. 20**a,b). At 24hpf, the *Pdu-hox1* expressing cells form a wedge-shaped territory in the lateral and ventral ectoderm (**Fig. 20**c,d) that is still separated on the ventral side by the large stomodaeal precursor cells (**Fig. 20**d, st, stippled line, see also **Fig. 26**c,d,h). Its distinct anterior boundary forms an angle of about 45° to the prototroch. I found a novel expression domain of *Pdu-hox1* in two cells that lie in the centre of the episphere and are part of the apical organ area (**Fig. 20**c, inlet). After 36h of development, the *Pdu-hox1* territory remains wedge-shaped and is situated several cell diameters posterior of the prototroch (**Fig. 20**e,f, dashed line) and the mouth

opening (**Fig. 20**f, "st"). The two initially separated regions have fused along the ventral midline, cover the neural plate and reach laterally into the parapodial area (**Fig. 20**e,f). The anterior boundary is now in parallel to the prototroch and has therefore rotated by almost 90° compared to the stage 19hpf. The expression at 48hpf is similar to 36hpf (**Fig. 20**g,h). It can now be recognised that laterally, *Pdu-hox1* is expressed in the first and second pair of parapodia (**Fig. 20**g, white arrowheads). In a 72h old worm, *Pdu-hox1* does not have a clear anterior boundary anymore, covers a major part of the neural plate and presents an expression gap posterior of the prototroch (**Fig. 20**i).

I have determined the exact position of the anterior *Pdu-hox1* boundary by performing double *in situ* hybridisations with *Pdu-engrailed* and *Pdu-gbx* (**Fig. 21**).

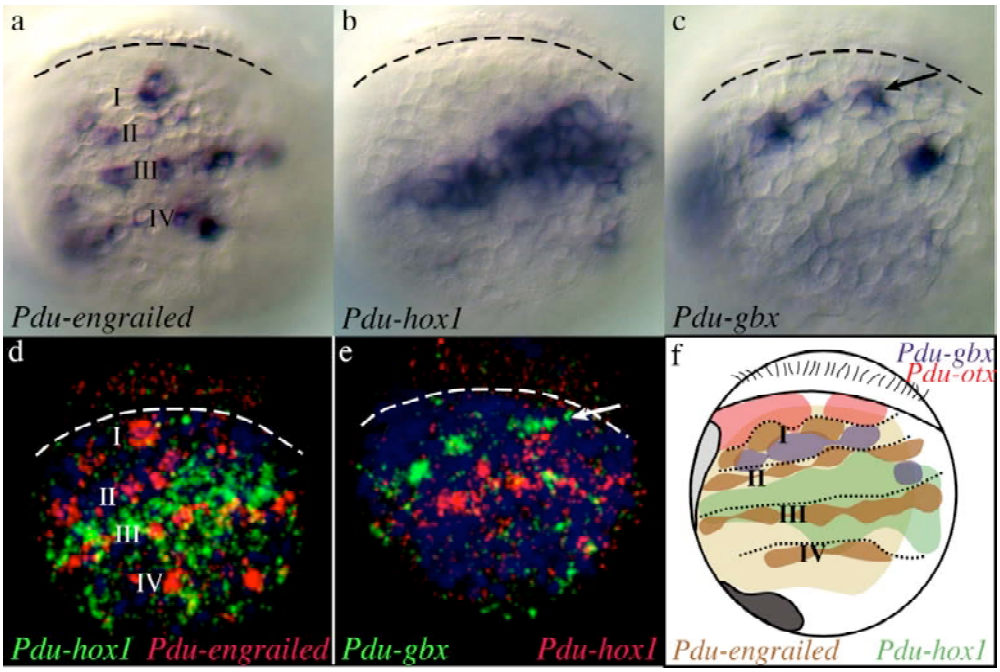

Fig. 21 Single detection (**a**-**c**), double detection (**d**, **e**) and schematics (**f**) of *Pdu-engrailed* (**a**, **d**, **f**), *Pdu-hox1* (**b**, **d**-**f**) and *Pdu-gbx* (**c**, **e**, **f**) expression at 48hpf.
I-IV: position of larval segments. **d**, **e**: reconstruction of confocal sections. Dashed lines: prototroch. Stippled lines: segment boundaries. Arrow depicts stripe of *Pdu-gbx*-expressing cells. Light brown: neural plate. Light grey: stomodaeal region. Dark grey: proctodaeal region. All posterior-lateral views.

The anterior boundary of *Pdu-hox1* is localised immediately posterior to and without overlapping the 2nd *Pdu-engrailed* stripe (**Fig. 21**a,b,d,f). Similar to the expression gap between *Pdu-otx* and *Pdu-gbx*, there is also a gap between the stripe of *Pdu-gbx* and *Pdu-hox1*, most probably also filled by *Pdu-engrailed* expressing cells (**Fig. 21**, compare d with e,f). Thus, the anterior boundary of *Pdu-hox1* does not define a segment boundary but lies within the 2nd metameric segment.

3.3.4 The formation and differentiation of the trunk mesoderm

In polychaetes, the origin and development of the trunk mesoderm is much better understood than the development of the so-called "ectomesoderm" in the polychaete head described before. The trunk mesoderm develops from the 4d micromere. The mesodermal marker *Pdu-fgfr* has been described already and is used as reference to compare the expression of other mesodermal marker genes (Steinmetz, 2002). I have cloned the following mesodermal genes to describe on the molecular level the development of the trunk mesoderm: *Pdu-mef2*, *Pdu-twist* and *Pdu-myoD*.

First, I describe general trunk muscle development in *Platynereis* by using *Pdu-troponin I*, cloned by F. Zelada, as a marker gene.

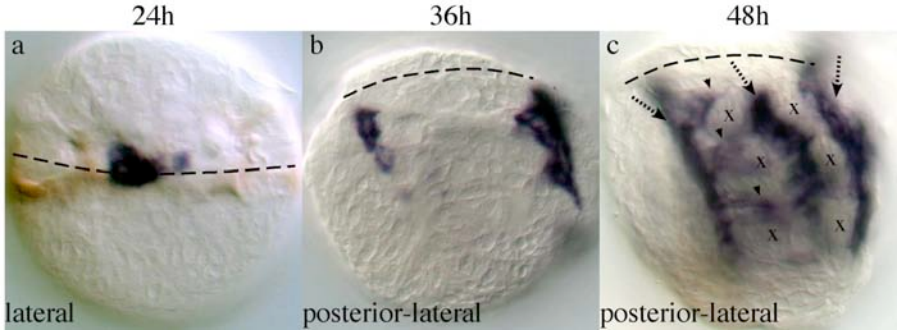

Fig. 22 Expression of *Pdu-troponin I* at different developmental stages of *Platynereis dumerilii*. Dashed line: prototroch. Dashed arrows: longitudinal muscles. Arrowheads: projections of transverse muscles. "x": position of chaetal sacs.

At 24hpf, the only differentiated muscle cells are two lateral cell cluster of 2-3 cells just below the prototroch ring (**Fig. 22**a). The origin of these muscle cells is completely unknown. They could derive from the 4d micromere as well as from the micromeres that form the peristomial mesoderm. The 36hpf stage shows that the first unambiguous differentiated trunk muscles are the longitudinal muscles running dorsal and ventral of the developing parapodial sacs (**Fig. 22**b). The ventral pair develops at the border between the neural plate and the parapodia. Whether any of them originates from the prototroch cell cluster described at 24hpf is unknown. Alternatively, these cell clusters degenerate and cannot be found anymore at 36hpf. This can be further addressed by analysing *Pdu-troponin I* expression in additional developmental stages between 24hpf and 36hpf. At 48hpf, a third, median longitudinal muscle has appeared in-between the ventral and dorsal parapodial sacs in addition to the ventral and dorsal longitudinal muscles (**Fig. 22**c, dashed arrows). Transverse muscles begin

to develop in-between the parapodial sacs in a dorso-ventral direction (**Fig. 22**c, arrowheads). At 72hpf, the staining is so strong that the muscle pattern cannot be discerned anymore (not shown). At this stage, a better resolution of the muscle pattern can be achieved by using confocal microscopy on fluorescent phalloidin stained larvae.

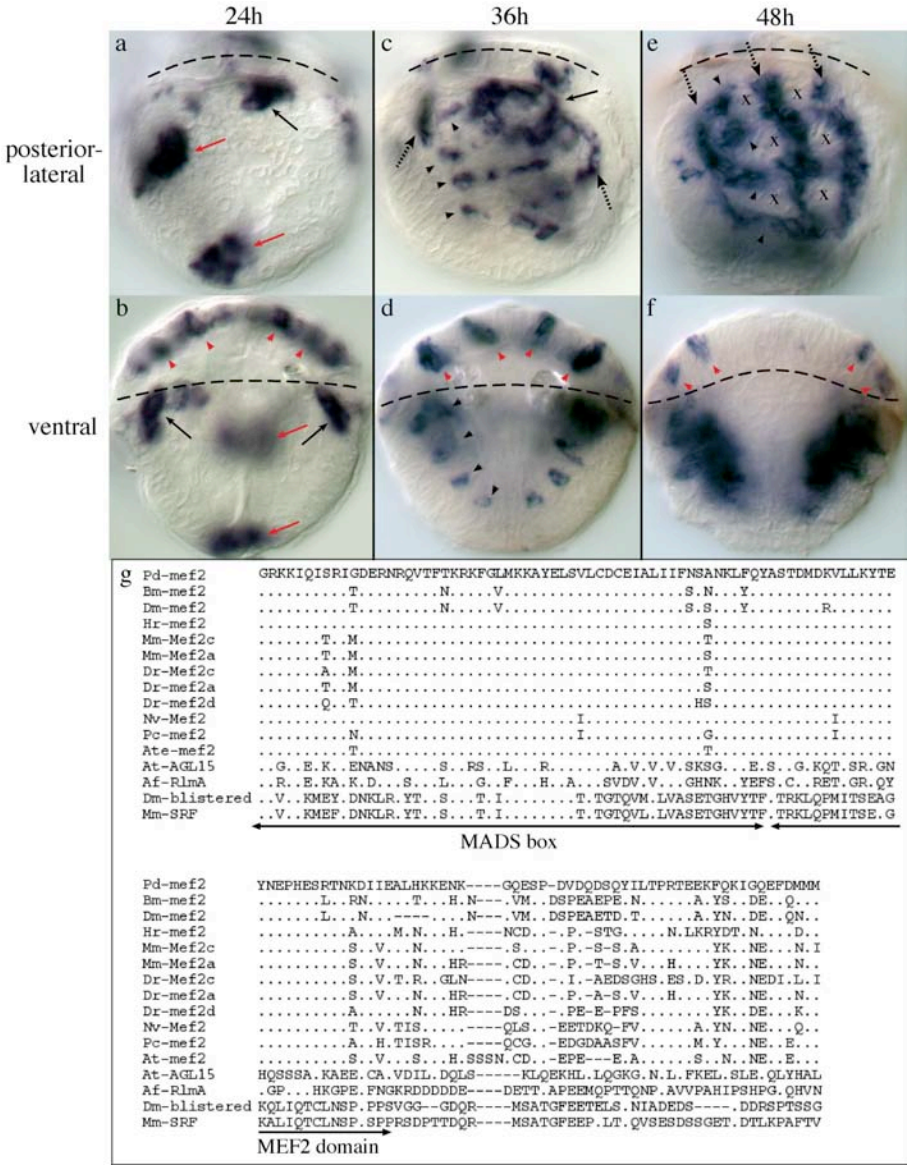

Fig. 23 Expression of *Pdu-mef2* (**a**-**f**) and multiple sequence alignment of the *Pdu-mef2* MADS and Mef2 domains with other MADS domain proteins (**g**).
Black arrows: Putative prototroch muscles. Red arrows: Stomodaeal and proctodaeal expression. Dashed arrows: Longitudinal muscles. Black arrowheads: Segmental transverse expression in putative transverse muscles. Red arrowheads: Neural expression. "x": Position of chaetal sacs. Dashed line: prototroch. In **g**: Domains as defined by (Molkentin et al., 1996). Dots represent amino acid identity; dashes represent gaps in the alignment. Species abbreviations: Af: *Aspergillus fumigatus*; At: *Arabidopsis thaliana*; Ate: *Achaearanea tepidariorum*; Bm: *Bombyx mori*; Dm: *Drosophila melanogaster*; Dr: *Danio rerio*; Hr: *Halocynthia roretzi*; Mm: *Mus musculus*; Nv: *Nematostella vectensis*; Pc: *Podocoryne carnea*; Pd: *Platynereis dumerilii*. AGL15: Agamous-like 15; SRF: serum-response factor; RlmA: SRF-type transcription factor. Accession numbers can be found in the materials and methods section.

I have cloned a 3'-RACE-fragment of the *Platynereis mef2* orthologue based on a short initial fragment cloned by B. Prud'homme (Balavoine lab, Gif-sur-Yvette). The fragment codes for a protein that has a much higher similarity to proteins of the Mef2 family than to other MADS-box proteins (**Fig. 23**g) (Molkentin et al., 1996). In *Platynereis*, Pdu-*mef2* appears to be a marker for differentiating and differentiated muscle cells (**Fig. 23**a-f), although its earliest expression implies a mesoderm-unrelated function. At 24hpf, it is mostly expressed in non-mesodermal cells, like stomodaeal and proctodaeal cells (**Fig. 23**a,b red arrows), but expression in those cells cannot be found at later stages. In contrast, expression in the developing brain can be seen until at least 48hpf (**Fig. 23**b,d,f, red arrowheads). The only putative mesodermal expression at 24hpf could correspond by position to the differentiated muscle cells below the prototroch (compare **Fig. 23**a, arrow with **Fig. 22**a). At 36hpf, *Pdu-mef2* appears in segmentally iterated stripes in-between the parapodial sacs anticipating the position of the prospective transverse muscles at 48hpf (**Fig. 23**c,d and **Fig. 22**c, black arrowheads). It is also expressed in longitudinal bands reminiscent of the ventral and dorsal longitudinal muscles (**Fig. 23**c,e, dashed arrows). The dorsal chaetal sac of the first chaetiferous segment is fully surrounded by *Pdu-mef2* expression, suggesting that the dorso-anterior muscles differentiate earliest (**Fig. 23**c, black arrow). This is also supported by the *Pdu-troponin I* expression data showing strongest expression in the dorso-anterior located longitudinal muscle (**Fig. 22**b). At 48hpf, *Pdu-mef2* is very similar to the *Pdu-troponin I* staining (compare **Fig. 23**e to **Fig. 22**c). Strong expression is seen in the three longitudinal (**Fig. 23**e, dashed arrows) and transverse muscles (**Fig. 23**e, black arrowheads) surrounding the chaetal sacs (**Fig. 23**c, "x").

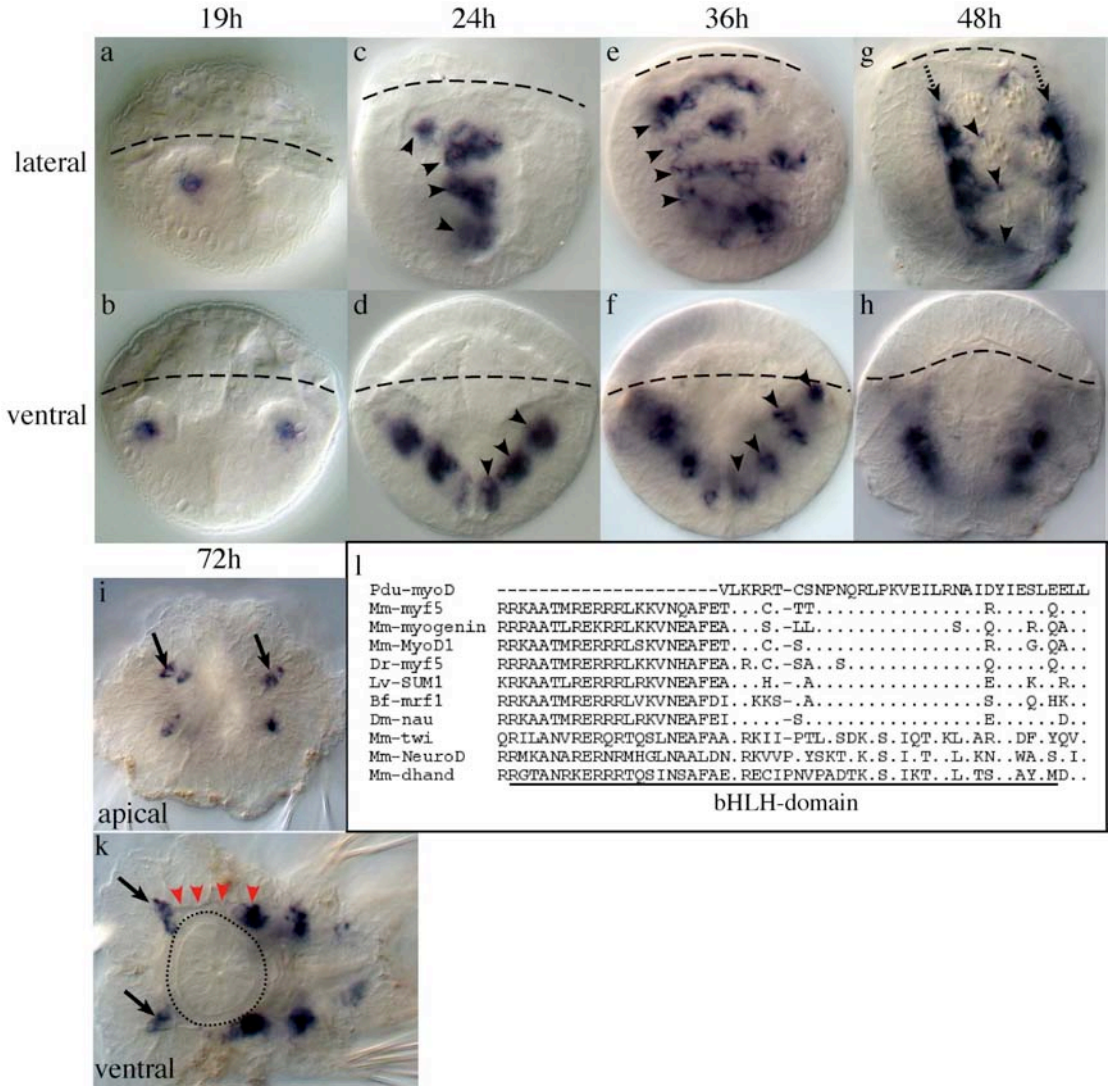

Fig. 24 Expression of *Pdu-myoD* (**a**-**k**) and multiple sequence alignment of the *Pdu-myoD* basic helix-loop-helix (bHLH) domains with other bHLH domain proteins (**l**).
Black arrows: Mesodermal "horns" in the brain region. Dashed arrows: Expression in longitudinal muscles. Black arrowheads: Expression in segmental clusters corresponding to the putative transverse muscle precursors. Red arrowheads: Putative connection between the "horns" in the brain and the trunk mesoderm. Dashed line: prototroch. Stippled line: Outer border of mesodermal envelope around the stomodaeum. Orientation in **k**: anterior to left. In **l**: Dots represent amino acid identity; dashes represent gaps in the alignment. Species abbreviations: Bf: *Branchiostoma floridae*; Dm: *Drosophila melanogaster*; Dr: *Danio rerio*; Lv: *Lytechinus variegates*; Mm: *Mus musculus*; Pdu: *Platynereis dumerilii*. Accession numbers can be found in the materials and methods section.

I have cloned a 3'-RACE-fragment of the *Platynereis myoD* orthologue based on a short initial fragment cloned by B. Prud'homme (Balavoine lab, Gif-sur-Yvette). The fragment encodes a protein sequence that covers partially the conserved basic helix-loop-helix (bHLH) domain. Multiple protein sequence alignments show high similarities of the partial bHLH of the putative *Platynereis myoD* orthologue to other members of the *myoD* family (Muller et al., 2003) and much less conservation to other myogenic and neurogenic bHLH-proteins (**Fig. 24**l).

In contrast to *Pdu-mef2*, *Pdu-myoD* is exclusively and much earlier expressed in mesodermal cells from 19hpf to 72hpf (**Fig. 24**a-k). At 19hpf, the earliest stage investigated, *Pdu-myoD* is expressed in two bilateral-symmetric clusters of 2-3 cells located in midst the lateral mesodermal bands (**Fig. 24**a,b). The expression expands considerably at 24hpf where *Pdu-myoD* is expressed in 4 clusters of cells in the lateral mesodermal bands (**Fig. 24**c,d, arrowheads). In the 36hpf larva, *Pdu-myoD* is expressed in four metamerically iterated, transverse stripes (**Fig. 24**e,f) that could partially include *Pdu-mef2*-expressing cells (compare **Fig. 24**e,f with **Fig. 23**c,d, black arrowheads). Between 36hpf and 48hpf, the expression pattern changes considerably from transverse to longitudinal stripes (**Fig. 24**e-h). While at 36hpf, *Pdu-myoD* could be interpreted as being expressed in differentiating transverse muscles, it marks the ventral and dorsal longitudinal muscles at 48hpf (compare **Fig. 24**g with **Fig. 22**c, dashed arrows) with only small transverse projections in-between the chaetal sacs (**Fig. 24**g,h, arrowheads). Notably, the median longitudinal muscle is totally devoid of *Pdu-myoD* expression (compare **Fig. 22**c and **Fig. 24**g). Assuming that *Pdu-myoD* keeps being expressed in the same cells, these changes imply that major cell sorting takes place. An alternative explanation is that *Pdu-myoD* is down regulated in transverse muscles, and up regulated in longitudinal muscles between 36hpf and 48hpf. At 72hpf, *Pdu-myoD* starts also being expressed in the head in the four horn-like structures (**Fig. 24**i,k, arrows) that have already been identified as *Pdu-fgfr*-positive (Steinmetz, 2002). Expression of *Pdu-myoD* supports the initial assumption that the "horns" correspond probably to the palpal and antennal head muscles. **Fig. 24**k might wrongly suggest that these horns are in direct continuation with the trunk muscles and form a second, outer layer of mesoderm around the stomodaeum (**Fig. 24**k, red arrowheads) that in contrast to the inner layer originates from the 4d micromere. Cell lineage analysis has shown that these horns are clearly of "ectomesodermal" origin (Ackermann et al., 2005). The time and localisation of *Pdu-myoD* expression suggest that it plays a role in early muscle specification and differentiation.

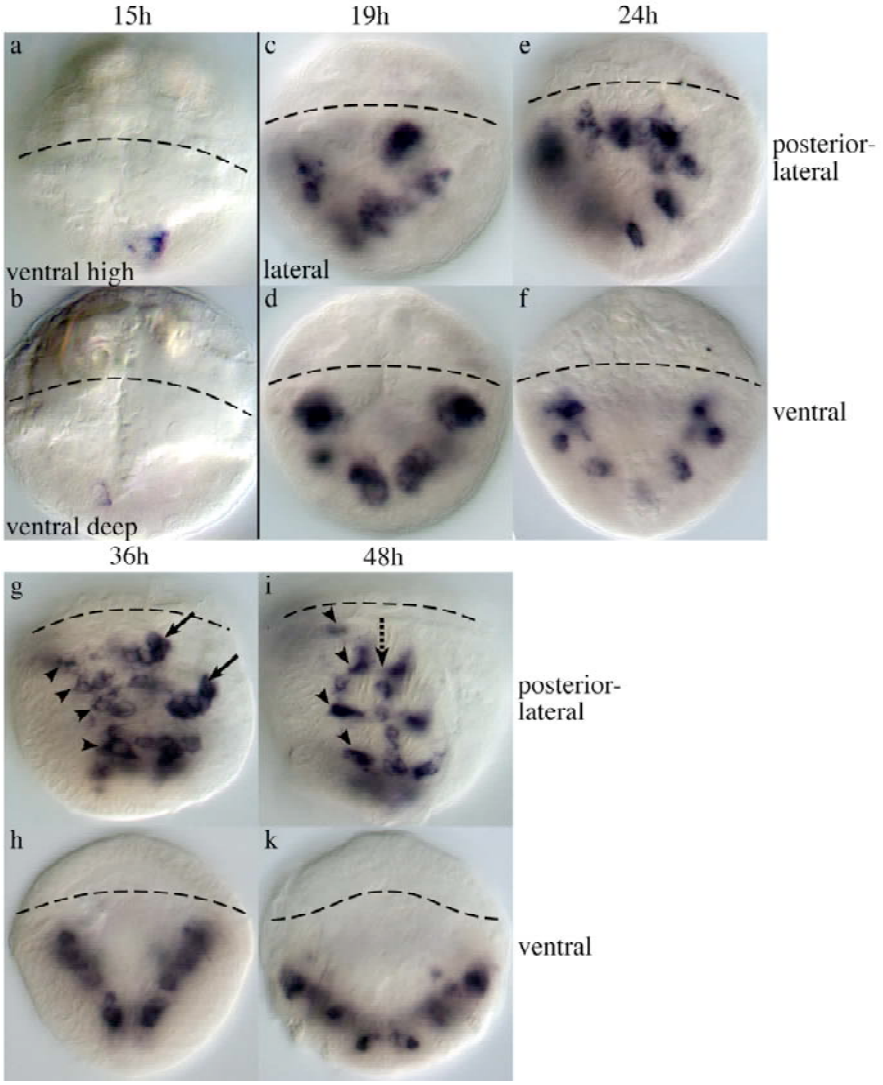

Fig. 25 Expression of *Pdu-twist* (**a**-**k**) at different developmental stages of *Platynereis dumerilii*. Arrows: Expression in cell cluster dorso-posterior of the chaetal sacs. Dashed arrow: Expression in the median longitudinal muscle. Arrowheads: Expression in the ventral longitudinal muscle region corresponding to the putative segmental transverse muscle precursors. Dashed line: prototroch.

From all mesodermal genes described so far, *Pdu-twist* is the most complex and difficult to interpret. It is found in two cells at 15hpf: one in the region of the future stomodaeum (**Fig. 25**a) at or just below the surface of the embryo and another cell much deeper at the posterior base of the mesodermal bands (**Fig. 25**b). The expression is much broader at 19hpf in non-metameric cell clusters of the lateral mesodermal band (**Fig. 25**c,d). These cell groups refine into about 6 clusters along the lateral mesodermal band at 24hpf (**Fig. 25**e,f). At 36hpf, the *Pdu-twist* expression adopts a complex pattern with most cells localised in a few clusters at the ventral side near the position of the developing ventral longitudinal muscles (**Fig. 25**g,h, arrowheads) and dorsally at a dorso-posterior position to the developing chaetal sacs (**Fig. 25**g,h arrows). Be-

tween 36hpf and 48hpf, a change in *Pdu-twist* expression similar to the change in *Pdu-myoD* expression is seen. Assuming again that the same cells keep expressing *Pdu-twist*, it supports a rearrangement of cells in-between 36hpf and 48hpf. The expression of *Pdu-twist* in the region of the transverse muscle cells (**Fig. 25**i, arrowheads) and in parts of the median longitudinal muscle region (**Fig. 25**i, dashed arrow) at 48hpf strikingly suggests that *Pdu-twist* and *Pdu-myoD* are expressed in a complementary fashion (compare **Fig. 25**i with **Fig. 24**g).

3.4 Closure of the Platynereis blastopore by amphistome gastrulation

I have analysed the morphogenesis of the polychaete trunk by *in vivo* time-lapse recordings. The use of the fluorescent membrane dye BODIPY5647/570 coupled to propionic acid has enabled me to use 4D laser confocal microscopy. The aim of the recordings was to follow the closure of the *Platynereis* blastopore, the formation of the neural plate and the origin of the neural midline cells. These processes have been analysed during a period that covers the fusion of the neural plate and the beginning of the ventral midline formation between approx. 17hpf and 29hpf (**Fig. 26**). The time-points of the observed processes cannot be directly compared to embryos developing under normal conditions (18°C) as the recordings have been performed at 25°C.

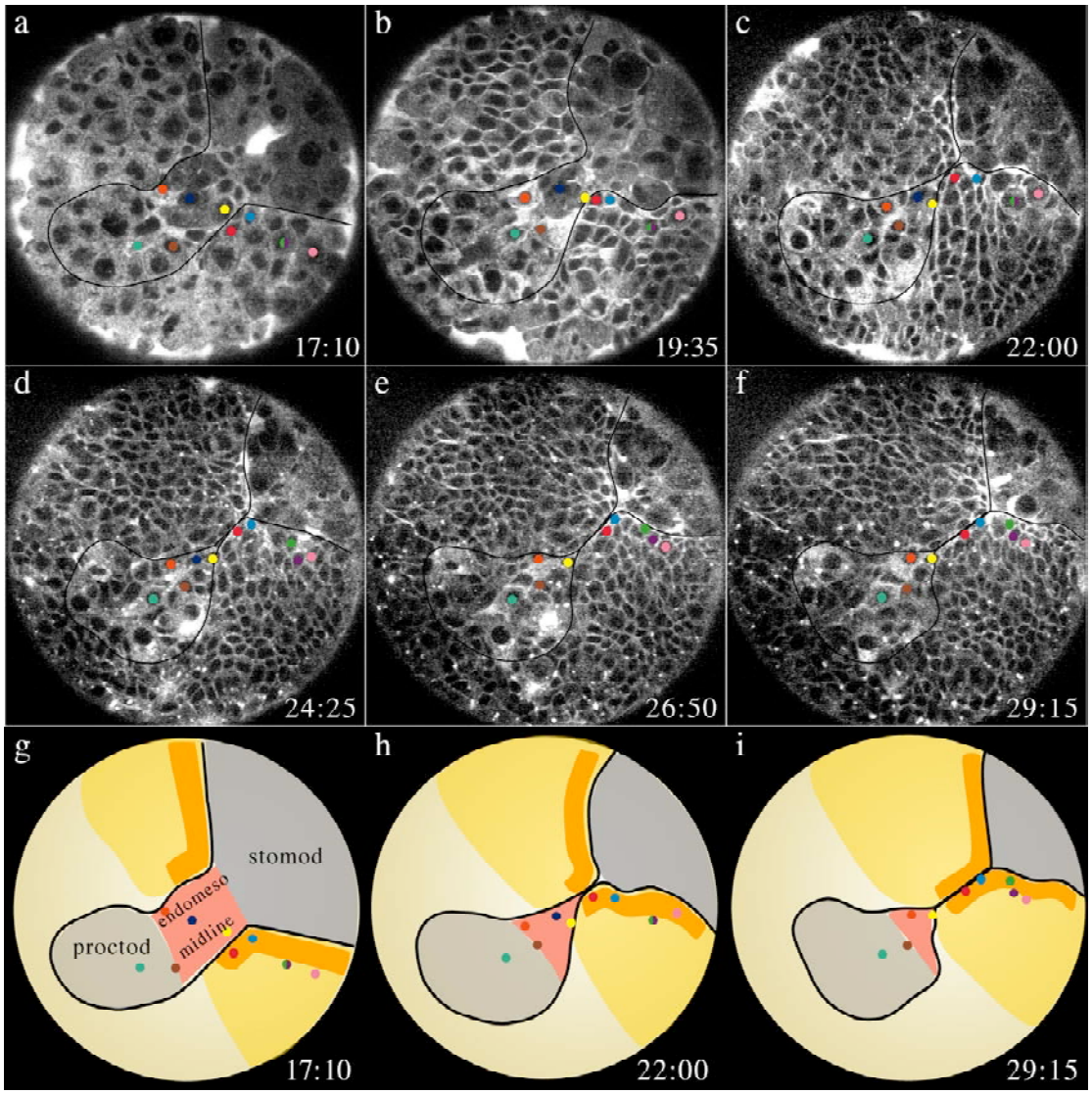

Fig. 26 Amphistome closure of the blastopore and formation of the neural midline in *Platynereis dumerilii*.
(**a**-**f**) Frames of a confocal time-lapse recording between 17:10 hrs and 29:15 hrs post-fertilisation at 25°C. (**g**-**i**) Schematics corresponding to the frames in (**a**), (**c**), and (**f**). Black line: Blastopore margin and border of the neural plate. Dark yellow: neural plate. Orange: Prospective neural midline. Dark grey, "stomod": stomodaeal region; light grey, "proctod": proctodaeal region; red area: "endomesodermal" midline of unknown fate. Coloured dots: Centres of tracked cells. Views onto blastopore, anterior to the top right corner.

The line of internalisation demarcates the border between internalising and non-internalising cells and represents the rim of the closing blastopore (**Fig. 26**a-f, black line). A true blastopore opening as seen in embryos with low yolk content in small macromeres is never present in *Platynereis dumerilii* that shows a moderate amount of yolk. In the time period analysed, some of the cells that are getting internalised during gastrulation are still superficial. They include the stomodaeal cells (**Fig. 26**g-i, dark grey), internalising midline cells of putative endomesodermal origin and unknown fate (**Fig. 26**g-i, red) and proctodaeal cells (**Fig. 26**g-i, light grey). The ecto-

dermal neural plate is the result of massive proliferation of the 2d somatoblasts from the dorsal towards the ventral side. These movements force the initially elliptic blastopore rim to adopt a slit-like shape. At the beginning of the recordings at about 17hpf, the neural plate (**Fig. 26**g, dark yellow) still lies laterally of the blastopore. Already before the fusion of the neural plate, the line of internalisation is morphologically apparent due to the different cell morphologies: the fast dividing neural plate cells are much smaller than the slowly dividing internalising cells. After complete formation of the neural midline (at about 36hpf), it is reminiscent of a suture line formed by the cells that directly abut the line of internalisation.

I have visualised the morphogenetic movements occurring during neural plate formation by following cells that only show low cell proliferation at representative locations (by tracking cells most of the times reversely on the timescale). After the fusion of the neural plate at about 22:00 hrs post-fertilisation (hpf) (**Fig. 26**c), the ectodermal cells positioned just below the fusion point (**Fig. 26**c-f. yellow dot) represent the posterior end of the neural midline. During development, the cells positioned lateral of the forming stomodaeum will gradually approach the fusion point and will be integrated into the neural midline that forms in a zipper-like manner from posterior to anterior (see blue, green, purple and pink dots in **Fig. 26** and orange band in **Fig. 26**g-i). By this process, the stomodaeal cells are pushed anteriorwards and forced away from the proctodaeal cells that stay at their initial posterior position (note the increasing distance between the brown and turquoise dots (proctodaeal cells) and the stomodaeal territory). The cells of the endomesodermal midline will be partly overgrown by this process (note the position of the yellow and dark blue dots in relation to line of internalisation and the disappearance of the dark blue dot between 22:00 hpf and 26:50 hpf).

This data shows that *Platynereis* gastrulation is not typically protostome, as the blastopore does not entirely give rise to the mouth, but amphistome. During amphistome gastrulation as presented here, the slit-like blastopore adopts the shape of an “8” after the fusion of the lateral lips from which the anterior part gives rise to the mouth and the posterior part to the anus. Notably *Platynereis* has two midlines: an endomesodermal midline connecting stomodaeal and proctodaeal cells before fusion of the neural plate, and the neural midline that originates from cells positioned along the left and right border of the stomodaeum at 24hpf. The neural plate is consequently positioned

lateral of the stomodaeum at 24hpf (**Fig. 26**g-i, orange line). This has important implications for the role of the stomodaeum in early neural patterning that will be discussed later.

3.5 Convergent extension in the Platynereis trunk neuroectoderm during the elongation of the larva into a juvenile worm

At 48hpf, most cells within the line of internalisation have internalised (this might not be the case for the proctodaeal cells yet) and the neural plate has formed with the neural midline along the ventral suture line. Although gastrulation is practically complete, the larva has still a spherical shape. The transformation into an elongated juvenile worm begins shortly after 48hpf. This transformation of a spherical into an elongated animal might be ancestral to all Bilateria but it is only described at the cellular level for chordates yet. In vertebrates, morphogenetic movements in the mesoderm and neuroectoderm drive this transformation from e.g. a spherical blastula into a tadpole in frogs. During this process, neuroectoderm and dorsal mesodermal tissue undergo convergent extension, meaning that the tissues simultaneously narrow and elongate. I have analysed the shape of the *Platynereis* neural plate at different larval stages by measuring its length and width in-between morphological landmarks stained by α-acetylated tubulin immunohistochemistry (**Fig. 27**).

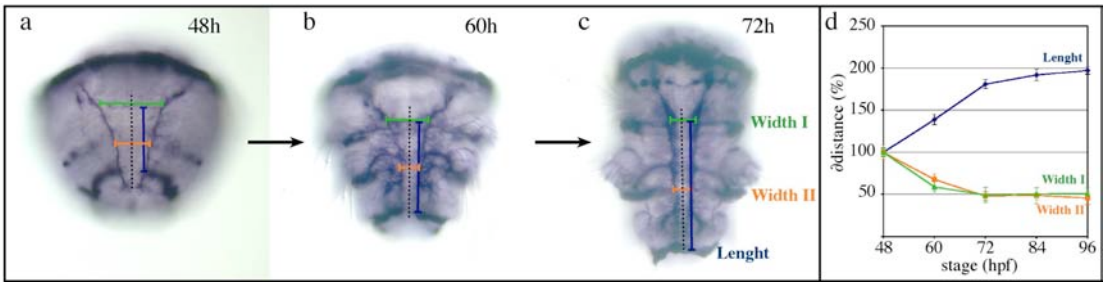

Fig. 27 Analysis of convergent extension in the *Platynereis* neuroectoderm during elongation of the trochophore into a juvenile worm by quantification of tissue transformation through morphological landmarks.
Axonal scaffold and ciliary bands stained by acetylated α-tubulin antibody. The plotted distances in the graph refer to the coloured dashed lines in the larvae. Note that axis elongation is almost complete at 72hpf. Blue length: from poststomodaeal commissure to telotroch; Green width I: between connectives at poststomodaeal commissure level; Orange width II: between connectives at level of 2nd paratroch. Black stippled line: neural midline. Ventral views.

In parallel to the elongation of the larva, the neural plate elongates (in-between the substomodaeal commissure and the telotroch) to 197±4% and narrows (in-between

the longitudinal axon tracts) to 45±6% between 48hpf and 96hpf (**Fig. 27**). Narrowing and elongation of the neural plate is mainly occurring between the 48hpf and 72hpf stages, during which it narrows to 48±9% and elongates to 181±5%. Such reshaping of tissue is reminiscent of the convergent extension movements of the trunk neuroectoderm (and underlying mesoderm) in vertebrates.

3.6 Mediolateral cell intercalation in the Platynereis neural plate during elongation of the trochophore larva

I have analysed convergent extension of the neural plate during elongation of the trochophore larva on the cellular level by time-lapse recordings between 53hpf and 58hpf. It is supposed that the embryo develops faster under the recording conditions (at 25°C) than at normal breeding conditions (18°C). The use of the fluorescent lipophilic dye BODIPY564/570 coupled to propionic acid allows using confocal microscopy to identify cellular outlines and track individual cells throughout the period of recording. I have tracked 139 individual cells in one half of the neural plate that were visible in one focal plane (**Fig. 28** and **Fig. 29**). Cells that could not be tracked either due to cell division or to their disappearance from the analysed focal plane are mainly located along the midline, at the presumptive segment boundaries and at the lateral border of the neural plate.

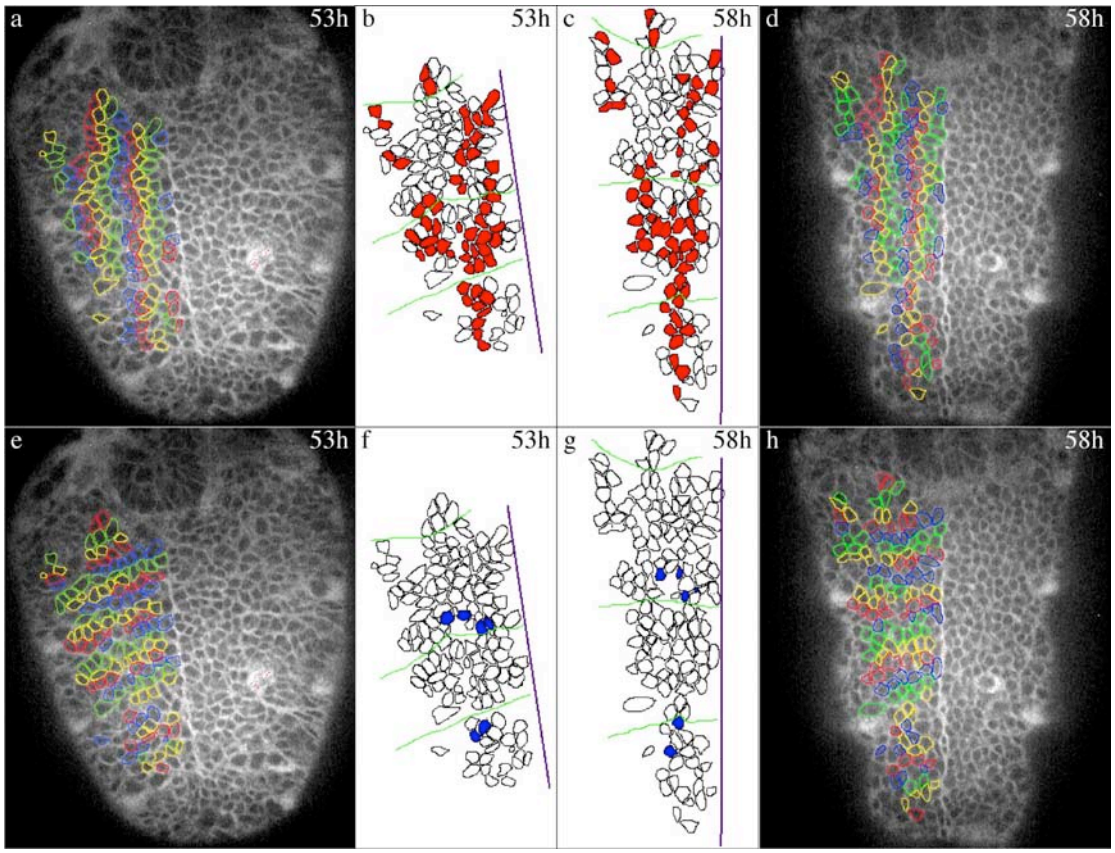

Fig. 28 Convergent extension by mediolateral cell intercalation in the *Platynereis* neural plate.
Cell intercalation events in mediolateral (**a**-**d**) and antero-posterior (**e**-**h**) direction. **a**, **d** , **e**, **h**: Frames of focal planes of a 300min time-lapse recording between approx. 53hpf and 58hpf. Traceable cells are artificially coloured in columns (**a**) or rows (**e**) and tracked in **d** and **h** to visualise intercalation events. **b**, **c**, **f** and **g** depict traced cells that are separated from one neighbour cell by at least one traced intercalating cell in mediolateral (red) or antero-posterior (blue) direction. Purple: ventral midline. Green: posterior boundaries of ciliary bands.

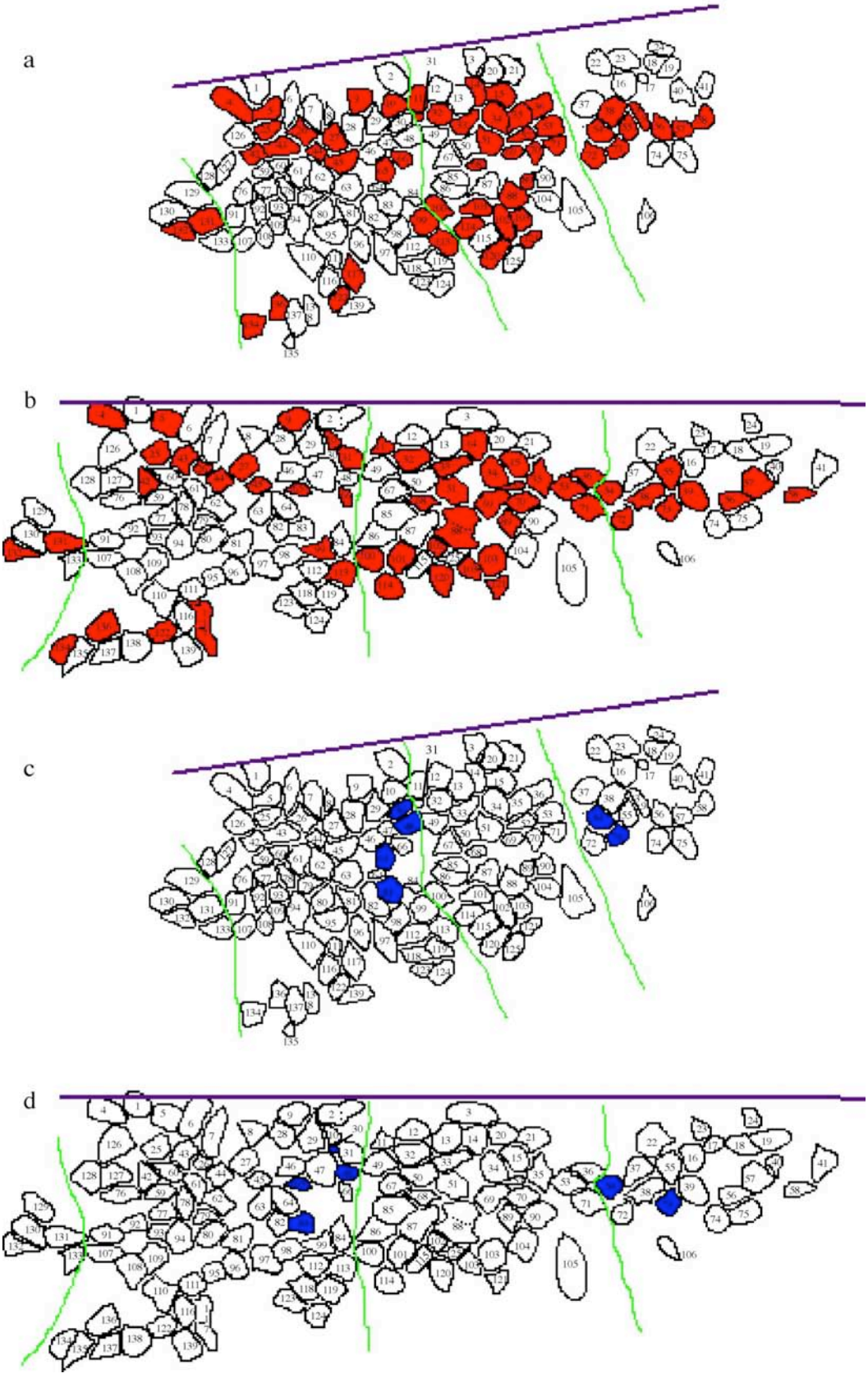

Fig. 29 Traced cells undergoing mediolateral (**a**, **b**) and antero-posterior intercalation (**c**, **d**). Same experiment as in (**Fig. 28**) but with numbers to identify and track individual cells.

I have found that in the *Platynereis* neural plate, polarised neighbour cell displacements occur (**Fig. 28**). I have found that cells strongly intercalate in the mediolateral direction (**Fig. 28**a-d), while they hardly ever intercalate in the antero-posterior direction (**Fig. 28**e-h). These data also show that mediolateral cell intercalation accounts for the observed elongation: In the 5h period documented in **Fig. 28**a-d, a given longitudinal column of cells on average increases in length to 129+/-6% (elongation index (Elul et al., 1997); n=6), while the number of tracked cells that contribute to this column on average augments to 126+/-14% by mediolateral intercalation (mediolateral intercalation index (Elul et al., 1997); n=6). In keeping with this, I have also determined that cell shape change (ratio of length/width) does not contribute significantly to convergent extension (p=0,42; n=25). Still, I have observed an increase in neuroectodermal surface area (to 111+/-14%; n=100) using tracked cells as landmarks, which is best explained by radial cell intercalation as cells selectively appearing in or disappearing from focal planes can be occasionally observed. Although the described polarised neighbour cell displacement is very reminiscent of the mediolateral cell intercalation in the vertebrate neuroectoderm, also differences exist mainly in the cellular morphology. Efforts to identify actin-based cellular protrusions (e.g. filopodia) on intercalating cells by phalloidin staining (staining F-actin) or by α-phospho-tyrosine immunohistochemistry (used in *Drosophila* to identify focal adhesion points) have remained unsuccessful.

3.7 The role of cell division during elongation of the neural plate

Although mediolateral cell intercalation can theoretically account for the elongation of the neural plate, cell proliferation could play an additional role during elongation. I tested this possibility by determining the amount of proliferating cells in the neural plate using the BrdU assay. I have functionally addressed the role of cell proliferation in embryo elongation by measuring the lengths of embryos where the cell cycle has been arrested in the G2/M-phase using the microtubule depolymerising drug Nocodazole.

3.7.1 Identification of mitotic cells using Bromodeoxyuridine (BrdU) incorporation and detection

I have determined the number and localisation of proliferating neural plate cells by incorporation and detection of the thymidine analogon bromodeoxyuridine (BrdU) during 2h intervals between 48hpf and 72hpf.

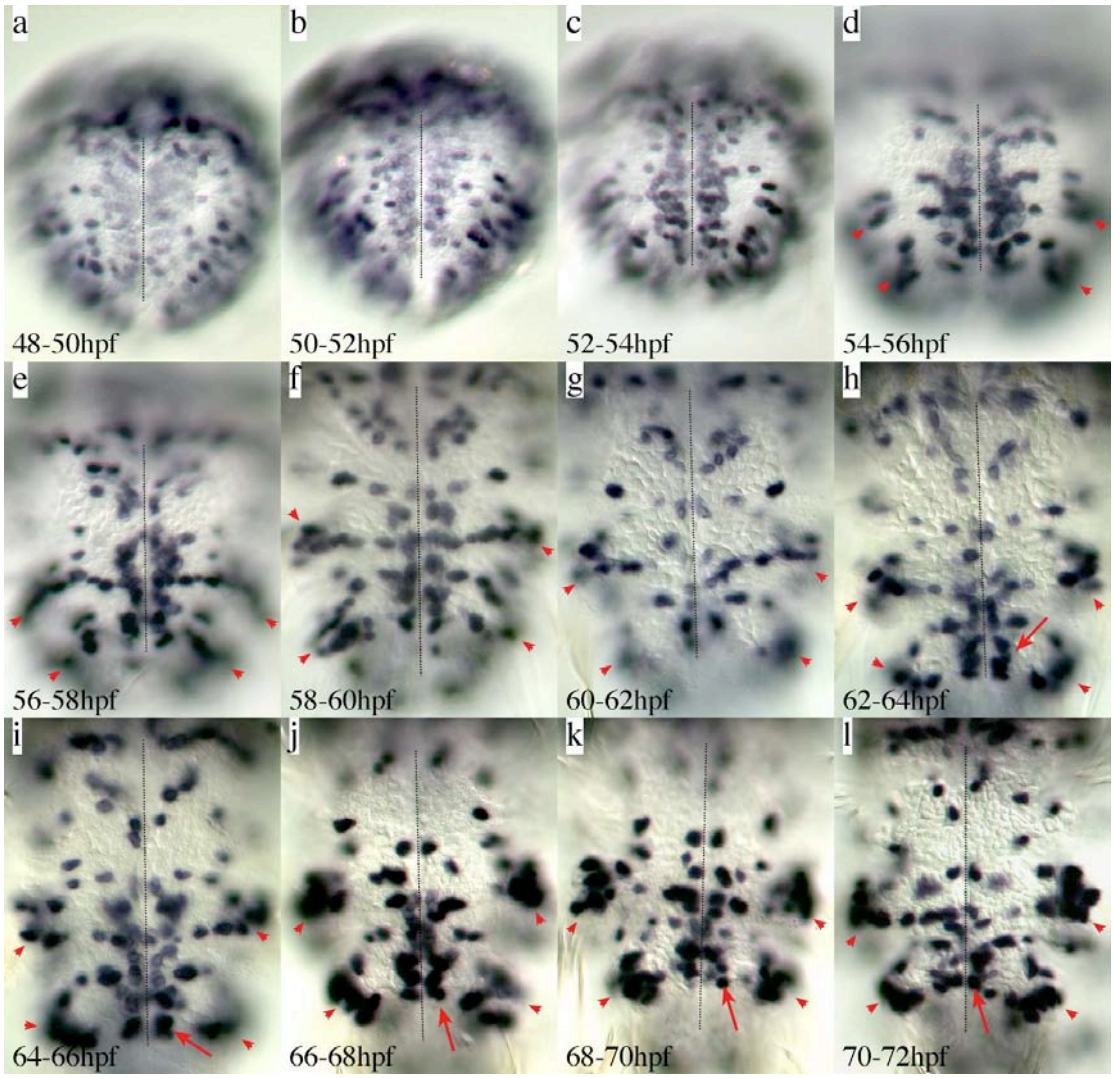

Fig. 30 Cell proliferation in the *Platynereis* neural plate as assayed by BrdU incorporation in 2h intervals between 48hpf and 72hpf.
Red arrowheads: Proliferating cells at the lateral neural plate border of the 2nd and 3rd chaetal sac. Stippled line: neural midline. Ventral views.

Between 48hpf and 52hpf, a broad domain of mitotic cells is located on either side of the midline (**Fig. 30**a,b). From 52hpf onwards, the domain starts to diminish in lateral extent to only 1-2 cell diameters at 58hpf (**Fig. 30**c-e) while larger patches of mitotic cells appear and stay until 72hpf at the lateral neural plate border at the position of the 2nd and 3rd chaetal sacs (**Fig. 30**d-l, red arrowheads). The diminution of proliferating

cells in the neural plate coincides within the beginning of mediolateral cell intercalation documented between 53hpf and 58hpf at 25°C. In the documented period recorded by time-lapse microscopy, the large majority of the neural plate cells are not proliferating (**Fig. 30**d-f). The proliferating areas during this period also match regions where some cells could not be tracked in the documented time-lapse recording: cells next to the midline, at segmental boundaries and at the lateral border of the neural plate (compare **Fig. 30**c with **Fig. 28**a). After 56hpf, the amount of mitotic cells along the midline diminishes further to a few scattered cells except in the third chaetiferous segment where even beyond 64hpf, the number of mitotic cells stays higher (**Fig. 30**h-l, red arrow). The third chaetal segment is also the segment where least cells could be tracked during the time-lapse analysis. Between 64hpf and 72hpf, the neural plate territory anterior of the 3rd chaetiferous segment contains only a few mitotic cells scattered along the midline and at the lateral border. As the majority of neural plate cells do not proliferate during the period where most elongation takes place, a major role for cell division in the elongation process cannot be ruled out but seems rather unlikely.

3.7.2 Cell cycle arrest by Nocodazole treatment has no effect on the elongation of the larva

I have functionally tested the role of mitosis during elongation by incubating embryos in the microtubule depolymerising drug Nocodazole at 0,2ug/ul and 20ug/ul between 48hpf and 72hpf that arrests the cells at the G2/M transition of the cell cycle.

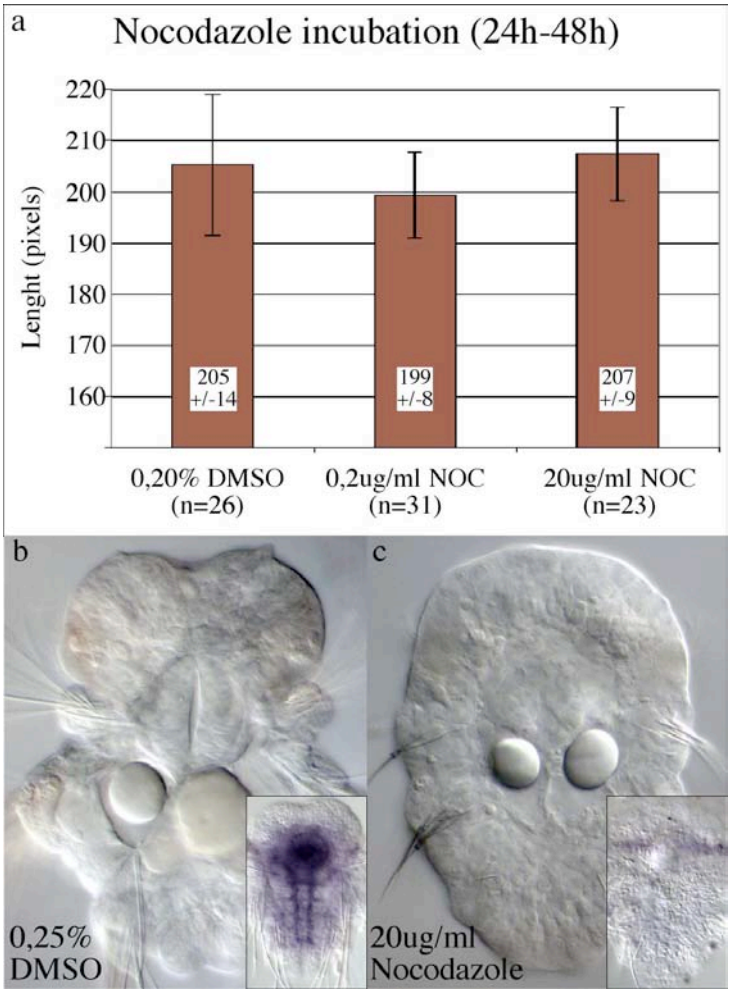

Fig. 31 Microtubule depolymerisation by Nocodazole does not affect elongation of the *Platynereis* larva between 48hpf and 72hpf.
(**a**) Nocodazole treatment does not reduce length significantly at 0,2ug/ml (p=0,13) or 20ug/ml (p=0,48) compared to controls (0,2%DMSO). (**b**, **c**) Nocodazole treatment depolymerises efficiently microtubules (insets: α-tubulin immunohistochemistry) but does not affect elongation in treated embryos (**c**) in comparison to control embryos (**b**). Ventral views. Error bars represent standard deviations. Probabilities calculated with two-tailed Student's t-test assuming equal variance in both samples.

The depolymerisation of microtubules has been controlled by α-tubulin immunohistochemistry (**Fig. 31**b,c, insets). I could not detect any significant reduction in embryo lengths (**Fig. 31**a) at 0,2ug/ml (p=0,13) or 20ug/ml (p=0,48) compared to controls (0,2%DMSO) although the embryos presented severe morphological defects (**Fig. 31**b,c). This rules out a major role for microtubule-dependent processes like cell division in elongating the *Platynereis* trunk neuroectoderm.

3.8 Depolymerisation of F-actin by Cytochalasin B treatment affects elongation of the larva

In vertebrates, mediolateral cell intercalation is dependent on actin-based filo-and lamellipodia (Keller et al., 2000). Although I could not detect filo- or lamellipodia on intercalating cells in the *Platynereis* neuroectoderm, I tested whether elongation in *Platynereis* is an F-actin-dependent process by depolymerising actin filaments using Cytochalasin B at 0,1ug/ml and 2,5ug/ml between 48hpf and 72hpf.

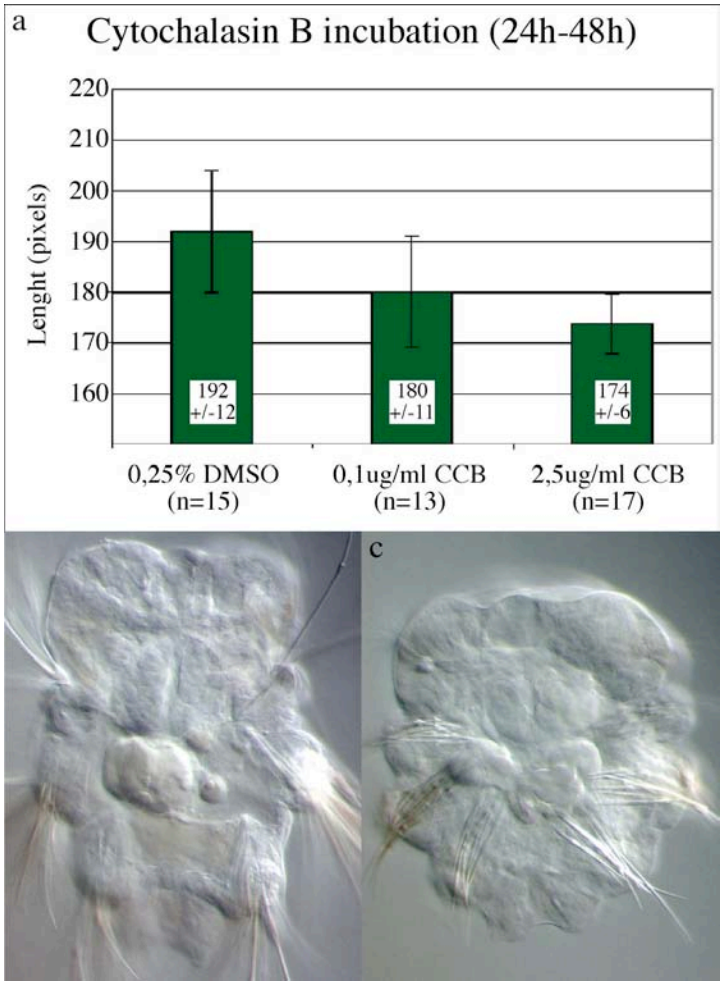

Fig. 32 Actin filament depolymerisation by Cytochalasin B affects elongation of the *Platynereis* larva between 48hpf and 72hpf.
(**a**) Cytochalasin B treatment significantly shortens larva in a concentration-dependent manner ($p_{0,1ug/ml\text{-}2,5ug/ml}$=0,0493) at 0,1ug/ml (p=0,0115) and 2,5ug/ml ($p=4,77*10^{-6}$) compared to 0,25%DMSO-controls. (**b**, **c**) Convergent extension phenotype of Cytochalasin B-incubated (**c**) in comparison to control embryos (**b**). Ventral views. Error bars represent standard deviations. Probabilities calculated with two-tailed Student's t-test assuming equal variance in both samples.

I found a significant, concentration-dependent reduction ($p_{0,1ug/ml\text{-}2,5ug/ml}$=0,0493) in embryo lengths (**Fig. 32**a) at 0,1ug/ml (p=0,0115) and 2,5ug/ml ($p=4,77*10^{-6}$) compared to 0,25%DMSO-controls (**Fig. 32**a). Treated embryos were shorter and wider

than control embryos very much reminiscent of a convergent extension phenotype (**Fig. 32**b,c). This shows that elongation is dependent on actin filaments, supporting the role of cell intercalation as a driving force for elongation by either still unidentified lamellipodia or by other actin-dependent cellular mechanisms like membrane rearrangements (Bertet et al., 2004).

3.9 Expression of members of the non-canonical Wnt pathway

Similarities between *Platynereis* and vertebrate convergent extension by mediolateral cell intercalation suggest that the non-canonical Wnt pathway, controlling mediolateral cell intercalation in vertebrates (Jessen et al., 2002), might also be conserved to control *Platynereis* convergent extension movements. One way to test this hypothesis was to analyse the expression of several specific members of the non-canonical Wnt pathway.

3.9.1 Pdu-strabismus

strabismus is a conserved five-transmembrane-domain protein that in *Drosophila* gets asymmetrically localised intracellularly to pattern the planar polarity of a cell upon non-canonical Wnt signalling.

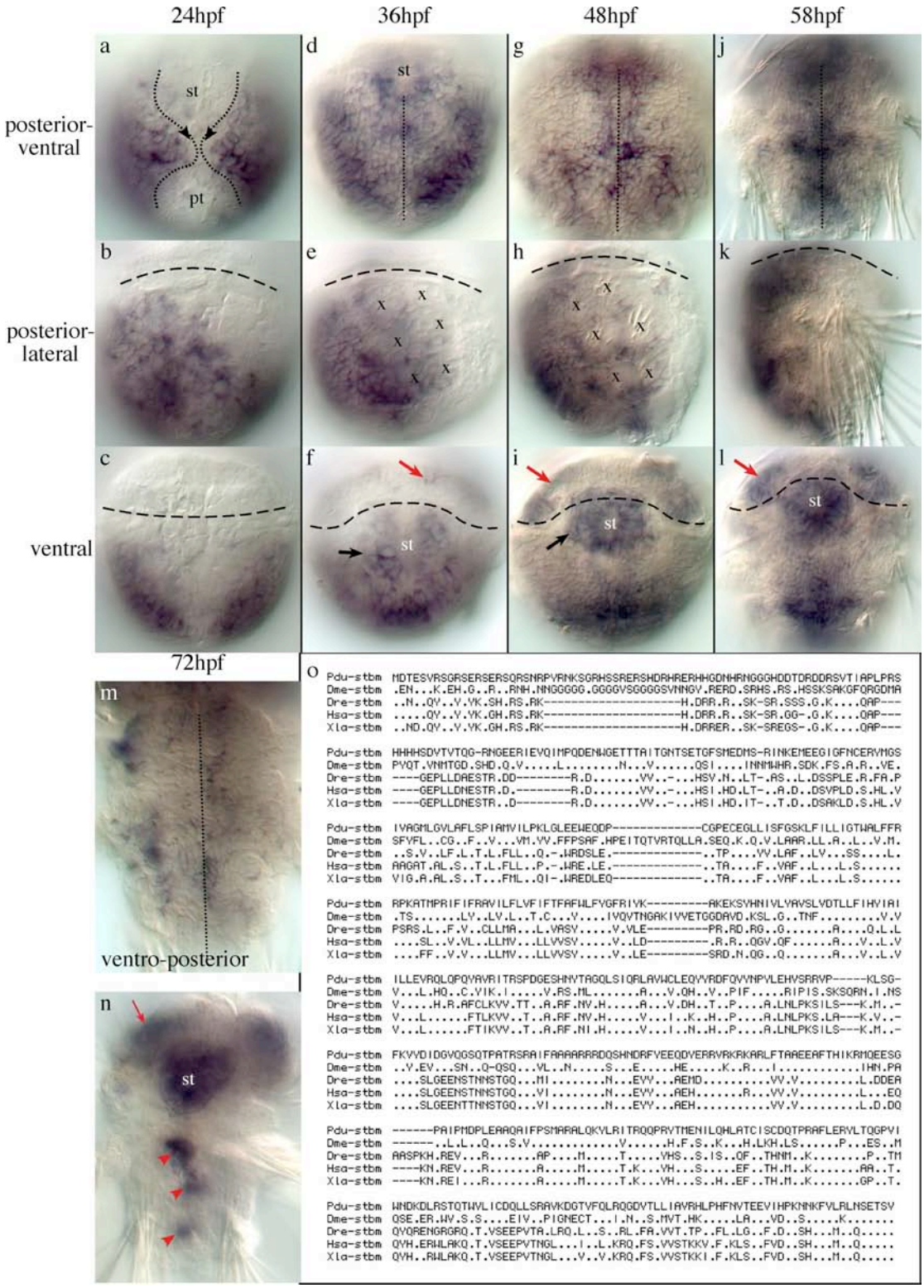

Fig. 33 Expression at different stages (**a**-**n**) and multiple sequence alignment (**o**) of *Pdu-strabismus.* Black arrow: expression in the mesodermal envelope around the stomodaeum. Red arrows: Expression in the brain region. Black arrowheads: Cells of left and right neural plate fusing at the future neural midline and exempt of *Pdu-strabismus* expression. Red arrowheads: Expression in prospective midgut cells. Dotted line: Blastopore margin giving rise to the neural midline. Dashed line: Prototroch. pr: proctodaeum; st: stomodaeum. "x": position of chaetal sacs. In **o**: dots represent amino acid identity; dashes represent gaps in the alignment. Species abbreviations: Dme: *Drosophila melanogaster*; Dre: *Danio rerio*; Hsa: *Homo sapiens*; Pdu: *Platynereis dumerilii*; Xla: *Xenopus laevis*. Accession numbers can be found in the materials and methods section.

I have cloned the *Platynereis* orthologue of *strabismus* the identity of which was confirmed by multiple sequence alignments with other *strabismus* orthologues (**Fig. 33**o). Pdu-*strabismus* is expressed as early as 24hpf in the entire future neural plate (except in the cells meeting along the midline; (**Fig. 33**a, arrowheads), and compare with **Fig. 34**a) and reaches laterally into the prospective chaetal sac region (**Fig. 33**b,e,h). On the ventral side at 24hpf, the prospective stomodaeal, endomesodermal midline and proctodaeal cells are free of expression marking the borders of the fusing neural plate (**Fig. 33**a "st", "pr", also compare with **Fig. 26**c and h). The episphere (**Fig. 33**b,c above the prototroch (dashed line)) and the dorso-anterior side are free of expression (**Fig. 33**b,c). At 36hpf, Pdu-strabismus is expressed in the neural plate (**Fig. 33**d) and the ventral chaetal sacs (**Fig. 33**e). Expression also appears in the forming stomodaeum (**Fig. 33**d,f, "st") and mesodermal cells surrounding the stomodaeum (**Fig. 33**f, black arrow) and very faintly in the ventral part of the episphere (**Fig. 33**f, red arrow). At 48hpf, the expression in the neural plate gets restricted to cells along the midline in the region of the first chaetal segment while it is down regulated laterally (**Fig. 33**g). *Pdu-strabismus* keeps being expressed broadly in the neuroectodermal region of approximately the second and third chaetal segment (**Fig. 33**g). Laterally, ectodermal *Pdu-strabismus* expression protrudes in-between the ventral chaetal sacs, but keeps the dorsal sacs free (**Fig. 33**h). The expression in the stomodaeum (**Fig. 33**i, "st"), stomodaeal mesoderm (**Fig. 33**i, black arrow) and ventral episphere (**Fig. 33**i, red arrow) appears stronger than at 36hpf. At the 58hpf stage, belonging to the documented period during which mediolateral cell intercalation elongates the embryo, *Pdu-strabismus* is strongly expressed in a few cell rows left and right of the midline and broadens approximately at the level of the second chaetal sac (**Fig. 33**j). Laterally, *Pdu-strabismus* appears restricted to the ventral plate and lateral ectodermal protrusions between the ventral chaetal sacs (**Fig. 33**k). Expression in the stomodaeal mesoderm is not apparent anymore, but persists in the stomodaeum (**Fig. 33**l, "st") and the ventral episphere (**Fig. 33**l, red arrow). At 72hpf, when most of the elongation has taken place (see 3.5), *Pdu-strabismus* is lost from most neural plate cells and remains in a few scattered cells along the midline (**Fig. 33**m). The expression in stomodaeum (**Fig. 33**n, "st") and episphere (**Fig. 33**n, red arrow) remain strong, while *Pdu-strabismus* appears strongly expressed in the forming midgut (**Fig. 33**n, red arrowheads).

3.9.2 Pdu-four-jointed

Four-jointed has been described in *Drosopila* as a member of the planar cell polarity pathway (non-canonical Wnt pathway) acting upstream of *strabismus*, but has not yet been described during vertebrate gastrulation. Although its role is not fully understood yet, it is thought to modulate the binding properties of some cadherins (like *fat* or *dachsous*) in the Golgi apparatus (Strutt et al., 2004). Although it is not secreted extra-cellularly, it has been found expressed in a gradient throughout the *Drosophila* eye and wing discs (Strutt et al., 2004). As it acts prior to the intracellular localisation of e.g. *strabismus*, it has been proposed to pre-pattern the planar polarity in the wing disc via modulation of cadherins.

I have analysed the expression of *four-jointed* that has been identified during a random EST sequencing project carried out in the lab. The sequenced 5'end of the EST clone (48-12-01-C) codes for the N-terminus of a protein that has similarities to *four-jointed* orthologues in vertebrates and insects and no similarity to any other metazoan protein family (in BLAST searches, not shown) (**Fig. 34**h).

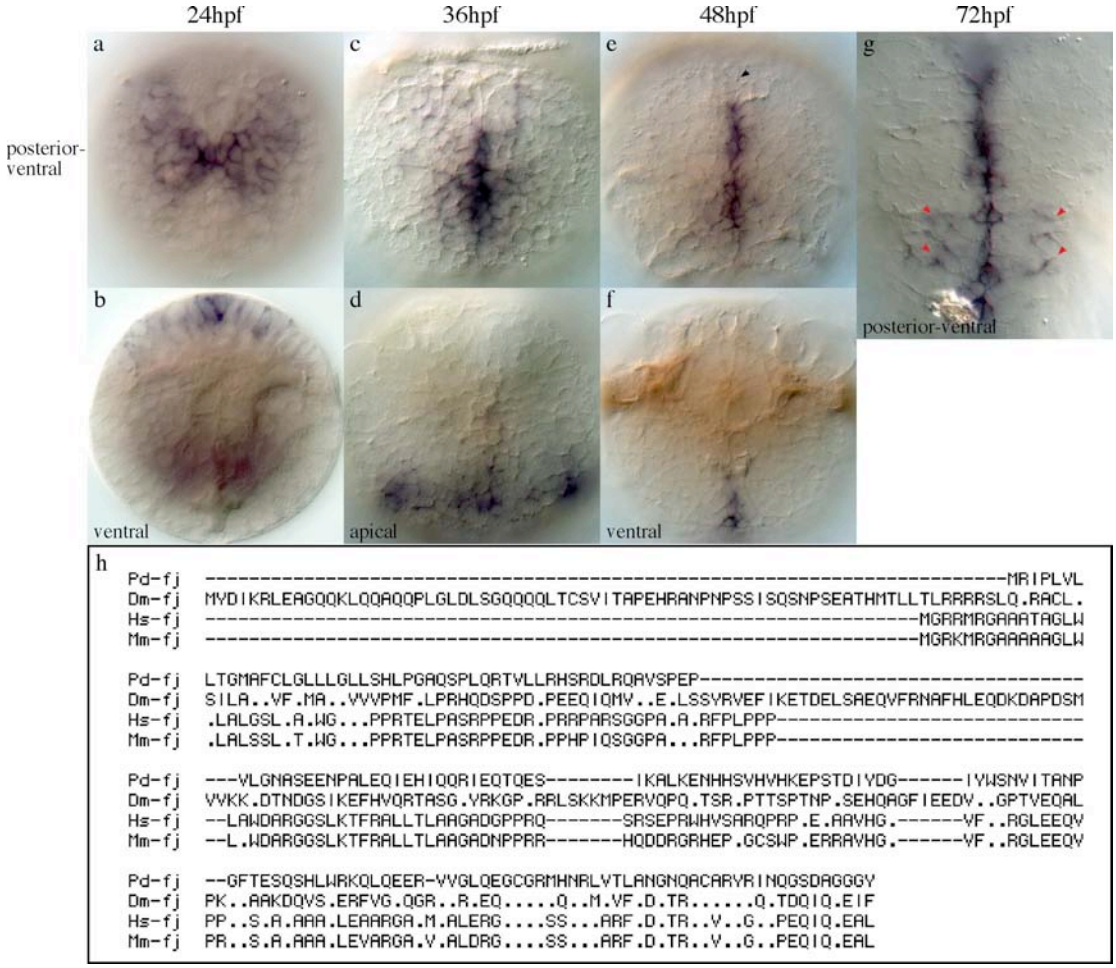

Fig. 34 Expression at different stages (**a**-**g**) and multiple sequence alignment of the N-terminus (**h**) of *Pdu-four-jointed*.
a-**g**: Black arrowhead: Lack of expression in the peristomium. Red arrowheads: Expression in the lateral neural plate. **h**: Species abbreviations: Dm: *Drosophila melanogaster*; Hs: *Homo sapiens*; Mm: *Mus musculus*; Pd: *Platynereis dumerilii*. Dots represent amino acid identity with *Pdu-four-jointed*. Dashes represent gaps in the alignment. Accession numbers can be found in the materials and methods section.

Pdu-jointed is expressed in a very conspicuous manner in the most ventral cells of the fusing neural plate at 24hpf, probably co-expressed in major parts with *Pdu-strabismus* (compare **Fig. 34**a with **Fig. 33**a). It appears to be expressed in a gradient with highest expression in the cells that have just touched along the fusing midline (compare **Fig. 34**a with **Fig. 26**c and h) and gradually decreasing laterally. Another domain of expression is located in a few median cells of the episphere (**Fig. 34**b). At 36hpf, after the fusion of the neural plate, *Pdu-four-jointed* is expressed in and lateral of the midline cells in a steeper gradient than at 24hpf (**Fig. 34**c). The brain expression is restricted to the ventral-most cells (**Fig. 34**d). *Pdu-four-jointed* is restricted to the midline cells at 48hpf and is absent from the most anterior part of the neural plate that supposedly belongs to the *otx*-expressing peristomium (compare **Fig. 34**e, arrow-

head with **Fig. 11**a). At 72hpf, it keeps being expressed in the midline cells but also appears in a few more lateral cells of the third chaetal segment (**Fig. 34**g, red arrowheads).

3.9.3 Pdu-dachsous

The *dachsous* gene is expressed in an opposing gradient to *four-jointed* in the *Drosophila* wing disc and has been proposed as a target of *four-jointed* to pattern the planar polarity within the epithelium of the *Drosophila* eye and wing discs. Although *dachsous* has no described function during vertebrate convergent extension, I have cloned and analysed the expression of *Pdu-dachsous*.

I have cloned a fragment coding for a 173 amino acids stretch of the *Platynereis dachsous* cadherin that only shows similarities to other *dachsous* orthologues near the C-terminal, cytoplasmic tail (**Fig. 35**). This domain is specific to *dachsous* orthologues and cannot be found in cadherins of other subfamilies (not shown).

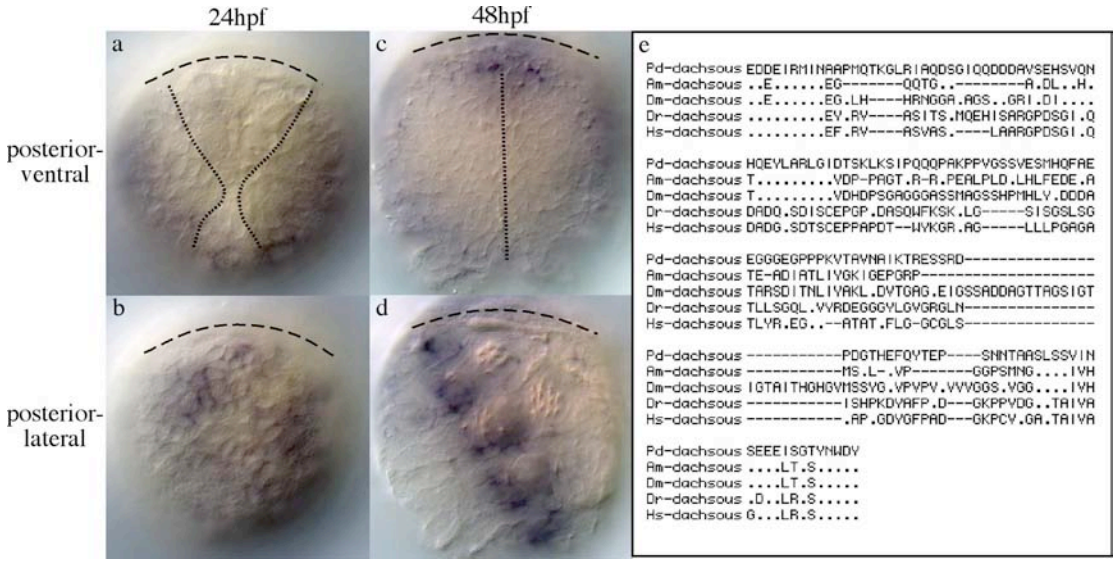

Fig. 35 Expression at different stages (**a**-**d**) and multiple sequence alignment of the cloned fragment (**e**) of *Pdu-dachsous*.
(**a**-**d**): Dotted line: Blastopore margin giving rise to the neural midline. Dashed line: Prototroch. (**e**) Species abbreviations: Am: *Apis millifera*; Dm: *Drosophila melanogaster*; Dr: *Danio rerio*; Hs: *Homo sapiens*; Pd: *Platynereis dumerilii*. Dots represent amino acid identity in comparison to the *Pdu-dachsous* sequence. Dashes represent gaps in the alignment. Accession numbers can be found in the materials and methods section.

At 24hpf, *Pdu-dachsous* expression is restricted to the dorsal and lateral ectoderm in the hyposphere (**Fig. 35**a,b), probably co-expressed with *Pdu-strabismus* (compare **Fig. 35**b with **Fig. 33**b). The ventral side that shows graded *Pdu-four*-jointed expres-

sion is free of *Pdu-dachsous* expression (**Fig. 35**a). A gradient of expression cannot be discerned for *Pdu-dachsous*. The data does not allow a conclusion on possible co-expression of both genes (compare **Fig. 35**a with **Fig. 34**a).

The lack of *Pdu-dachsous* expression in the neural plate at 48hpf excludes a direct role in mediolateral cell intercalation (**Fig. 35**c). At this stage, *Pdu-dachsous* is found to be expressed in the ectoderm between the neural plate and the ventral chaetal sacs. These cells also express *Pdu-strabismus* (compare **Fig. 35**d with **Fig. 33**h).

3.10 Chemical inhibition of Jun N-terminal kinase (JNK) by SP600125 affect elongation of the larva

I have functionally analysed the role of the non-canonical Wnt pathway by inhibiting the downstream target Jun N-terminal kinase (JNK) with the chemical inhibitor SP600125 (Bennett et al., 2001) between 48hpf and 72hpf at a concentration of 2,5uM and 25uM in comparison to 0,25%DMSO-incubated embryos.

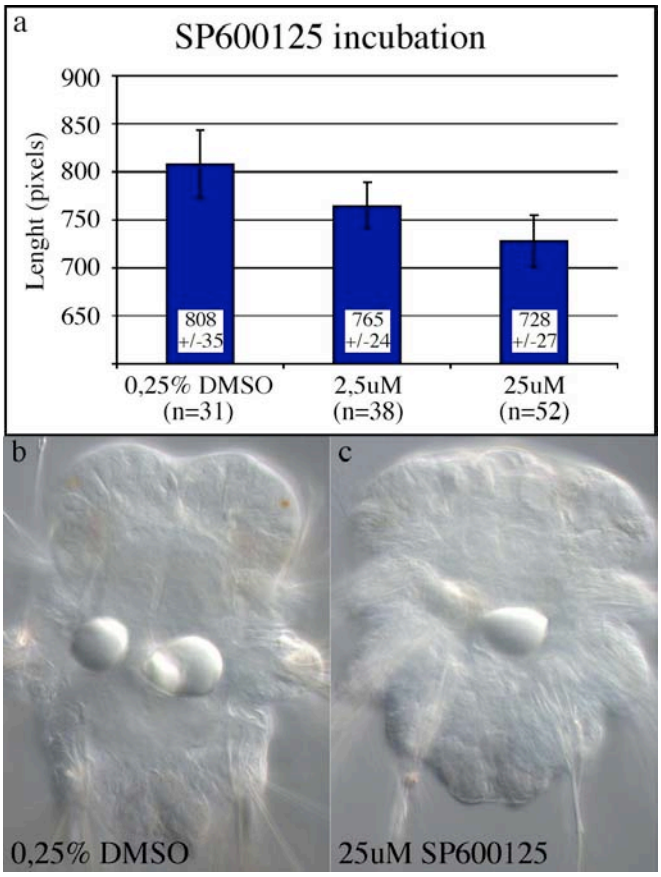

Fig. 36 Jun N-terminal kinase inhibition by SP600125 incubation affects elongation of the *Platynereis* larva between 48hpf and 72hpf.
SP600125 treatment significantly shortens larva in a concentration-dependent manner ($p_{2,5ug/ml-25ug/ml}=3,96*10^{-9}$) at 2,5uM ($p=8,74*10^{-8}$) and 25uM ($p=3,68*10^{-18}$) compared to 0,25%DMSO-controls. (**b**, **c**) Convergent extension phenotype of SP600125-incubated (**c**) in comparison to control embryos (**b**). Ventral views. Error bars represent standard deviations. Probabilities calculated with two-tailed Student's t-test assuming equal variance in both samples.

I have observed that SP600125 treatment significantly shortens larvae in a concentration-dependent manner ($p_{2,5ug/ml-25ug/ml}=3,96*10^{-9}$) at 2,5uM ($p=8,74*10^{-8}$) and 25uM ($p=3,68*10^{-18}$) compared to 0,25%DMSO-controls (**Fig. 36**a). Upon inhibition, embryos looked shorter and wider than control embryos very much reminiscent of a convergent extension phenotype and strongly resembling Cytochalasin B-incubated embryos (compare **Fig. 36**c to **Fig. 32**c).

I have analysed the axonal scaffold of treated embryos by acetylated α-tubulin immunohistochemistry to determine whether the elongation defect could be due to a general misdevelopment of the ventral neuroectoderm.

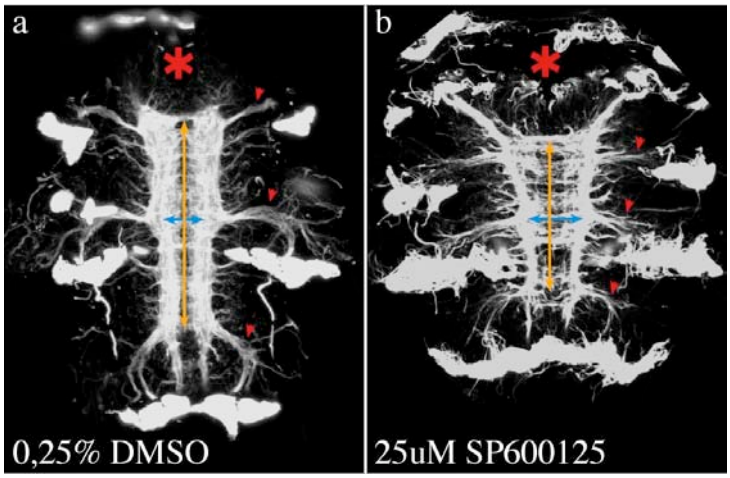

Fig. 37 Axonal scaffold of SP600125-treated embryo (**b**) in comparison to control embryos (**a**). Reconstructions of confocal sections of acetylated α-tubulin immunostainings. Asterisk: mouth opening. Red arrowhead: parapodial axonal bundles. Orange arrows: length between most anterior and posterior trunk commissural axons is reduced in SP600125-incubated embryos in comparison to control embryos. Blue arrows; connectives at the level of the second parapodial axonal bundles are further apart in SP600125-incubated embryos in comparison to control embryos.

The axonal scaffold in treated embryos is at 72hpf similar to its appearance at 48hpf and has failed to undergo convergent extension (**Fig. 37**b). The distance between the substomodaeal commissure and the connective of the fourth larval segment is shorter (**Fig. 37**, orange arrow) and the longitudinal axons are further apart (**Fig. 37**, blue arrow). Besides its failure to converge and extend, it appears to present an axonal fasciculation defect. Especially the two longitudinal axonal tracts in the control embryo appear thicker and more compact than in the treated embryo, where the axons appear frayed and less fasciculated. This is likely not due to a general retardation of the embryo's development because the two paratrochs, the ciliary bands at the posterior border of the larval segments II and III that cannot be detected at 48hpf, have fully developed in treated embryos.

Also the axons innervating the parapodia have grown out, but also appear to be more frayed than in control embryos (**Fig. 37**, red arrowheads).

4 Discussion

4.1 The molecular regionalisation of the Platynereis larval neuroectoderm

The analysis of the developing axonal scaffold and the molecular regionalisation of the *Platynereis* larval neuroectoderm by homeobox transcription factors supports the traditional primary tripartite subdivision of the polychaete larva into pro-, peri- and metastomium based on morphological characters (Hatschek, 1878; Schroeder and Hermans, 1975). The patterning of the different regions, as can be judged by the expression of the analysed regionalisation genes, occurs between 19hpf and 24hpf with the exception of the peristomium. Between 19hpf and 24hpf, almost all analysed genes get expressed in a region-specific pattern implying their role in regionalisation, e.g. the refinement of ectodermal *Pdu-six3* expression to the prostomium or the segmental appearance of *Pdu-engrailed* and *Pdu-gbx*. Therefore, the 24hpf stage has been taken as reference to compare the expression of regionalisation marker genes to each other and to other phyla.

4.1.1 The primary subdivision of the *Platynereis* larva

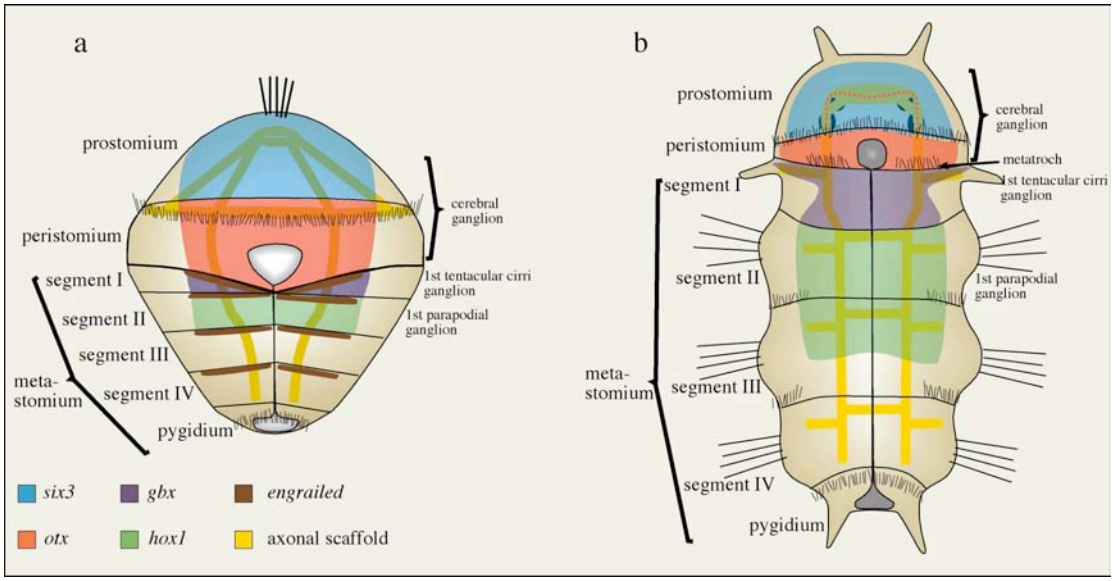

Fig. 38 Schematic representation and fate of neuroectodermal regions specified by *Pdu-six3* (blue), *Pdu-otx* (red), *Pdu-gbx* (purple), *Pdu-hox1* (green) and *Pdu-engrailed* (brown) at 48hpf (**a**) and 72hpf (**b**).

4.1.1.1 The prostomium

The pre-oral prostomium located anterior of the prototroch ciliated band bears the ciliated apical organ plexus as in many other polychaete larvae (Lacalli, 1981). It is mainly composed of neurosecretory cells (K. Tessmar-Raible, unpublished). In nereidids, the cerebral ganglion connects to antennae, palpae, nuchal organs (Gilpin-Brown, 1958; Orrhage, 1993) and adult eyes (Arendt et al., 2002) and harbours the ciliary photoreceptors (Arendt et al., 2004). I have shown that together with parts of the peristomial prototroch nerve ring, it develops into the cerebral ganglia of the juvenile and adult worm. I propose *Pdu-six3* as a regionalisation marker broadly covering the prostomial neuroectoderm (**Fig. 38**, blue) that is posteriorly encircled by the *Pdu-otx* expressing peristomium (**Fig. 38**, red). The fate of the few cells co-expressing both genes in the ventral apical organ region and at the dorsal rim of the prostomium is not known (**Fig. 10**e). The larval eye photoreceptors situated in the lateral larval head would have been a candidate cell type that co-expresses both transcription factors (Nishida et al., 2003; Toy et al., 1998; Vandendries et al., 1996; Zuber et al., 2003), but I could not find any co-expressing cells at the respective position in the lateral head. The affiliation of the larval eyes to either the *six3* or *otx* territory was also not possible because a molecular marker to relate the position of the larval eyes to either gene was not available. The apical organ region is devoid of *Six3* expression. In contrast to the larval eyes, the *Pdu-otx* and *Pdu-six3* expression at 48hpf indicates co-expression in the prospective adult eyes anlagen (Arendt et al., 2002). The comparison of the prostomium with body and brain regions of deuterostomes and arthropods will be discussed later.

4.1.1.2 The peristomium

The peristomium has been defined as the region surrounding the mouth, including the prototroch and posteriorly demarcated by the metatroch (Schroeder and Hermans, 1975). It bears the prototroch nerve ring. I have shown that the part of the nerve ring in-between the ventral and dorsal connectives to the apical organ plexus forms a major part of the dorsal root entering the juvenile cerebral ganglion. Consequently, the juvenile cerebral ganglion has contributions from the pro- and the peristomium (**Fig. 38**). The fate of the rest of the prototroch nerve ring is unknown and gets either integrated into the cerebral ganglion or disappears.

The early regionalisation of the peri-oral peristomium marks an exception during the development of the *Platynereis* larva. *Pdu-otx* is already at 19hpf and before (not shown) a marker clearly demarcating the primary and accessory cells of the prototroch ciliated band (Arendt et al., 2001). The reason for the early patterning of the peristomium might be that the differentiation of the prototroch, indispensable for larval locomotion and dispersal, occurs before larval hatching at about 16hpf. In *Platynereis*, the metatroch ciliated cells that morphologically determine the posterior border of the peristomium (Rouse, 1999; Schroeder and Hermans, 1975) can be detected earliest at 48hpf by α-tubulin mRNA detection. They posteriorly delimitate the *Pdu-otx* expressing region that includes the prototroch and is delimitated by the metatroch (**Fig. 11**b,d). *Pdu-otx* therefore fulfils the requirements as a regionalisation marker for the peristomium (**Fig. 38**, red). The region between prototroch and metatroch constitutes the mouth field that surrounds the mouth opening. In other polychaete larva, this region bears food-collecting cilia. The late appearance of the metatroch and the lack of cilia in the *Platynereis* mouth field is probably a secondary loss in adaptation to the lecithotrophic feeding mode. The expression of *otx* orthologues in ciliary bands surrounding the mouth of deuterostome primary larvae supports the homology of the mouth openings between protostome and deuterostome primary larvae and the ciliary bands that surround them (Arendt et al., 2001). The homology of the peristomium with deuterostome and arthropod body regions will be discussed later.

Prior to the appearance of the metatroch, *Pdu-otx* expression in the mouth region (**Fig. 38**a,b, red) is posteriorly bound by the expression of the first *Pdu-engrailed* stripe (**Fig. 15** and **Fig. 38**a,b, brown), marking the anterior boundary of the first larval segment. This shows that the larval peristomium is positioned anterior of the first larval segment and does not represent a metameric segment as speculated by some authors (Anderson, 1973; Goodrich, 1897). Notably, the adult peristomium in *Platynereis* is a compound structure that results from the fusion of the larval peristomium (non-metameric) and the first two metameric larval segments.

4.1.1.3 The metastomium

The metatroch ciliary band located at the border between peristomium and metastomium represents the morphologically important head-trunk boundary in *Platynereis* (**Fig. 38**b). It also splits the larva into the ontogenetically radial-symmetric head (originating from all four quadrants) and the ontogenetically bilateral-symmetric trunk (originating from the 2d somatoblast) (Ackermann et al., 2005; Nielsen, 2004). The metastomium is secondarily subdivided into the larval segments as will be discussed in the next section. It is also a fundamental morphogenetic boundary and represents the anterior border of the converging and extending trunk neuroectoderm as discussed later.

4.1.2 The secondary subdivision of the *Platynereis* larva

The number of metameric larval segments developing during the secondary subdivision of the metastomium has long been disputed due to the controversial metameric nature of the first tentacular cirri. I present evidence that the larval trunk consists of four larval segments and that the first tentacular cirri originate from an incomplete, first larval segment located anterior of the first chaetiferous segment as proposed before (**Fig. 38**)(Gilpin-Brown, 1958; Hempelmann, 1911; Rouse and Pleijel, 2001). At 24hpf, the ectoderm of the metastomium is morphologically uniform but the subdivision into four metameric segments (although only three chaetiferous segments develop) is already molecularly apparent by four *Pdu-engrailed* stripes (**Fig. 14**b and **Fig. 38**a, brown) marking the anterior segment boundaries (**Fig. 13**). I have shown that the first incomplete *Pdu-engrailed* stripe (fused ventrally to the second stripe) represents the anterior border of an incomplete segment anterior of the first chaetiferous segment (**Fig. 38**). Similarly to the following chaetiferous segments, it shows a structure reminiscent of a chaetal sac at the position of the future first tentacular cirri. In addition, the metameric nature of the tentacular cirri is supported by their common clonal origin with all other larval metameric segments from the 2d micromere and their similarity to second tentacular cirri that develop by metamorphosis of the first pair of parapodia (Ackermann et al., 2005). Unusually, the axonal projections of the first tentacular cirri (in larval segment I) project onto the circumoesophageal connectives without forming a detectable commissure (**Fig. 38**b, yellow line in the segment I). This distinguishes the first larval segment from all following segments. It could

either be a result of cephalisation due to the secondary reduction of the parapodia of first larval segment or it is primarily simple and has never possessed parapodia. In other polychaete species, though, the first larval segment (comparable to the first, reduced larval segment in *Platynereis*) undergoes secondary reduction and subsequent cephalisation, as described in the *Hydroides* (formerly known as *Eupomatus*, Serpulidae), *Pisione* (Aphroditiformia), *Pholoe* (Aphroditiformia) and *Protula* (Sabellida) (Åkesson, 1963). Similar as in nereidids, the corresponding ganglia of the reduced first larval segment are localised on the circumoesophageal connectives left and right of the mouth opening (Åkesson, 1963).At 24hpf, the neuroectoderm of the first larval segment is marked by the expression of the most anterior stripe of *Pdu-gbx* (**Fig. 18**d, arrow, and **Fig. 38**, purple).

The second larval (first chaetiferous) segment expresses the second *Pdu-engrailed* stripe at its anterior border (**Fig. 38**a, brown) and harbours, as in *Chaetopterus* (Irvine and Martindale, 2000), the anterior expression boundary of *Pdu-hox1* (**Fig. 21**d, **Fig. 38** green). Notably, *Pdu-hox1* does not co-localise with *Pdu-engrailed* and therefore does not mark the anterior border of the second larval segment in *Platynereis*. In *Chaetopterus*, the precise anterior boundary of *hox1* has not been determined (Irvine and Martindale, 2000) and *engrailed* is not marking segment boundaries (Seaver et al., 2001). A comparison with arthropod segments and vertebrate brain regions will be made later.

The expression of *Pdu-hox1* in the region of the apical organ is unusual as it is expressed anterior of the *otx* domain. Remarkably, a similar situation exists in vertebrates where a *hox1* orthologue is expressed at the fore-/midbrain boundary (McClintock et al., 2003).

4.2 The subdivision and molecular patterning of the Platynereis *mesoderm*

The *Platynereis* mesoderm has several ontogenetic origins. The major part is giving rise to the trunk mesoderm and derives from the 4d micromere as typical for animals with spiral cleavage. In addition to the trunk mesoderm founder cell, “ectomesodermal” founder cells were identified in many animals with spiral cleavage. In those

animals, some mesodermal contribution also derives from the 3rd quartet (most polychaetes and many molluscs), 2nd quartet (many molluscs and nemerteans, only described for one polychaete species: *Polygordius*) or very atypically from the 1st quartet (in Echiura) (Boyer et al., 1996). In *Platynereis*, it has been proposed that the 3rd quartet is a major source of "ectomesoderm" (Ackermann et al., 2005).

4.2.1 The molecular characterisation of the *Platynereis* head "ectomesoderm"

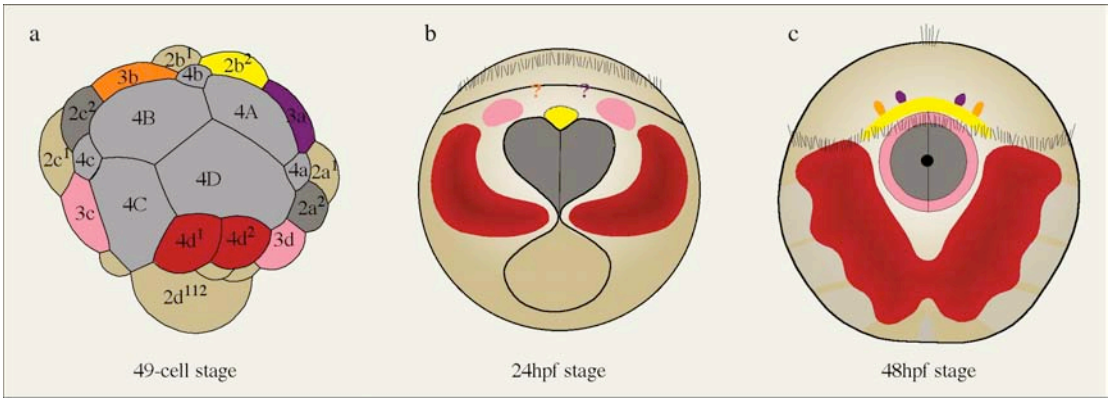

Fig. 39 Schematics depicting putative origin and localisation of the mesoderm in *Platynereis dumerilii*.
(**a**, **b**): Views onto the blastopore. (**c**): Ventral view. Dark grey; stomodaeal precursors. Light grey: endoderm precursors. Red: 4d descendants. Rose: stomodaeal envelope precursors. Orange: 3b descendants. Purple: 3a descendants. Yellow: $2b^2$ descendants. The position of the 3a and 3b descendants is unknown in a 24hpf larva. The fate of the $2b^2$, 3a and 3b descendants is speculative at 48hpf. **a** modified after (Ackermann et al., 2005).

I have found molecular markers that characterise the ectomesodermal populations recently determined by cell lineage tracings in the 4-5 days old *Platynereis* head (Ackermann et al., 2005):

Cells in the region "of the great central commissure of the brain" are proposed to be descendants of the 3a and 3b micromeres (Ackermann et al., 2005). I have found *Pdu-six3* expressing cells (**Fig. 39**c, yellow) located in a very similar position between the neuropil of the cerebral ganglion and the (mesodermal) stomodaeal envelope (**Fig. 8** and **Fig. 39**c, pink). Some *Pdu-six3* cells also express *Pdu-fgfr* and *Pdu-twist* in a more temporally and spatially restricted fashion (**Fig. 8** and **Fig. 12**). The co-expression still has to be shown by double fluorescent *in situ* hybridisation of *Pdu-six3*, *Pdu-fgfr* and *Pdu-twist*. The mesodermal identity of these cells cannot be stated beyond doubt. If *Pdu-fgfr* and *Pdu-twist* act as differentiation genes, it is highly probable that these cells have a mesodermal identity. Alternatively, both genes have been

shown to play essential roles in epithelial-mesenchymal transitions (Ciruna and Rossant, 2001; Yang et al., 2004) and could also control the internalisation of the cells from the surface of the larva. This would not necessarily mean that these cells adopt a mesodermal identity. The expression of *Pdu-six3*, assuming it is stably expressed and can be used as a reliable marker to follow cells through development, gives valuable insights in the origin and morphogenesis of this prospective "brain mesoderm". In an early trochophore, the prospective "brain mesoderm" cells appear embedded within the *Pdu-six3* expressing stomodaeal region (**Fig. 8**a,b and **Fig. 39**b, dark grey) and bulge out anteriorly at 24hpf (**Fig. 8**c and **Fig. 39**b, yellow). This is reminiscent of the enterocoel mode of mesoderm formation from pouches of the digestive tract (Remane, 1950; Tautz, 2004). The cells that bulged out from the stomodaeal region form a single cluster of cells (**Fig. 8**d,f) anterior of both the stomodaeum (**Fig. 39**c, dark grey) and the mesodermal stomodaeal envelope (**Fig. 39**c, pink) that are both of paired origin (**Fig. 39**a, pink, dark grey) (Ackermann et al., 2005). The proposed movements of the cells during larval development can be shown by tracing the cells using either transgenesis (with a *Pdu-six3* promotor-GFP construct) or by photo-inducing caged GFP in the putative precursor cells discussed in the next paragraph.

I propose that at least some of the *Pdu-six3* expressing cells originate from the $2b^2$ micromere in contrast to the 3a and 3b cells, as proposed by Ackermann, for several reasons. First, the $2b^2$ is located at the anterior border of the blastopore at the 49-cell stage (**Fig. 39**a yellow), at the corresponding position where the cells will bulge out at 24hpf (**Fig. 39**b, yellow). Secondly, the corresponding micromeres $2a^2$ and $2c^2$ from other quadrants give rise to the stomodaeum (**Fig. 39**a, dark grey) while their sister cells $2a^1$ and $2c^1$ adopt and epidermal fate (Wilson, 1892). Wilson has even considered the $2b^2$ micromere to be the median stomatoblast although cell lineages have recently proven that the B quadrant does not contribute to the stomodaeum (Ackermann et al., 2005; Wilson, 1892). Therefore, $2b^2$ might form part of the stomodaeal region in the early trochophore, explaining the initial position of the prospective "brain mesoderm" cells before undergoing out-bulging as described. Third, cell lineage tracings have shown that the cells located at a similar position as the *Pdu-six3* cells are entirely labelled upon injection of the 1B macromere (Ackermann et al., 2005), reducing the probability of a major contribution of the A quartet (and therefore the 3a

micromere), but still leaving the possibility of a major contribution of 3b. The contribution of the 3a and 3b micromeres might still be mesodermal, but restricted to the developing head muscles as discussed in the forthcoming section.

a) The four (horn-like) paired strands of muscles of which one pair forms at the base of the antennae have also been proposed as being 3a and 3b derivatives (Ackermann et al., 2005). Cells corresponding by position and shape to these horns have already been described by *Pdu-fgfr* marker gene expression and their presumptive identity as antennal and palpal muscle anlagen is now confirmed by the presence of *Pdu-myoD* transcripts (**Fig. 39**c, orange and purple) (Steinmetz, 2002). An epithelial continuity of at least one pair of horns with the trunk muscle strands that reach into the head suggests a common clonal origin, but cell lineage tracings have clearly shown a non-4d origin of the horns. They might be the only contribution of the 3a and 3b micromeres to the head mesoderm (**Fig. 39**a, orange, purple). The localisation of their precursor cells in a 24hpf embryo is not known (**Fig. 39**b).

b) The left and right "half-envelopes" of the stomodaeum are most probably derived from the 3c (right) and 3d (left) micromeres (**Fig. 39**a-c, pink) (Ackermann et al., 2005) and express the mesodermal marker genes *Pdu-fgfr* and *Pdu-twist*. A subset of those cells also expresses *Pdu-tinman* and *Pdu-bagpipe*, two NK2-class genes that mark heart (only *tinman*) and visceral mesoderm (*tinman* & *bagpipe*) in *Drosophila* (Azpiazu and Frasch, 1993; Bodmer, 1993) (G. Balavoine, unpublished, personal communication). *Pdu-fgfr* marks the entire envelope, while *Pdu-twist* is only expressed in a subset of cells. In contrast to the "brain mesoderm" precursors, the paired origin of the stomodaeal sheath lateral of the stomodaeal region is apparent at 24hpf by the bilateral-symmetric expression of *Pdu-fgfr* as a robust marker of the stomodaeal sheath in two patches of cells anterior-lateral of the developing stomodaeum (**Fig. 39**b, pink). The paired arrangement of the precursor cells supports the proposed descendance from the 3c and 3d cells (**Fig. 39**a, pink).

c) Two pairs of mesodermal strands in the pre-trochal head are 4d descendants. They can be distinguished as an epithelial sheath surrounding the stomodaeal envelope from posterior as described by *Pdu-myoD* expression analysis at 72hpf. The position and origin of those strands have been confirmed by expression of muscle differentiation genes identified by a random EST expression screen performed in the lab (not shown).

4.2.2 The molecular characterisation of the *Platynereis* trunk mesoderm

The development of the trunk mesoderm in polychaetes has been the subject of many morphological studies (Anderson, 1973; Iwanoff, 1928). Common features of the polychaete trunk mesoderm are the origin from the 4d micromere and the almost simultaneous subdivision of the initially uniform trunk mesoderm into the metameric larval segment mesoderm. I have described *Pdu-twist*, *Pdu-myoD*, *Pdu-mef2* and *Pdu-troponin I* as mesodermal markers that allow characterising the development of the mesoderm on a molecular level, identifying mesodermal cell types and studying the emergence of segmentation in the developing mesoderm. The expression of the mesodermal marker genes can be compared to their described orthologues in insects and vertebrates.

4.2.2.1 The time-course of trunk mesodermal gene expression

I have focussed on the differentiation of the mesoderm from 15hpf onwards. As described before, mesodermal expression of *Pdu-fgfr* can be found already at 15hpf (Steinmetz, 2002). The earliest mesodermal marker gene described in this work is *Pdu-twist*, which is very restrictedly expressed already at 15hpf. *Pdu-myoD* expression is found at 19hpf and has not been analysed at preceding stages. Before 24hpf, *Pdu-mef2* is only expressed in non-mesodermal cells. At 24hpf, *Pdu-myoD* starts to be broadly expressed while the mesodermal expression of *Pdu-mef2* is probably restricted to a few lateral cells located very anteriorly almost below the prototroch that could correspond to about four differentiated muscle cells that express *Pdu-troponin I*. *Pdu-mef2* appears broader in the mesoderm only at 36hpf. The temporal succession of expression might indicate that the genes analysed act during different stages of mesodermal differentiation. While *Pdu-twist* and *Pdu-myoD* are markers for both

early and late mesodermal differentiation, *Pdu-mef2* appears to be only a late differentiation marker as it is detectable at a similar stage than *Pdu-troponin I* that marks differentiated muscle cells.

At 48hpf, there appears to be a difference in cell type specificity as well. While *Pdu-myoD* and *Pdu-twist* are specific markers for subsets of mesodermal cells, *Pdu-mef2* is probably a marker for all differentiating muscle cells.

4.2.2.2 Mesodermal segmentation

The expression of *Pdu-twist* does not support a clear segmental subdivision of the mesodermal bands before 48hpf. In contrast, *Pdu-myoD* expression appears in four segmental cell clusters supposedly belonging to the four larval segments between 19hpf and 24hpf (**Fig. 24**c,d). This strongly suggests a segmental patterning of the mesodermal bands at this stage meaning that the molecular subdivision of the mesoderm and ectoderm into larval segments occurs around the same developmental stage. The segmental nature of the *Pdu-myoD* cell clusters at 24hpf is supported by the later expression of *Pdu-myoD* in four segmental stripes at 36hpf that seem to be located at the boundaries of the larval segments. Also, *Pdu-mef2* appears to be partially expressed in segmental stripes, but only at 36hpf, possibly in the same cells as *Pdu-myoD*. Strikingly, the clear segmental expression of *Pdu-myoD* is almost completely lost at 48hpf, while the expression patterns of *Pdu-twist* and *Pdu-mef2* get at least partially segmentally iterated at that stage. The significance of this transition between 36hpf and 48hpf is not clear. It could on the one hand reflect an expression change of *Pdu-myoD*, or show that important rearrangements of mesodermal cells occur during this interval. The latter is supported by the drastic change of expression pattern also for *Pdu-twist*.

4.2.2.3 Defining mesodermal cell types by putative co-expression of marker genes

The comparison of the described gene expression patterns and the expression of orthologous genes in vertebrate and insect model species can provide insights into their possible function and identify conserved aspects of mesodermal patterning in bilaterians.

The cloned *Platynereis twist* gene contains coding regions for the highly conserved bHLH-domain as well as the characteristic WR motif that is highly conserved in vertebrates and cnidarians, but less conserved in *Branchiostoma* and *Drosophila* and absent in *C. elegans* (Castanon and Baylies, 2002). The expression of *Platynereis twist* is consistent with the proposed evolutionary conservation as an early differentiation factor for a subset of mesodermal cells (Castanon and Baylies, 2002). Given the highly probable co-expression of *Pdu-twist* and *Pdu-fgfr*, a functional link between FGF signalling and *twist* as shown genetically for other models species (Harfe et al., 1998; Shishido et al., 1993; Zuniga et al., 2002), could also be conserved in *Platynereis*.

It can only be speculated whether the *Platynereis twist* gene is rather a myogenic activator as in *Drosophila* (Baylies and Bate, 1996) or inhibitor as in vertebrates (Spicer et al., 1996). The broad expression in *Platynereis* at 24hpf and 36hpf, and the restriction to a few cells at 48hpf would rather suggest an expression in less differentiated muscle cells to prevent premature differentiation that would be more similar to vertebrates than to *Drosophila*. This is also supported by the apparent mutual exclusive expression of *Pdu-twist* and *Pdu-myoD* in a 48hpf trochophore reminiscent to the described mutual exclusive expression to prevent premature myogenic differentiation in vertebrates (Spicer et al., 1996). This implies the evolutionary conservation of *twist* as a myogenic inhibitor in *Platynereis* and therefore in Bilateria. Comparison with the currently only known expression pattern from another lophotrochozoan, the mollusc *Patella vulgata*, suggests that molluscs have secondarily lost the expression of *twist* in the trunk mesoderm as it can only be found in the ectomesoderm (Nederbragt et al., 2002a).

The orthologues of *Pdu-myoD* play an early and important role in vertebrate skeletal muscle determination and differentiation while the *Drosophila* orthologue has only a minor role to specify a small subset of muscle precursors (Berkes and Tapscott, 2005). The expression of *Platynereis myoD* implies a more important role than in *Drosophila* as it is expressed in a larger subset of mesodermal cells. The expression of *Pdu-myoD* from the early trochophore and beyond 72hpf suggests that *Pdu-myoD*, as

the MRFs in vertebrates, plays a role in both determination and differentiation of muscle cells (Berkes and Tapscott, 2005). The expression pattern first in metameric transverse stripes at 36hpf, and twelve hours later in the longitudinal muscles suggests that *Pdu-myoD* first drives differentiation of the transverse and later the longitudinal muscles, but this cannot be supported by *Pdu-troponin I* expression that shows that the longitudinal muscles differentiate before the transverse muscles. Another explanation for the drastic expression change between 36hpf and 48hpf is the occurrence of massive cell sorting at this stage.

The orthologues of *Pdu-mef2* have crucial functions during myogenesis in both vertebrates and insects. *Drosophila mef2* (*D-mef2*) is a direct downstream target of *twist* but is not necessary for initial cell fate determination (Taylor et al., 1995). It is rather required for the further differentiation of somatic, cardiac and visceral myoblasts (Bour et al., 1995). In vertebrates, *mef2* genes play a rather late role to regulate cardiac and skeletal muscle-specific genes (Edmondson et al., 1994; Ticho et al., 1996). Similar to insects and vertebrates, the *Platynereis mef2* gene cannot play a major role in early muscle specification as the gene is only transcribed prominently in the mesoderm at 36hpf. The probably overlapping expression with *Pdu-myoD* in both the segmental stripes at 36hpf and the longitudinal muscles at 48hpf shows that *Pdu-mef2* could play a similar role to potentiate *myoD* transcriptional activity in differentiating muscle cells.

Long before mesodermal expression is obvious, *Pdu-mef2* is strongly expressed in non-mesodermal cells. This expression gets restricted to different regions of the brain. It can be speculated that *Pdu-mef2* marks, as in *Drosophila*, also the developing mushroom bodies (Schulz et al., 1996). As the non-mesodermal expression appears rather late in insects and vertebrates, the early expression in non-mesodermal cells in *Platynereis* has so far no correlate in other bilaterian animals. Nevertheless, the early ectodermal head expression might be comparable to the ectodermal expression of the *mef2* gene in putative neuronal cells in the anthozoan *Nematostella* (Martindale et al., 2004). Also the *mef2* expression around the mouth opening of the hydrozoan *Podocoryne* bears striking similarities to the *Platynereis* expression in the developing stomodaeum and proctodaeum, both derived from the blastopore (Spring et al., 2002).

4.3 Comparison with archimeric deuterostomes

4.3.1 The subdivision of the *Platynereis* mesoderm in the light of the archicoelomate theory

The body of some bilaterian animals is characterised by the tripartite subdivision into the “archimeres” prosoma, mesosoma and metasoma (also termed “archimeric segments” although no metamery is apparent) based on the three coelomic cavities (archicoels: procoel, mesocoel and metacoel) (Remane, 1950; Tautz, 2004)(**Fig. 40**a,b). These animals were classified within the phylum Archicoelomata due to their common mode of coelom formation by enterocoely (Siewing, 1985). Molecular phylogenetic studies have now shown that they fall into both Deuterostomia (Hemichordata, Echinodermata) and Lophotrochozoa (Phoronida, Brachiopoda, Bryozoa, Chaetognatha)(de Rosa et al., 1999; Mallatt and Winchell, 2002; Papillon et al., 2004) therefore indicating that the tripartite body and coelom subdivision might be ancestral to all Bilateria.

The enterocoely theory, as recently reviewed (Tautz, 2004), proposes the evolution of the five archimeric coelomic sacs in Bilateria from the gastric pouches of an anthozoan-like ancestor therefore inferring their ancestry in Bilateria (Remane, 1950). It has further been suggested that Spiralia have reduced or lost their pro- and mesocoel, while the larval segments (deutomeric segments) represent metameric subdivisions of the metacoel. The recent classification of the beard worms (Pogonophora) – that might have kept all three archicoels (Siewing, 1976; Siewing, 1985) – as derived annelids (Boore and Brown, 2000; McHugh, 1997) indicates that annelids might still have preserved remnants of archimeric coeloms.

The large set of neuroectodermal regionalisation genes recently described in the enteropneust *Saccoglossus* (Hemichordata, Deuterostomia) (Lowe et al., 2003) allows comparing the *Platynereis* trochophore regions to the archimeric segments of a basal deuterostome. In addition, the molecular identification and characterisation of the *Platynereis* mesodermal structures combined with recent cell lineage data (Ackermann et al., 2005) allow comparing the putative remnants of archicoeloms in the

Platynereis trochophore on the morphological and molecular basis with the tripartite coelom in Enteropneusta as representatives of archicoelomate deuterostomes.

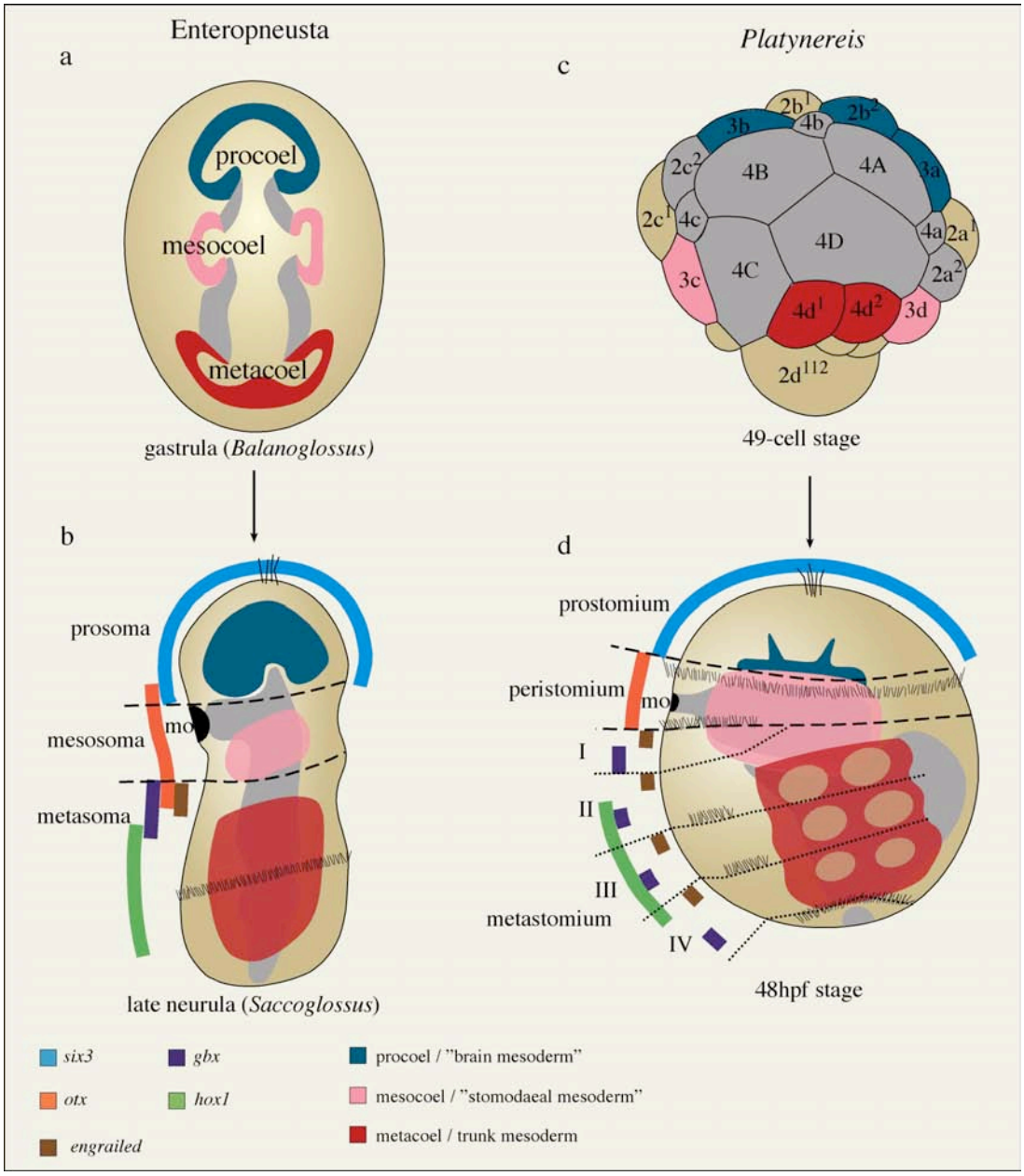

Fig. 40 Schematic comparison of the origin and molecular regionalisation of the mesoderm and ectoderm between enteropneusts (**a**, **b**) and *Platynereis* (**c**, **d**).
Dashed lines: Primary body region borders. Grey: digestive tracts. Stippled lines: secondary larval segment borders. I-IV: *Platynereis* larval segments. mo: mouth opening. (**a**) and (**c**): views onto blastopore. (**b**) and (**d**): lateral views. (**a**) modified after (Remane, 1950). (**b**) modified after (Lowe et al., 2003). (**c**) modified after (Ackermann et al., 2005)

The prosoma is the rostral archimere and carries the procoel (**Fig. 40**a,b, dark blue) as a coelomic sac that originates from a non-paired out-pouching of the anterior larval archenteron. The reduction of the procoelic coelom as in Brachiopoda and Phoronida (Bartolomaeus, 2001; Lüter, 2000) appears frequently although mesodermal cells can

still be found. In the enteropneust *Saccoglossus kowalevskii*, the mesodermal coelom of the procoel is prominent and expresses a *six3* orthologue (**Fig. 40**a,b dark blue) (Lowe et al., 2003). Strikingly similar, the *Platynereis* "brain mesoderm" also expresses *Pdu-six3* and appears to originate from the anterior border of the digestive tract, the stomodaeal region, although it is not of endodermal origin (**Fig. 40**c,d dark blue). I propose that it represents together with the mesodermal "horns" the remnants of a procoelic mesoderm in *Platynereis*. This is supported by the presence of an unpaired coelomic sac at a very similar position – directly adjacent to the brain neuropil – in the trochophore larvae of *Lanice conchilega* (Heimler, 1981), *Owenia* (Wilson, 1932) and *Scoloplos* (Anderson, 1959). In addition, the most rostral, pre-oral neuroectodermal body regions in *Platynereis* (prostomium) and *Saccoglossus* (prosoma), both characterised by the presence of an apical organ, are delimitated by the expression of the regionalisation gene *six3* (**Fig. 40**b,d light blue line).

I propose that the prostomium (**Fig. 40**d, light blue line) and corresponding "brain mesoderm" (**Fig. 40**c,d, dark blue) of *Platynereis* are homologous to the prosoma (**Fig. 40**b, light blue line) and procoel (**Fig. 40**a,b dark blue) of *Saccoglossus* and therefore represent a conserved body region already present in Urbilateria, the last common ancestor of Bilateria.

The mesosoma is the median archimere bearing the mouth opening at the anterior border and containing the mesocoel, a pair of coelomic sacs that develops from a pair of lateral pouches from the larval archenteron (**Fig. 40**a,b, pink). The mesocoel generally surrounds the pharynx. In Enteropneusta, the mesocoel is situated in the collar, while in Phoronida and Brachiopoda, it forms the complex coelom of the food-collecting tentacles (Nielsen, 2001). Although mesodermal markers from enteropneusts have not been described yet, the stomodaeal envelope in polychaetes resembles the mesocoel in several aspects. It originates in *Platynereis* from a pair of cells (3c and 3d) at the lateral blastopore margin located posterior of the stomodaeal precursor cells (**Fig. 40**c,d, pink). It will then embrace the stomodaeum and later form the pharyngeal musculature. More similarities exist between the *Saccoglossus* mesosomal ectoderm and the peristomial ectoderm bearing the ciliated mouth opening. Both regions are patterned by orthologues of the regionalisation gene *otx* (**Fig.**

40b,d, light red line) (Arendt et al., 2001). Notably, the tornaria larva of the indirect developing enteropneust *Ptychodera flava* carries a pre- and postoral ciliated band in the mesosomal region that just as the prototroch and metatroch of the *Platynereis* peristomium express *otx* orthologues (Arendt et al., 2001; Harada et al., 2000).

The metasoma is the posterior archimere that bears the anus and contains the paired metacoel that forms the trunk mesoderm (**Fig. 40**a,b, dark red). The metacoel originates as a paired out-bulging from the posterior archenteron (**Fig. 40**a,b, dark red). It forms the trunk mesoderm and is assumed to be homologous to the polychaete trunk mesoderm in the metastomium (**Fig. 40**c,d, dark red) (Remane, 1950; Tautz, 2004). The polychaete trunk mesoderm has a single origin from the 4d micromere and gets secondarily subdivided into two metamerically segmented mesodermal bands. The molecular comparison with the enteropneust metacoel is not possible due to the lack of molecular data from any enteropneust. Nevertheless, molecular markers support the homology between the metasomal neuroectoderm in enteropneusts and the metastomial neuroectoderm in polychaetes (**Fig. 40**b,d). Both regions are anteriorly delimited by the expression of *gbx* orthologues (**Fig. 40**b,d, purple lines) followed by the expression of *hox1* orthologues (**Fig. 40**b,d, green lines) (Arendt et al., 2001; Lowe et al., 2003).

The molecular and morphological similarities of body region patterning between polychaetes and enteropneusts on the ectodermal and mesodermal level supports the presence of three archimeric body regions in the last common ancestor of Bilateria and their evolutionary conservation in the trochophore and enteropneust larvae. It also supports the ancestry of primary larva in Bilateria (Arendt et al., 2001).

4.3.2 Comparison with vertebrate brain regions

Enteropneust neuroectoderm and vertebrate brain regions have recently been homologised based on similar expression of transcription factors and secreted growth factors: prosoma – forebrain, mesosoma – midbrain and metasoma – hindbrain/spinal chord (Gerhart et al., 2005). This suggests the following indirect homologies between vertebrate and polychaete brain regions: forebrain – cerebral ganglion (prostomial part);

midbrain – cerebral ganglion (peristomial part); hindbrain – metameric ventral nerve chord.

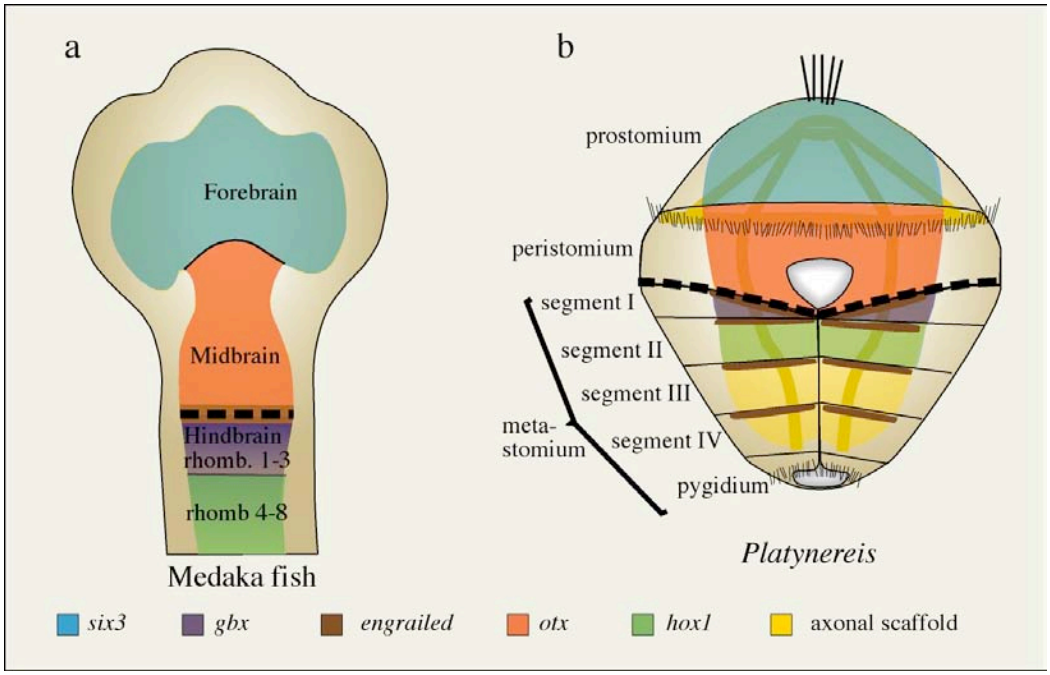

Fig. 41 Comparison of larval regions specified by *six3*, *otx*, *gbx*, *hox1* and *engrailed* orthologues between fish (**a**) and *Platynereis* (**b**).
Thick dashed line: Midbrain-hindbrain-boundary in fish and head-trunk border in *Platynereis*. Light yellow: Neuroectoderm.

And indeed, the direct comparison of *Platynereis* with vertebrates supports these homologies suggesting conservation in the last common ancestor of Bilateria (**Fig. 41**). The *six3-otx* dichotomy described in *Platynereis* and *Saccoglossus* is found in fish (Loosli et al., 1998) and possibly also in frogs (Kablar et al., 1996; Pannese et al., 1995; Zhou et al., 2000) (although co-expression studies are lacking in frogs) during the earliest phase of *six3* expression to pattern forebrain (*six3*, **Fig. 41** blue) and midbrain respectively (*otx*, **Fig. 41** red). In other vertebrates, *six3* is similarly expressed at the rostral tip of the neural plate (Loosli et al., 1998; Oliver et al., 1995; Zhou et al., 2000), but the dichotomy to *otx* is less pronounced. Further morphological support for a homology between the forebrain and the CNS in the polychaete prostomium is the presence of the main olfactory, neurosecretory and optic centres (Starck, 1982). The midbrain-peristomium homology is morphologically supported by the direct connection to optic nerves in vertebrates and polychaetes (only larval eyes) (Starck, 1982). The comparison with polychaetes suggests an expansion of the pro- and peristomial neural territories to give rise to fore- and midbrain during the evolution of vertebrates (**Fig. 41**). The homology of the polychaete peristomium-metastomium (head-trunk)

border and the midbrain-hindbrain boundary (MHB) in vertebrates finds even higher support (**Fig. 41**, thick dashed line). In both polychaetes and vertebrates, it is the boundary between *otx* and *gbx* orthologue expression with *hox1*-orthologues further patterning the metastomium/hindbrain, between convergent extension-negative and –positive regions (as discussed in the next section), and between non-metameric and metameric regions (Keynes and Lumsden, 1990; Kiecker and Lumsden, 2005). A conclusive statement on the homology between the segmental entities of the polychaete trunk and the vertebrate hindbrain cannot be made, as *engrailed* - the most reliable marker of segment borders so far described in protostomes - is not determining segment boundaries in the nervous system of any basal chordate (*Amphioxus*, tunicates, enteropneusts) or vertebrate. Nevertheless, the robust anterior expression borders of *hox1* orthologues suggest the homology of the territory posterior and including the vertebrate rhombomere 4 (Kiecker and Lumsden, 2005) to the region posterior of the 2nd *Pdu-engrailed* stripe in *Platynereis* (**Fig. 41**, green).

4.4 Platynereis elongation by convergent extension

In the previous section, I have proposed the homology between the polychaete peristomium-metastomium (head-trunk) boundary and the vertebrate midbrain-hindbrain boundary both positioned at the border between the expression of *otx* and *gbx* orthologues. In vertebrates, this boundary is also a morphogenetic boundary between the hindbrain/spinal chord-territory that undergoes convergent extension movements and the forebrain-/midbrain-territory that does not extend (Hirose et al., 2004; Keller et al., 1992). The convergent extension movements of the posterior neuroectoderm and mesoderm are conserved among vertebrates to transform a spherical into an elongated larva (Keller et al., 2000). I have found evidence that this fundamental process is evolutionary conserved in the neuroectoderm of *Platynereis* on the tissue, cellular and molecular level.

Using the early forming commissures and connectives of the axonal scaffold and the ciliary bands as morphological landmarks, I have shown that during the transformation of the spherical *Platynereis* trochophore larva into an elongated juvenile worm, the neural plate doubles in length and halves in width. Such reshaping of tissue is reminiscent of convergent extension movements of the trunk neuroectoderm (and

mesoderm) in vertebrates, which is driven in large parts by polarised neighbour cell displacements such as mediolateral cell intercalation in *Xenopus*, although a role of cell division cannot be excluded in other vertebrates (Elul et al., 1997; Glickman et al., 2003; Keller et al., 1992; Schoenwolf and Alvarez, 1989; Warga and Kimmel, 1990). Time-lapse recordings show that *Platynereis* neural plate cells strongly intercalate into mediolateral direction while barely any intercalations can be found in the antero-posterior direction. The amount of mediolateral cell intercalation events can fully account for the observed elongation during the analysed time-span. The observed mediolateral cell intercalation in the *Platynereis* neural plate is highly reminiscent of the cellular mechanism that drives convergent extension of the *Xenopus* neuroectoderm where convergent extension has been most carefully analysed within vertebrates. Notably, convergent extension is, as described for *Xenopus* (Keller et al., 1992) and medaka fish (Hirose et al., 2004), restricted to the region posterior of the *otx-gbx* boundary. The *Platynereis* overall 2-fold elongation by convergent extension is less pronounced than in the *Xenopus* spinal chord (displaying 12-fold elongation (Keller et al., 1992)), but comparable to the elongation of the medaka fish hindbrain (exhibiting 2-fold elongation (Hirose et al., 2004)).

Similar convergent extension by mediolateral cell intercalation is also found during *Drosophila* germband extension (Irvine and Wieschaus, 1994). The major difference to vertebrates and *Platynereis* is that mediolateral cell intercalation during germband extension is not elongating the *Drosophila* embryo. Instead, the *Drosophila* oocyte has already an elongated shape and germband extension is soon after compensated by germband retraction. A transformation of a spherical into an elongated embryo therefore never takes place in *Drosophila* that shows germband extension, a process the biological significance of which is still enigmatic. From an evolutionary point of view, *Drosophila* germband extension could represent an evolutionary remnant of convergent extension by mediolateral cell intercalation.

The *Platynereis* neural plate also increases in surface during the elongation. This can be explained by radial intercalation, the intercalation of cells along the Z-axis, also occurring during *Xenopus* convergent extension (Keller et al., 2000). The presence of radial intercalation in *Platynereis* is supported by the observation of some cells en-

tering and exiting the analysed focal planes. I have failed to analyse radial intercalation in more detail because in many cases cells could not be followed through multiple focal planes.

I have further analysed whether other cellular mechanisms could be partly responsible for elongation of the *Platynereis* neural plate. The non-significant difference in the length/width ratio of observed cells rules out a major role of cell shape changes during convergent extension. A major role of cell proliferation could be excluded by the failure to detect a significant elongation phenotype after arresting the cell cycle at the G2/M phase using the microtubule-depolymerising drug Nocodazole. Notably, the beginning of elongation (and mediolateral intercalation as shown) of the neural plate appears to be paralleled by a decline of cell proliferation as shown by BrdU-incorporation assays. The block of convergent extension by depolymerising the actin cytoskeleton further supports a major role of polarised neighbour cell displacements that use actin filaments to generate the necessary biomechanical force. In *Xenopus*, the intercalating cells show actin-based cellular protrusions like filopodia or lamellipodia. In *Platynereis*, the detection of cellular protrusions on neural plate cells either by staining of actin filaments with phalloidin or by visualising focal adhesion points with anti-phospho-tyrosine immunostaining remained unsuccessful. This means that either cell intercalation is independent of cellular protrusions or the protrusions could not be identified with the techniques available. In the first case, it is also possible that cell membrane rearrangements using Myosin V as a motor protein as described for *Drosophila* (Bertet et al., 2004) is the mechanism driving mediolateral cell intercalation also in *Platynereis*. In the second case, the use of electron microscopy techniques could allow visualising the presence of cellular protrusions in the neural plate.

Convergent extension movements in vertebrates are molecularly controlled by the non-canonical Wnt pathway (Wallingford et al., 2002), in *Drosophila* known as the planar polarity pathway (Fanto and McNeill, 2004; Strutt and Strutt, 2005). Yet, an involvement of the *Drosophila* planar polarity pathway in morphogenetic processes involving neighbour cell displacements (e.g. germband extension) has not been described. The high similarity of *Platynereis* and vertebrate convergent extension on the tissue and cellular level prompted me to analyse the possible involvement of the non-

canonical Wnt pathway in *Platynereis* by several means: first, by studying the expression of *Pdu-strabismus*, a specific marker gene of the non-canonical Wnt pathway (Axelrod, 2002; Darken et al., 2002; Park and Moon, 2002); and second, by chemically inhibiting the downstream target Jun N-terminal kinase (Weber et al., 2000; Yamanaka et al., 2002) with the chemical inhibitor SP600125 (Bennett et al., 2001). *Pdu-strabismus* is expressed throughout the ventral neuroectoderm during the time-period when mediolateral cell intercalation has been described, suggesting that the non-canonical Wnt pathway might play a role during this process. This is further supported by the elongation phenotype in Jun N-terminal kinase-inhibited embryos, reminiscent of the phenotype following F-actin depolymerisation. Nevertheless, it can only be speculated about the role of the non-canonical Wnt pathway during convergent extension in *Platynereis*. It is possible that although *strabismus* mRNA is expressed at the right time and place, it is further translationally regulated or has a still undescribed role in other cellular processes. It is also not clear how specific SP600125 inhibits the Jun N-terminal kinase of *Platynereis*, whether any other kinases are inhibited, and to what extent the observed phenotype is a secondary effect due to unrelated functions of Jun N-terminal kinase during other cellular processes. The role of the non-canonical Wnt pathway can only be reliably tested by more gene-specific gain- and loss-of-function assays such as injection of mRNA, Morpholino or siRNA.

Four-jointed and *dachsous* have both been described to play roles upstream of *strabismus* in the *Drosophila* wing and eye disc. Their proposed roles are the establishment of the planar polarity throughout the epithelium before the establishment of the intracellular planar polarity (by localisation of proteins such as *strabismus*) (Peifer and McEwen, 2002; Strutt and Strutt, 2002). This is reflected by the gradient-like expression of both genes (Clark et al., 1995; Matakatsu and Blair, 2004; Zeidler et al., 2000). Orthologues of both genes are very conspicuously expressed in the *Platynereis* 24hpf ventral plate neuroectoderm, more than 24h before the described mediolateral cell intercalation. While *Pdu-four-jointed* displays a gradient-like expression, *Pdu-dachsous* appears expressed opposing and partly overlapping *Pdu-four-jointed*. *Pdu-strabismus* is also expressed uniformly in the same region already at that stage. It can be speculated that the non-canonical Wnt pathway has another early role in *Platyne-*

reis. As described by time-lapse recording, the blastopore closes and the ventral plate starts to fuse along the midline around the same stage. The morphogenetic movements that lead to the blastopore closure might be orchestrated by oriented cell divisions. It is suggestive that the non-canonical Wnt pathway might play a role in oriented cell division as described for vertebrates (Ciruna et al., 2006; Gong et al., 2004) during this process, and that the opposing expression of *four-jointed* and *dachsous* helps directing the orientation of the spindles.

4.5 Comparison with arthropod head segments

The identification of marker genes specifying the larval neuroectodermal regions in *Platynereis* allows molecular comparisons with the CNS of the arthropod head segments (**Fig. 42**). As described in the introduction, the brain subdivisions proto-, deuto-, and tritocerebrum have been homologised throughout Arthropoda by the shared expression of molecular markers (**Fig. 42**a-c).

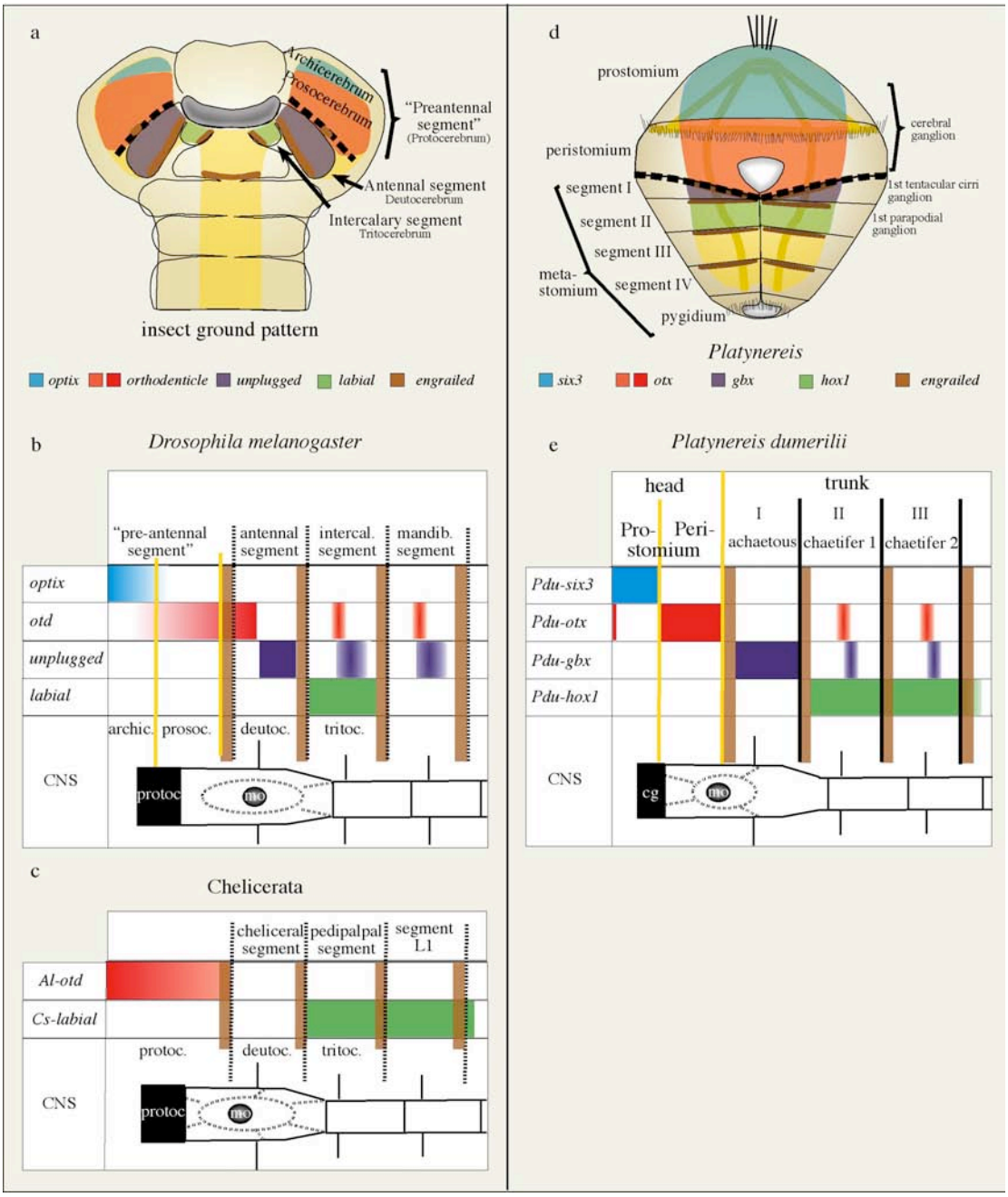

Fig. 42 Schematic comparison of larval regions (**a**, **d**) and regional expression patterns (**b**, **c**, **e**) of *six3*/*optix*, *otx*/*orthodenticle*, *gbx*/*unplugged*, *labial*/*hox1* and *engrailed* orthologues between arthropods (**a**-**c**) and *Platynereis* (**d**, **e**).
In (**a**) and (**d**):Thick dashed line: Proto-deutocerebral border in *Drosophila*; head-trunk border in *Platynereis*. In (**b**), (**c**) and (**e**): yellow lines: border between putative archimeric segment remnants. Thick black lines: Segment borders. Stippled lines: parasegmental boundaries. Double-dotted lines: stomatogastric nervous system. mo: mouth opening. I-III: larval segments. Species abbreviations: Al: *Archegozetes longisetosus*; Cs: *Cupiennius salei*; Pdu: *Platynereis dumerilii*. archic: archicerebrum; cg.: cerebral ganglion; deutoc.: deutocerebrum; prosoc.: prosocerebrum; protoc.: protocerebrum; tritoc.: tritocerebrum. References to expression patterns: *optix*: (Seo et al., 1999); *orthodenticle* (*Drosophila*): (Hirth et al., 2003; Hirth et al., 1995; Urbach and Technau, 2003b); *labial*: (Diederich et al., 1991; Hirth et al., 1998); *engrailed* (*Drosophila*): (Hirth et al., 1995; Schmidt-Ott and Technau, 1992); *unplugged*: (Hirth et al., 2003); *Al-otd*: (Telford and Thomas, 1998); *Cs-labial*, *Cs-engrailed*: (Damen et al., 1998)

I have shown that the *Platynereis* cerebral ganglion has contributions from both the *Pdu-six3*-expressing prostomium (**Fig. 42**d,e, blue) and the *Pdu-otx*-expressing peristomium (**Fig. 42**d,e, red), both located anterior of the first patch of *Pdu-engrailed* (**Fig. 42**d,e, brown). In *Drosophila*, the protocerebrum expresses during its development an *orthodenticle/otx* orthologue (**Fig. 42**a,b, red) omitting the most rostral and dorsal areas (Hirth et al., 2003; Hirth et al., 1995; Urbach and Technau, 2003b) where an *optix/six3* orthologue is expressed (**Fig. 42**a,b, blue) (Seo et al., 1999). The precise spatial correlation of the two genes has still to be confirmed by co-expression studies in *Drosophila* and/or other arthropods. I consider *otd/otx* expression limited to the protocerebrum (as described in *Tribolium* (Insecta, Coleoptera) (Li et al., 1996) and the more basal chelicerate *Archegozetes* (Telford and Thomas, 1998)) (**Fig. 42**a,c, red) as the ancestral state for Arthropoda and the *Drosophila otd/otx* brain expression in the deutocerebral region as evolutionary derived within arthropods (**Fig. 42**b, red). On the basis of *optix/six3* and *otd/otx* expression, I propose homology between the arthropod protocerebrum and the polychaete cerebral ganglion that both connect to the eyes (Bullock and Horridge, 1965) and express marker genes for circadian rhythmicity (Arendt et al., 2004) (**Fig. 42**a,d). This homology is also supported by the expression of the genes defining specific cell types in the arthropod protocerebrum as well as the *Platynereis* cerebral ganglia, e.g. *Pdu-rx*, *Pdu-pax6*, *Pdu-six1/2*(Arendt et al., 2002; Arendt et al., 2004). The protocerebral expression of *otx* and *six3* orthologues, defining two distinct regions that fuse during the development of the cerebral ganglia in the trochophore larva, implies that the arthropod protocerebrum has a split origin from the pro- and peristomial parts of the CNS of an annelid-like ancestor (**Fig. 42**a,d). This hypothesis is supported by classical morphologists who have proposed that the arthropod preantennal head bearing the protocerebrum is split on the neural (into archi- and prosocerebrum) (**Fig. 42**a) and coelomic level into two regions (Rempel, 1975; Siewing, 1963; Urbach and Technau, 2003a; Weber, 1952; Weygoldt, 1979). Although I have support for a split protocerebrum, it has to be stressed that my data does not support a metameric nature of either of these two parts. Rather, as comparison with enteropneusts has shown, they are probably remnants of the pro- and mesosoma and thus archimeric body regionalisation. Notably, the *engrailed* stripe of the arthropod "preantennal segment" belongs to the most anterior parasegment and shifts in front of the first segment due to the segment-parasegment

frame shift (**Fig. 42**b). In the grasshopper *Schistocerca*, the parasegmental boundary of the first metameric segment is still apparent as the "preantennal" *engrailed* stripe gets partially integrated into the antennal segment (Boyan and Williams, 2000). The presence of an acron in polychaetes is dependent on its definition: if defined as a uniform, unsegmented region anterior of the first metameric segment, it would not exist in polychaetes as the cerebral ganglion has a split origin from pro- and peristomium. If one defines the acron only as the unsegmented anterior tip of the animal, the acron would correspond to the prostomium of the polychaete larva. Yet, using this definition, the acron would be followed by a second non-metameric region, the peristomium.

The metameric larval segments of the *Platynereis* larva, expressing *Pdu-engrailed* at their anterior border, would correspond to arthropod parasegments as already proposed on the basis of *Pdu-engrailed* expression in regenerating segments (Prud'homme et al., 2003).

Recently, the deutocerebrum that innervates the 1st pair of antenna (in Mandibulata and Crustacea) (Bullock and Horridge, 1965) or the cheliceres (in Chelicerata) (Damen et al., 1998; Mittmann and Scholtz, 2003; Telford and Thomas, 1998) has been homologised throughout arthropods by three main arguments: it originates from the region between first and second *engrailed* stripes, lies in the segment directly anterior of the first *labial/hox1* expressing segment (Damen et al., 1998), and forms a commissure-less ganglion on the circumoesophageal connective lateral of the mouth opening (**Fig. 42**a-c) (Mittmann and Scholtz, 2003). All these criteria are fulfilled by the first larval segment of *Platynereis* that gives rise to the ganglia of the first quartet of tentacular cirri (**Fig. 42**d,e). It is, as in *Drosophila*, also the most anterior segment defined by the expression of a *gbx* orthologue (**Fig. 42**b,e, purple) (Hirth et al., 2003). I therefore propose homology between the *Platynereis* "segment I" and the parasegmental part of the 1st antennal/cheliceral segment of Arthropoda innervated by the deutocerebrum (**Fig. 42**a,d, purple). During the ontogeny of chelicerates, insects, crustaceans and myriapods, the 1st antennae are initially post-orally positioned and subsequently move anteriorwards in the course of cephalisation, reflecting their evolutionary origin from an initial post-oral position as seen for *Platynereis* (Anderson,

1973; Telford and Thomas, 1998). Importantly, the polychaete antennae, innervated directly by the cerebral ganglion in the prostomium, cannot be homologous to the mandibulate antennae that are innervated by the deutocerebrum. This does not necessarily mean that the polychaete homologues of the olfactory glomeruli (situated in the insect antennae and projecting into the mushroom bodies) have to be localised in the nereidid tentacular cirri, but would consolidate that their position is, as in chelicerates (Strausfeld et al., 1998) and onychophorans (Eriksson et al., 2003; Scholtz and Edgecombe, 2005), not fixed to the first metameric segment. The presence of antennae in Onychophora (basal arthropods) which in contrast to mandibulates are innervated by the protocerebrum supports their homology to polychaete antennae or palpae and corroborates the presence of protocerebral appendages at the base of Protostomia (Eriksson et al., 2003).Therefore, the antennae are the most probable homologues of the recently characterised chelifore appendages connected to the protocerebrum in pycnogonids (sea spiders) (Maxmen et al., 2005). This implies that during the evolution of higher arthropods, the "primary" antennae directly innervated by the protocerebrum have been lost and replaced by "secondary" antennae from modified appendages of the first metameric segment (Scholtz and Edgecombe, 2005).

The arthropod tritocerebrum that innervates the intercalary (Mandibulata), 2nd antennal (Crustacea) or pedipalpal segment (Chelicerata) (Bullock and Horridge, 1965) is characterised by the expression of *hox1*/*labial* (**Fig. 42**a-c, green) (Abzhanov and Kaufman, 1999; Damen et al., 1998; Diederich et al., 1991; Hirth et al., 1998) and bears the first substomodaeal commissure (**Fig. 42**b,c) (Bullock and Horridge, 1965). The presence of both characters allows proposing the homology between the *Platynereis* "segment II" and the parasegmental part of the arthropod intercalary/2nd antenna/pedipalpal segment bearing the tritocerebrum (**Fig. 42**d,e).

As the new animal phylogeny highly supports the division of Protostomia into Ecdysozoa (including arthropods) and Lophotrochozoa (including annelids) (Aguinaldo et al., 1997; Philippe et al., 2005), the comparison with arthropods suggests the conservation of two non-metameric head regions followed by at least two conserved metameric segments in the last common ancestor of Protostomia. Yet, the majority of phyla within Ecdysozoa and Lophotrochozoa are "unsegmented" animals (e.g. nema-

todes, molluscs, flatworms). The ancestry of at least two metameric segments in Protostomia postulates the secondary loss of these metameric segments in "unsegmented" protostome animals. The proposed correlation of the anterior-most polychaete metameric segments to the anterior-most arthropod parasegments is very close to the concept based entirely on morphology and proposed by Siewing (Siewing, 1963), not covering however the non-metameric origin of the peristomium and the corresponding brain part in arthropods ("prosocerebrum") as proposed here. Conclusions about the level of cephalisation present at the base of the protostomian phylogenetic tree cannot be drawn.

4.6 The evolution of the elongated bilaterian body form from a cnidarian-like ancestor and the emergence of the bilaterian body axes

4.6.1 Amphistome gastrulation in *Platynereis*

Platynereis belongs to Protostomia originally defined by Grobben (Grobben, 1908) as animals in which the blastopore generally gives rise to the mouth only (protostomy). In *Platynereis* as in many other "protostomes", though, the blastopore fate derives from this general scheme. Time-lapse recordings have shown that the *Platynereis* blastopore gives rise to mouth and anus, a process termed amphistomy, found also in other polychaetes (as in *Polygordius* (Woltereck, 1904)), nematodes (*Potonema*, (Nielsen, 2001)) and onychophorans (*Peripatopsis*, (Nielsen, 2001)). Before the lateral lips of the blastopore fuse, the stomodaeal (future mouth) and proctodaeal (future anus) cells are located in close proximity inside of the blastopore. The blastopore splits by the rapprochement and fusion of the lateral neural plate cells from the left and right. When the cells of the neural plate first touch at the position of the future midline, the blastopore adopts a slit-like form, resembling the shape of an "8" and splitting off the anterior mouth from the posterior anus. The zipper-like fusion of the blastopore lips from posterior to anterior forces apart the future mouth anteriorly and the future anus that stays at the posterior end of the larva. As during this process the neural plate cells are strongly proliferating, it is conceivable but remains to be proven that directed cell divisions underlie the concerted movement of the neural plate resulting in the closure of the blastopore. Suggestively, the expression of *Pdu-four-*

jointed, *Pdu-dachsous* and *Pdu-strabismus* at 24hpf supports a possible role of the non-canonical Wnt pathway during this process as described during vertebrate blastopore closure (Gong et al., 2004). In the course of blastopore closure in *Platynereis*, the cells located at the lateral border of the stomodaeal region become the neural midline that represents the fusion line of the blastopore. The fact that initially the prospective neural plate lies left and right of the stomodaeum that is a major source of secreted signalling proteins (e.g. Hedgehog, personal communication by K. Tessmar-Raible; BMP2/4, not shown) makes it likely that the stomodaeum has a major role in the induction and early patterning of the neuroectoderm.

4.6.2 Convergent extension as an ancestral characteristic of amphistome gastrulation

About one day after the neural plate has started to fuse along the future neural midline, the spherical *Platynereis* trochophore larva transforms into an elongated juvenile worm. As discussed before, the transformation of a spherical into an elongated larva by convergent extension (driven by mediolateral cell intercalation) and the regional restriction to the *gbx*/*hox1*-region posterior of the *otx*-expressing mouth region in *Platynereis* are very reminiscent of the processes that elongate the spherical larva in vertebrates, strongly arguing for evolutionary conservation in Bilateria.

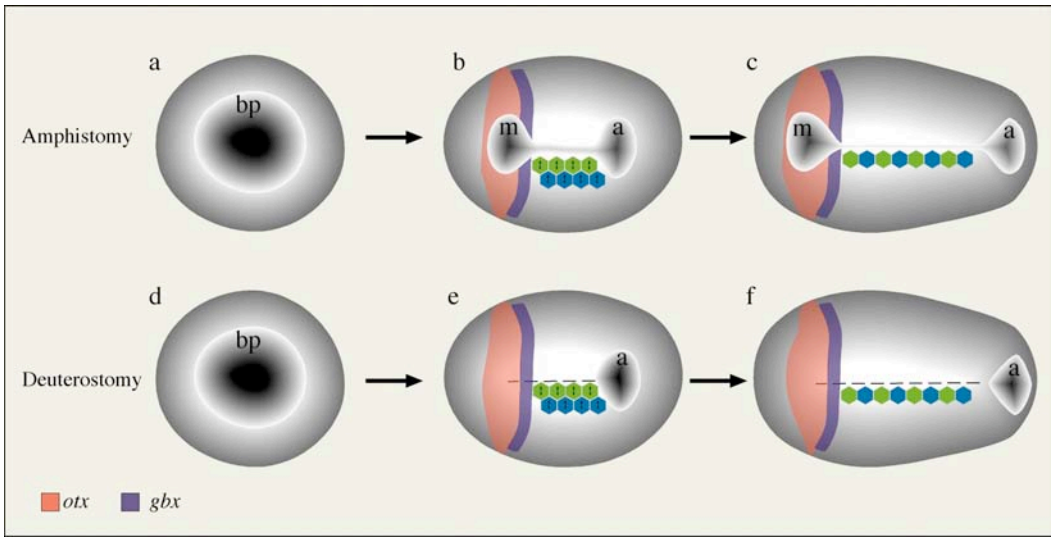

Fig. 43 Convergent extension by mediolateral cell intercalation in an amphistome (**a-c**) and in a deuterostome (**d-f**).
In the amphistome, mediolateral intercalation drives apart mouth (m) and anus (a). *otx* expression (red area) prevents elongation of the mouth. In the deuterostome, the slit-like blastopore no longer forms, but the corresponding movements persist. Dashed line in **e, f**: neural midline. Red: *otx*; purple: *gbx*; a: anus; bp: blastopore; m: mouth. Views onto blastopore and neural side; anterior to the left.

The reason why those features have evolved are not readily understood in vertebrates, but make much more sense in the context of amphistome gastrulation. Assuming that amphistome gastrulation is ancestral in Bilateria as both protostome and deuterostome modes can be derived from it (Arendt and Nübler-Jung, 1997; Jaegersten, 1955; Naef, 1927; Sedgwick, 1884; Shankland and Seaver, 2000; Siewing, 1985), I propose that convergent extension by mediolateral cell intercalation evolved in early bilaterians to further separate mouth and anus along the slit-like blastopore, as seen in today's polychaetes (**Fig. 43**a-c). In order to prevent the mouth opening from elongating and keep it at an anterior-ventral position, the mouth region was restricted from convergent extension by the expression of *otx* anterior of the *gbx*-expressing region (**Fig. 43**a-c, red and purple). Persisting during the development of today's polychaetes (as described for *Platynereis*), this ancestral pattern of axis elongation was modified to different extent in other lines of bilaterian evolution. For example, today's pterygote insects no longer develop through a spherical embryo, but start development from an elongated egg (Anderson, 1973). Still, the extension of their germband involves mediolateral cell intercalation (Irvine and Wieschaus, 1994) and thus can be regarded an evolutionary remnant of the ancestral elongation mode. In the chordate line of evolution, amphistomy would have changed into deuterostomy where the blastopore gives rise exclusively to the anus, but convergent extension by mediolateral cell intercalation along the neural midline (**Fig. 43**d-f) and regional restriction posterior to the midbrain-hindbrain boundary (**Fig. 43**d-f, red and purple) would have persisted.

This scenario also predicts that similar mechanisms should be found during elongation of other polychaetes (*Polygordius* (Woltereck, 1904)), nematodes (*Potonema*, (Nielsen, 2001)) and onychophorans (Peripatopsis, (Nielsen, 2001)) that present a slit-like blastopore characteristic for amphistome gastrulation.

4.6.3 Convergent extension movements establish the main body axes in polychaetes and vertebrates

Convergent extension movements are not only transforming spherical into elongated larvae in vertebrates and polychaetes, but also establish the two principal bilaterian body axes of the trunk: the antero-posterior and the dorso-ventral axis.

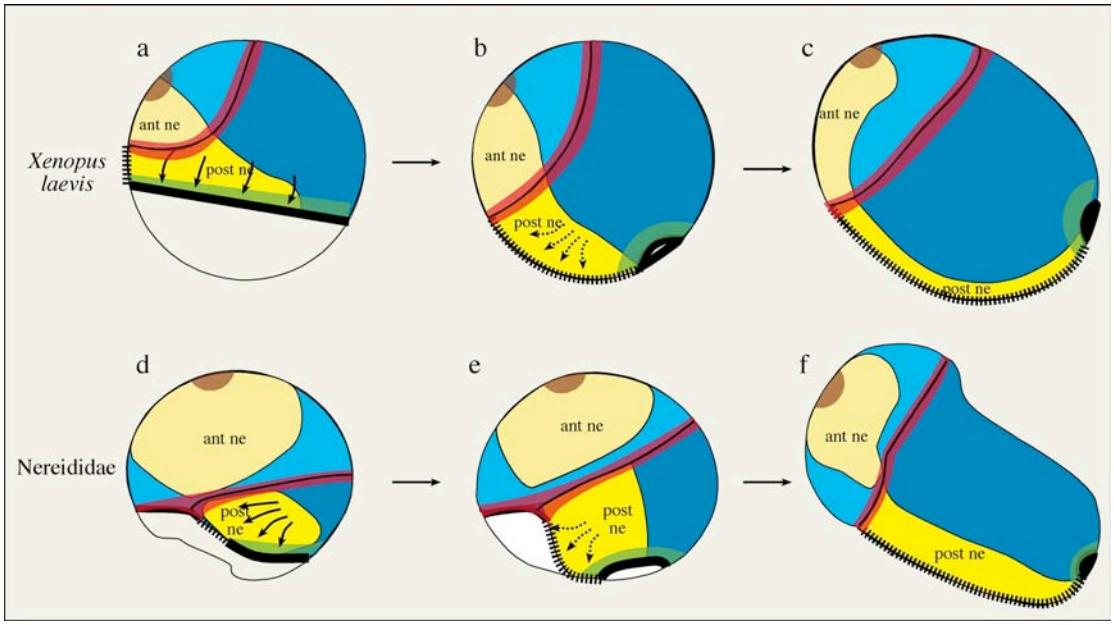

Fig. 44 Schematic ectodermal fate maps before (**a**, **d**), during (**b**, **e**) and after (**c**, **f**) the establishment of the bilaterian axes by gastrulation movements in *Xenopus laevis* (**a-c**) and *Platynereis dumerilii* (**d-f**).
Light yellow; ant ne: anterior neuroectoderm. Dark yellow; post ne: posterior neuroectoderm. Light blue: anterior epidermis. Dark blue: posterior epidermis. Brown: rostral pole. Red: Boundary between posterior trunk region undergoing and anterior head region not undergoing convergent extension movements; in *Xenopus*: midbrain-hindbrain-boundary; in *Platynereis*: peristomial-metastomial boundary. Green: posterior pole (prospective anal cells). Stippled line: prospective neural midline. Thick line: Prospective anal part of the blastopore margin. Arrows: epibolic movements. Stippled arrows: convergent extension movements. **a**-**c** after (Keller, 1975) **d**-**f** after (Wilson, 1892) and personal observations.

The fate maps of *Xenopus* (as a representative for deuterostome vertebrates) and *Nereis* resp. *Platynereis* (as representatives for amphistome polychaetes) before and after the occurrence of convergent extension movements highlight the importance of those morphogenetic movements to establish the principal bilaterian axes in a very similar manner (**Fig. 44**). In principle, two regions of fundamentally different morphogenetic behaviour can be distinguished: the rostral, future "head region" (**Fig. 44**, light yellow and light blue) located anterior of the *otx-gbx* boundary (**Fig. 44**, red stripe) that does not undergo convergent extension, and the prospective "trunk region" located posterior of the *otx-gbx* boundary that undergoes convergent extension (**Fig. 44**, dark yellow and dark blue). The *otx-gbx* boundary, giving rise to the vertebrate midbrain-hindbrain boundary and the polychaete border between peristomium and metastomium, marks the most posterior border of the "head region" and the most anterior border of the "trunk region".

In the “head region” of both *Xenopus* and nereidids, the relative positions of the most rostral pole (**Fig. 44**, brown spot) and the posterior *otx-gbx* boundary (**Fig. 44**, red stripe) do not change during development, but only get tilted indirectly so that the most rostral part takes a final position at the anterior pole of the larva.

This is in sharp contrast to the “trunk region” where the antero-posterior axis is established only during epiboly and subsequent convergent extension movements of the trunk. In the early *Xenopus* gastrula, the prospective anal cells of the future posterior pole (**Fig. 44**a-c, green stripe) lie at the line of internalisation between mesoderm and ectoderm representing the late blastopore rim that in all deuterostomes gives rise to the anus (**Fig. 44**a-c, thick black line). The future neural midline (**Fig. 44**a, stippled line) region spans an extremely short territory in early gastrulae with anterior and posterior fated cells just adjacent (**Fig. 44**a, compare red and green stripes at the stippled line). It is therefore not possible to distinguish an anterior and a posterior pole in the early gastrula. Also the dorso-ventral axis cannot be easily defined. The cells becoming hindbrain and spinal chord structures (**Fig. 44**a-c, dark yellow) represent the most dorsal structures of the trunk but span very laterally in an early gastrula. Only the morphogenetic movements during epiboly (**Fig. 44**a, arrows) and subsequent convergent extension (**Fig. 44**b, stippled arrows) separate anterior and posterior extremities and bring the dorsal neuroectoderm to its definite position. This makes it impossible to define clear axes in an early gastrula, which led to conflicting models of axial designation in early *Xenopus* gastrulae (Kumano and Smith, 2002).

The fate map of nereidids presents strikingly similar peculiarities. While the relative position between apical organ (as most rostral head structure, **Fig. 44**d-f, brown spot) and the head-trunk boundary (**Fig. 44**d-f, red stripe) do not change during development, the trunk undergoes similar rearrangements as in vertebrates. As characteristic for amphistome gastrulation, the blastopore closes by fusion along its lateral lips to form the neural midline (**Fig. 44**d, stippled line). As in vertebrates the future neural midline is initially short and barely separates anterior (mouth region) (**Fig. 44**d, green line) and posterior (anal region) (**Fig. 44**, red line) fates. This makes a clear designation of an antero-posterior axis in the future trunk of early trochophore larvae difficult. As described in previous sections, mouth and anus get only forced apart by pro-

liferating 2d cell descendants (**Fig. 44**d, arrows) followed by convergent extension movements along the neural midline (**Fig. 44**e, stippled arrows) that place the neural plate cells at their final ventral position (**Fig. 44**d-f, dark yellow). The cells of the future neural plate, the most ventral structure, have a broad lateral expansion in an early trochophore (**Fig. 44**d, dark yellow). Therefore also the dorso-ventral axis cannot be clearly assigned in the trunk of an early *Platynereis* larva.

In summary, the strong difference that exists between the axis determination in the head and trunk regions are shared between both vertebrates and polychaetes and suggest inheritance from a common ancestor. The ontogeny of axial morphogenesis common to vertebrates and polychaetes could recapitulate the evolutionary appearance of the bilaterian AP and DV axes from a pre-bilaterian ancestor. By using *Nematostella*, *Platynereis* and *Xenopus* as representative species still showing ancestral characteristics of Cnidaria, Protostomia and Deuterostomia, I propose a scenario that describes the evolution of the bilaterian AP and DV axes from a cnidarian-like ancestor with an oral-aboral and a directive axis (**Fig. 45**). I assume that the nereidid polychaetes, as they develop by an amphistome gastrulation mode, present a more ancestral gastrulation mode for Bilateria than the deuterostome vertebrates that have undergone secondary modifications due to the evolution of deuterostomy and yolk-rich eggs (Arendt and Nübler-Jung, 1999).

4.6.4 The evolution of the bilaterian body axes from a cnidarian-like ancestor

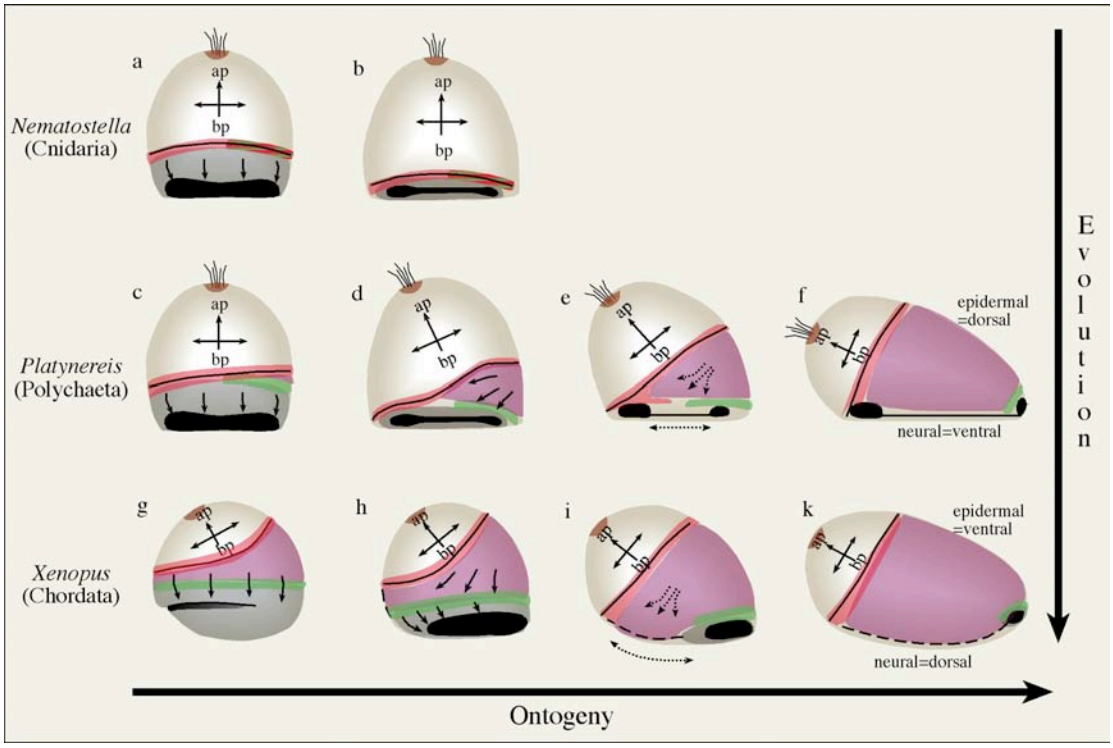

Fig. 45 Ontogenetic comparison between *Nematostella* (**a**,**b**), *Platynereis* (**c**-**f**) and *Xenopus* (**g**-**k**) as representatives of Cnidaria, Protostomia and Deuterostomia to explain the evolutionary origin of the trunk and main body axes from Cnidaria to Bilateria.
Selected species are considered ancestral and prototypic but do not represent stem species of phyla. Axes only refer to the head regions anterior of the red lines. The double arrow represents the directive axis in *Nematostella* and its evolutionary remnants in the bilaterian heads. Brown: apical pole; apical organ region in *Nematostella* and *Platynereis*. Red: Prospective head-trunk boundary. Green: prospective anus. Green-red hatched area: Blastoporal region from which the bilaterian trunk evolved. Purple: trunk. Dashed line: neural midline. Arrows: epibolic movements. Stippled arrows: convergent extension movements. ap: apical; bp: blastoporal.

Anthozoans, suggested to exhibit many ancestral characteristics of Cnidaria, have two main body axes: the oral-aboral axis and the directive axis along the slit-like mouth opening. The correlation of both axes to the bilaterian antero-posterior (AP) and dorso-ventral (DV) axes is highly debated. The oral-aboral axis of cnidarians (as exemplified for *Nematostella*, **Fig. 45**a,b), has recently been assigned to either the bilaterian anterior-posterior axis (Martindale, 2005), the posterior-anterior axis (Meinhardt, 2002) or proposed to have only a correlate in the bilaterian head, while the AP and DV axes of the bilaterian trunk would not have a correlate in cnidarians (Shankland and Seaver, 2000). The directive axis could represent a primitive bilateral sym-

metry in Cnidaria (**Fig. 45**a,b) (Finnerty et al., 2004) and similarities to the dorso-ventral axis in Bilateria have been described (Martindale, 2005).

The oral-aboral axis in adult cnidarians develops directly from the blastoporal-apical axis present in the planula larva. The blastopore gives rise to the mouth opening while the apical tuft develops into the foot (Nielsen, 2001). In polychaete blastulae prior to the proliferation of the 2d trunk ectoderm precursor cells, the ectoderm of the embryo consists almost entirely of the head ectoderm that develops quadriradial-symmetric from the four quadrants of the spiralian embryo (Shankland and Seaver, 2000). The polychaete blastula presents – as cnidarian planulae – an apical-blastoporal axis that coincides with the antero-posterior axis in the adult polychaete head (**Fig. 45**a,c). In polychaetes, the early trunk develops by directed proliferation of the 2d cell at the anal end of the blastopore rim that marks the future non-neural body side (**Fig. 45**c,d pink). The head with the initial blastoporal-apical axis is consequently tilted in the direction of the prospective mouth (**Fig. 45**c,d), bringing the sensory apical organ present in many bilaterian primary larvae in front of the mouth opening. From an evolutionary perspective this bilaterian novelty was a major advantage in the directional detection of food. In *Xenopus*, the antero-posterior (identical to the apical-blastoporal) axis in the "head region" of the early gastrula, expressing the same orthologous genes as the polychaete "head region" (*six3*, *otx*), is already tilted. It is very likely that this represents a secondary modification due to the premature proliferation of the trunk ectoderm at the non-neural side of the embryo (compare **Fig. 45**c and g, purple). The polychaete ontogeny of the head and trunk could thus represent the ancestral condition in Bilateria. Assuming the homology of cnidarian and bilaterian blastopores (Technau, 2001) as well as the homology between cnidarian and bilaterian apical tufts, the anterior-posterior axis within the bilaterian head would therefore be the only direct correlate of the cnidarian aboral-oral axis in Bilateria as both derive from the initial apical-blastoporal axis (**Fig. 45**a,c,g). On the other hand, the bilaterian trunk would be a novel evolutionary invention in Bilateria without a distinct corresponding structure in Cnidaria as proposed before (Shankland and Seaver, 2000).

As described for polychaetes, the early 2d trunk precursors at the anal blastopore rim (**Fig. 45**c, purple) form anterior, posterior and ventral trunk ectoderm and therefore

unite three of the four poles that define the AP and DV axis in Bilateria. As the epibolic (**Fig. 45** arrows) and convergent extension movements (**Fig. 45** stippled arrows) of the polychaete (**Fig. 45**c-f) and vertebrate (**Fig. 45**g-k) trunk precursors are most probably evolutionary conserved, it can be speculated that the trunk originated from one end of the slit-like blastopore – defined by the directive axis – in a cnidarian-like ancestor. One opening then evolved into the mouth opening, while the other end proliferated to form the anus, the precursor cells of the trunk that separate mouth and anus by the described morphogenetic movements (**Fig. 45**a,b, green and red hatched line). The cnidarian blastopore rim therefore unifies several bilaterian axial features. It has evolved the neural midline and therefore can be proposed to correspond to the neural side of Bilateria. On the other hand, the neural plate just as the opposing non-neural cells has probably evolved from one end of the slit-like blastopore that therefore unifies both ventral and dorsal fates. This is supported by the expression of genes in *Nematostella* that in Bilateria induce the neural (*chordin*) and non-neural (*BMP2/4* and *BMP5-8*) sides. In contrast to Bilateria, they are neither patterning the oral-aboral, nor the directive axis, but are first co-expressed at one end of the blastopore and then show an expression boundary exactly at the blastopore rim (Matus et al., 2006). This supports the notion that the bilaterian body has no correlate in Cnidaria and that one end of the cnidarian blastopore rim along the directive axis is already patterned by a BMP-chordin antagonism. Therefore, one end of the slit-like blastopore of Cnidaria could correspond to the anterior mouth opening, while the opposing blastopore end has probably evolved all bilaterian trunk structures (**Fig. 45**a,b, green and red hatched line).

5 References

Abzhanov, A. and Kaufman, T. C. (1999). Homeotic genes and the arthropod head: expression patterns of the labial, proboscipedia, and Deformed genes in crustaceans and insects. *Proc Natl Acad Sci U S A* **96**, 10224-9.

Ackermann, C. (2002). Markierung der Zellinien im Embryo von *Platynereis*. In *Fachbereich Biologie*, (ed. Mainz: Johannes Gutenberg-Universität.

Ackermann, C., Dorresteijn, A. and Fischer, A. (2005). Clonal domains in postlarval Platynereis dumerilii (Annelida: Polychaeta). *Journal of Morphology* **266**, 258-280.

Aguinaldo, A. M., Turbeville, J. M., Linford, L. S., Rivera, M. C., Garey, J. R., Raff, R. A. and Lake, J. A. (1997). Evidence for a clade of nematodes, arthropods and other moulting animals. *Nature (London)* **387**, 489-93.

Åkesson, B. (1963). The comparative morphology and embryology of the head in scale worms (Aphroditidae, Polychaeta). *Arkiv För Zooloi* **16**, 125-163.

Alberts, B., Johnson, A., Lewis, J., Raff, M., Roberts, K. and Walter, P. (2002). Molecular biology of the cell. New York: Garland Science.

Anderson, D. T. (1959). The embryology of the polychaete *Scoloplos armiger*. *Quarterly Journal of Microscopical Science* **100**, 89-166.

Anderson, D. T. (1973). Embryology and Phylogeny in Annelids and Arthropods. Oxford, New York, Toronto, Sydney, Braunschweig: Pergamon Press.

Ang, S., Jin, O., Rhinn, M., Daigle, N., Stevenson, L. and Rossant, J. (1996). A targeted mouse Otx2 mutation leads to severe defects in gastrulation and formation of axial mesoderm and to deletion of rostral brain. *Development* **122**, 243-252.

Arendt, D. and Nübler-Jung, K. (1997). Dorsal or ventral: similarities in fate maps and gastrulation patterns in annelids, arthropods and chordates. *Mech Dev* **61**, 7-21.

Arendt, D. and Nübler-Jung, K. (1999). Rearranging gastrulation in the name of yolk: evolution of gastrulation in yolk-rich amniote eggs. *Mech Dev* **81**, 3-22.

Arendt, D., Technau, U. and Wittbrodt, J. (2001). Evolution of the bilaterian larval foregut. *Nature (London)* **409**, 81-85.

Arendt, D., Tessmar, K., de Campos-Baptista, M. I., Dorresteijn, A. and Wittbrodt, J. (2002). Development of pigment-cup eyes in the polychaete Platynereis dumerilii and evolutionary conservation of larval eyes in Bilateria. *Development* **129**, 1143-54.

Arendt, D., Tessmar-Raible, K., Snyman, H., Dorresteijn, A. W. and Wittbrodt, J. (2004). Ciliary Photoreceptors with a Vertebrate-Type Opsin in an Invertebrate Brain. *Science* **306**, 869-871.

Axelrod, J. D. (2002). Strabismus comes into focus. *Nature Cell Biology* **4**, E6-E8.

Azpiazu, N. and Frasch, M. (1993). tinman and bagpipe: two homeo box genes that determine cell fates in the dorsal mesoderm of *Drosophila*. *Genes & Development* **7**, 1325-40.

Balagopalan, L., Keller, C. A. and Abmayr, S. M. (2001). Loss-of-function mutations reveal that the *Drosophila nautilus* gene is not essential for embryonic myogenesis or viability. *Dev Biol* **231**, 374-82.

Banerjee-Basu, S. and Baxevanis, A. D. (2001). Molecular evolution of the homeodomain family of transcription factors. *Nucleic Acids Res* **29**, 3258-69.

Bartolomaeus, T. (2001). Ultrastructure and formation of the body cavity lining in *Phoronis muelleri* (Phoronida, Lophophorata). *Zoomorphology* **120**, 135-148.

Baylies, M. K. and Bate, M. (1996). *twist*: a myogenic switch in *Drosophila*. *Science* **272**, 1481-1484.

Baylies, M. K. and Michelson, A. M. (2001). Invertebrate myogenesis: looking back to the future of muscle development. *Curr Opin Genet Dev* **11**, 431-439.

Bely, A. E. and Wray, G. A. (2001). Evolution of regeneration and fission in annelids: insights from engrailed- and orthodenticle-class gene expression. *Development* **128**, 2781-91.

Bennett, B. L., Sasaki, D. T., Murray, B. W., O'Leary, E. C., Sakata, S. T., Xu, W., Leisten, J. C., Motiwala, A., Pierce, S., Satoh, Y. et al. (2001). SP600125, an anthrapyrazolone inhibitor of Jun N-terminal kinase. *Proc Natl Acad Sci U S A* **98**, 13681-6.

Berkes, C. A. and Tapscott, S. J. (2005). MyoD and the transcriptional control of myogenesis. *Semin Cell Dev Biol* **16**, 585-595.

Bertet, C., Sulak, L. and Lecuit, T. (2004). Myosin-dependent junction remodelling controls planar cell intercalation and axis elongation. *Nature (London)* **429**, 667-71.

Black, B. L. and Olson, E. N. (1998). Transcriptional control of muscle development by myocyte enhancer factor-2 (MEF2). *Annu Rev Cell Dev Biol* **14**, 167-196.

Bodmer, R. (1993). The gene tinman is required for specification of the heart and visceral muscles in *Drosophila*. *Development* **118**, 719-29.

Boore, J. L. and Brown, W. M. (2000). Mitochondrial genomes of *Galathealinum*, *Helobdella*, and *Platynereis*: Sequence and gene arrangement comparisons indicate thet Pogonophora is not a phylum and Annelida and Arthropoda are not sister taxa. *Mol Biol Evol* **17**, 87-106.

Bour, B. A., O'Brien, M. A., Lockwood, W. L., Goldstein, E. S., Bodmer, R., Taghert, P. H., Abmayr, S. M. and Nguyen, H. T. (1995). *Drosophila* MEF2, a transcription factor that is essential for myogenesis. *Genes & Development* **9**, 730-741.

Bovolenta, P., Mallamaci, A., Puelles, L. and Boncinelli, E. (1998). Expression pattern of *cSix3*, a member of the *six/sine oculis* family of transcription factors. *Mechanisms of Development* **70**, 201-203.

Boyan, G. and Williams, L. (2000). Building the antennal lobe: *engrailed* expression reveals a contribution from protocerebral neuroblasts in the grasshopper *Schistocerca gregaria*. *Arthropod Structure & Development* **29**, 267-274.

Boyer, B. C., Henry, J. Q. and Martindale, M. Q. (1996). Dual Origins of Mesoderm in a Basal Spiralian: Cell Lineage Analyses in the Polyclad Turbellarian *Hoploplana inquilina*. *Developmental Biology* **179**, 329-338.

Buck, L. and Axel, R. (1991). A novel multigene family may encode odorant receptors: a molecular basis for odor recognition. *Cell* **65**, 175-87.

Bullock, T. H. and Horridge, G. A. (1965). Structure and Function in the Nervous System of Invertebrates. San Francisco, London: Freeman and company.

Carpenter, E. M., Goddard, J. M., Chisaka, O., Manley, N. R. and Capecchi, M. R. (1993). Loss of Hox-A1 (Hox-1.6) function results in the reorganization of the murine hindbrain. *Development* **118**, 1063-75.

Castanon, I. and Baylies, M. K. (2002). A Twist in fate: evolutionary comparison of Twist structure and function. *Gene* **287**, 11-22.

Chisaka, O., Musci, T. S. and Capaci, T. M. (1992). Developmental defects of the ear, cranial nerves and hindbrain resulting from targeted disruption of the mouse homeobox gene Hox-1.6. *Nature (London)* **355**, 516-20.

Ciruna, B., Jenny, A., Lee, D., Mlodzik, M. and Schier, A. F. (2006). Planar cell polarity signalling couples cell division and morphogenesis during neurulation. *Nature (London)* **439**, 220-4.

Ciruna, B. and Rossant, J. (2001). FGF signaling regulates mesoderm cell fate specification and morphogenetic movement at the primitive streak. *Dev Cell* **1**, 37-49.

Clark, H. F., Brentrup, D., Schneitz, K., Bieber, A., Goodman, C. and Noll, M. (1995). *Dachsous* encodes a member of the cadherin superfamily that controls imaginal disc morphogenesis in *Drosophila*. *Genes & Development* **9**, 1530-42.

Corsi, A. K., Kostas, S. A., Fire, A. and Krause, M. (2000). *Caenorhabditis elegans* Twist plays an essential role in non-striated muscle development. *Development* **127**, 2041-2051.

Damen, W. G., Hausdorf, M., Seyfarth, E. A. and Tautz, D. (1998). A conserved mode of head segmentation in arthropods revealed by the expression pattern of Hox genes in a spider. *Proc Natl Acad Sci U S A* **95**, 10665-70.

Damen, W. G. M. (2002). Parasegmental organization of the spider embryo implies that the parasegment is an evolutionary conserved entity in the arthropod embryogenesis. *Development* **129**, 1239-1250.

Darken, R. S., Scola, A. M., Rakeman, A. S., Das, G., Mlodzik, M. and Wilson, P. A. (2002). The planar polarity gene *strabismus* regulates convergent extension movements in *Xenopus*. *The EMBO Journal* **21**, 976-85.

de Rosa, R., Grenier, J. K., Andreeva, T., Cook, C. E., Adoutte, A., Akam, M., Carroll, S. B. and Balavoine, G. (1999). Hox genes in brachiopods and priapulids and protostome evolution. *Nature (London)* **399**, 772-6.

Diederich, R. J., Merrill, V. K. L., Pultz, M. A. and Kaufman, T. C. (1989). Isolation, structure, and expression of *labial*, a homeotic gene of the Antennapedia Complex involved in *Drosophila* head development. *Genes & Development* **3**, 399-414.

Diederich, R. J., Pattatucci, A. M. and Kaufman, T. C. (1991). Developmental and evolutionary implications of *labial*, *Deformed* and *engrailed* expression in the *Drosophila* head. *Development* **113**, 273-281.

Dolle, P., Lufkin, T., Krumlauf, R., Mark, M., Duboule, D. and Chambon, P. (1993). Local Alterations of Krox-20 and Hox Gene Expression in the Hindbrain Suggest Lack of Rhombomeres-4 and Rhombomere-5 in Homozygote null Hoxa-1 (Hox-1.6) Mutant Embryos. *Proceedings of the National Academy of Sciences of the United States of America* **90**, 7666-7670.

Dorresteijn, A. W. C. (1990). Quantitative analysis of cellular differentiation during early embryogenesis of *Platynereis dumerilii*. *Roux Arch. Dev. Biol.* **196**, 51-58.

Dorresteijn, A. W. C., O'Grady, B., Fischer, A., Porchet-Henere, E. and Boilly-Marer, Y. (1993). Molecular specification of cell lines in the embryo of *Platynereis* (Annelida). *Roux's Arch. Dev. Biol.* **202**, 264-273.

Edmondson, D. G., Lyons, G. E., Martin, J. F. and Olson, E. N. (1994). *Mef2* gene expression marks the cardiac and skeletal muscle lienages during mouse embryogenesis. *Development* **120**, 1251-1263.

Elul, T., Koehl, M. A. and Keller, R. (1997). Cellular mechanism underlying neural convergent extension in Xenopus laevis embryos. *Dev Biol* **191**, 243-58.

Eriksson, B. J., Tait, N. N. and Budd, G. E. (2003). Head development in the onychophoran *Euperipatoides kanangrensis* with particulart reference to the central nervous system. *Journal of Morphology* **255**, 1-23.

Fanto, M. and McNeill, H. (2004). Planar polarity from flies to vertebrates. *Journal of Cell Science* **117**, 527-33.

Finkelstein, R., Smouse, D., Capaci, T. M., Spradling, A. C. and Perrimon, N. (1990). The orthodenticle gene encodes a novel homeo domain protein involved in the development of the Drosophila nervous system and ocellar visual structures. *Genes Dev* **4**, 1516-27.

Finnerty, J. R., Pang, K., Burton, P., Paulson, D. and Martindale, M. Q. (2004). Origins of bilateral symmetry: Hox and dpp expression in a sea anemone. *Science* **304**, 1335-7.

Fioroni, P. (1992). Allgemeine und vergleichende Embryologie. Berlin, Heidelberg, New York: Springer.

Fischer, A. and Dorresteijn, A. W. C. (2004). The polychaete Platynereis dumerilii (Annelida): a laboratory animal with spiralian cleavage, lifelong segment proliferation and a mixed benthic/pelagic life cycle. *Bioessays* **26**, 314-325.

Füchtbauer, E.-M. (1995). Expression of M-Twist during postimplantation development of the mouse. *Developmental Dynamics* **204**, 316-322.

Galliot, B., de Vargas, C. and Miller, D. J. (1999). Evolution of homeobox genes: Q_{50} Paired-like genes founded the Paired class. *Dev Genes Evol* **209**, 186-97.

Garda, A.-L., Echevarría, D. and Martínez, S. (2001). Neuroepithelial co-expression of *Gbx2* and *Otx2* precedes *Fgf8* expression in the isthmic organizer. *Mech Dev* **101**, 111-8.

Gerhart, J., Lowe, C. and Kirschner, M. (2005). Hemichordates and the origin of chordates. *Current Opinion in Genetics and Development* **15**, 461-467.

Ghanbari, H., Seo, H. C., Fjose, A. and Brandli, A. W. (2001). Molecular cloning and embryonic expression of Xenopus Six homeobox genes. *Mech Dev* **101**, 271-7.

Gilpin-Brown, J. B. (1958). The development and structure of the cephalic nerves in Nereis. *Journal of Comparative Neurology* **109**, 317-348.

Glickman, N. S., Kimmel, C. B., Jones, M. A. and Adams, R. J. (2003). Shaping the zebrafish notochord. *Development* **130**, 873-887.

Goddard, J. M., Rossel, M., Manley, N. R. and Capecchi, M. R. (1996). Mice with targeted disruption of *Hoxb-1* fail to form the motor neuron nucleus of the VIIth nerve. *Development* **122**, 3217-28.

Gong, Y., Mo, C. and Fraser, S. E. (2004). Planar cell polarity signalling controls cell division orientation during zebrafish gastrulation. *Nature (London)* **430**, 689-93.

Goodrich, E. S. (1897). On the relation of the arthopod head to the annelid prostomium. *Quarterly Journal of Microscopical Science* **40**, 247-268.

Grobben, K. (1908). Die systematische Einteilung des Tierreichs. *Verh. Zool. Bot. Ges. Wien* **58**, 491-511.

Habas, R., Kato, Y. and He, X. (2001). Wnt/Frizzled activation of Rho regulates vertebrate gastrulation and requires a novel Formin homology protein Daam1. *Cell* **107**, 843-54.

Haeckel, E. (1874). Die Gastraea-Theorie, die phylogenetische Classification des Thierreiches und die Homologie der Keimblätter. *Jena Z. Naturwiss.* **8**, 1-55.

Han, K., Levine, M. S. and Manley, J. L. (1989). Synergistic activation and repression of transcription by *Drosophila* homeobox proteins. *Cell* **56**, 573-83.

Harada, Y., Okai, N., Taguchi, S., Tagawa, K., Humphreys, T. and Satoh, N. (2000). Developmental expression of the hemichordate *otx* ortholog. *Mechanisms of Development* **91**, 337-9.

Harfe, B. D., Gomez, A. V., Kenyon, C., Liu, J., Krause, M. and Fire, A. (1998). Analysis of a *Caenorhabditis elegans* Twist homolog identifies conserved and divergent aspects of mesodermal patterning. *Genes & Development* **12**, 2623-2635.

Hatschek, B. (1878). Studien über Entwicklungsgeschichte der Anneliden. *Arb.Zool.Inst.Wien Tom.I.*, 277-405.

Hauenschild, C. and Fischer, A. (1969). Platynereis dumerilii. Mikroskopische Anatomie, Fortpflanzung, Entwicklung. *Großes Zoologisches Praktikum* **10b**, 1-54.

Heimler, W. (1981). Untersuchungen zur Larvalentwicklung von *Lanice conchilega* (Pallas) 1766 (Polychaeta, Terebellomorpha) Teil II: Bau und Ultrasturktur der Trochophora-Larve. *Zool.Jb.Anat.* **106**, 236-277.

Heisenberg, C. P., Tada, M., Rauch, G. J., Saude, L., Concha, M. L., Geisler, R., Stemple, D. L., Smith, J. C. and Wilson, S. W. (2000). Silberblick/Wnt11 mediates convergent extension movements during zebrafish gastrulation. *Nature (London)* **405**, 76-81.

Helfrich-Forster, C. (2002). The circadian system of *Drosophila melanogaster* and its light input pathways. *Zoology (Jena)* **105**, 297-312.

Hempelmann, F. (1911). Zur Naturgeschichte von Nereis dumerilii Aud. et Edw. *Zoologica* **62**, 1-135.

Herpin, A., Lelong, C., Becker, T., Rosa, F. M., Favrel, P. and Cunningham, C. (2005). Structural and functional evidences for a type 1 TGF-beta sensu stricto receptor in the lophotrochozoan Crassostrea gigas suggest conserved molecular mechanisms controlling mesodermal patterning across bilateria. *Mech Dev* **122**, 695-705.

Hirose, Y., Varga, Z. M., Kondoh, H. and Furutani-Seiki, M. (2004). Single cell lineage and regionalization of cell populations during Medaka neurulation. *Development* **131**, 2553-2563.

Hirth, F., Hartmann, B. and Reichert, H. (1998). Homeotic gene action in embryonic brain development of Drosophila. *Development* **125**, 1579-89.

Hirth, F., Kammermeier, L., Frei, E., Walldorf, U., Noll, M. and Reichert, H. (2003). An urbilaterian origin of the tripartite brain: developmental genetic insights from Drosophila. *Development* **130**, 2365-73.

Hirth, F., Therianos, S., Loop, T., Gehring, W. J., Reichert, H. and Furukubo-Tokunaga, K. (1995). Developmental defects in brain segmentation caused by mutations of the homeobox genes orthodenticle and empty spiracles in Drosophila. *Neuron* **15**, 769-78.

Hopwood, N. D., Pluck, A. and Gurdon, J. B. (1989). A Xenopus mRNA related to Drosophila *twist* is expressed in response to induction in the mesoderm and the neural crest. *Cell* **59**, 893-903.

Huelsken, J. and Behrens, J. (2002). The Wnt signalling pathway. *J Cell Sci* **115**, 3977-8.

Ingham, P., Martinez-Arias, A., Lawrence, P. A. and Howard, K. (1985). Expression of *engrailed* in the parasegment of *Drosophila*. *Nature (London)* **317**, 634-6.

Irvine, K. D. and Wieschaus, E. (1994). Cell intercalation during Drosophila germband extension and its regulation by pair-rule segmentation genes. *Development* **120**, 827-41.

Irvine, S. Q. and Martindale, M. Q. (2000). Expression patterns of anterior Hox genes in the polychaete Chaetopterus: correlation with morphological boundaries. *Dev Biol* **217**, 333-51.

Iwanoff, P. P. (1928). Die Entwicklung der LArvalsegmente bei den Anneliden. *Zeitschrift für Morphologie und Ökologie der Tiere* **10**, 62-161.

Jacobsohn, S. (1999). Characterization of novel F-actin envelopes surrounding nuclei during cleavage of a polychaete worm. *Int J Dev Biol* **43**, 19-26.

Jaegersten, G. (1955). On the early phylogeny of the Metazoa. *Zool. Bidr. Uppsala* **30**, 321-354.

Jessen, J. R., Topczewski, J., Bingham, S., Sepich, D. S., Marlow, F., Chandrasekhar, A. and Solnica-Krezel, L. (2002). Zebrafish trilobite identifies new roles for Strabismus in gastrulation and neuronal movements. *Nature Cell Biology* **4**, 610-5.

Kablar, B., Vignali, R., Menotti, L., Pannese, M., Andreazzoli, M., Polo, C., Giribaldi, M. G., Boncinelli, E. and Barsacchi, G. (1996). Xotx genes in the developing brain of Xenopus laevis. *Mech Dev* **55**, 145-58.

Keller, C. A., Grill, M. A. and Abmayr, S. M. (1998). A role for *nautilus* in the differentiation of muscle precursors. *Dev Biol* **202**, 157-71.

Keller, R., Davidson, L., Edlund, A., Elul, T., Ezin, M., Shook, D. and Skoglund, P. (2000). Mechanisms of convergence and extension by cell intercalation. *Philos Trans R Soc Lond B Biol Sci* **355**, 897-922.

Keller, R., Davidson, L. A. and Shook, D. R. (2003). How we are shaped: the biomechanics of gastrulation. *Differentiation* **71**, 171-205.

Keller, R., Shih, J. and Sater, A. (1992). The Cellular Basis of the Convergence and Extension of the *Xenopus* Neural Plate. *Developmental Dynamics* **193**, 199-217.

Keller, R. E. (1975). Vital dye mapping of the gastrula and neurula of *Xenopus laevis*. I. Prospective areas and morphogenetic movements of the superficial layer. *Developmental Biology* **42**, 222-241.

Keynes, R. and Lumsden, A. (1990). Segmentation and the origin of regional diversity in the vertebrate central nervous system. *Neuron* **2**, 1-9.

Kiecker, C. and Lumsden, A. (2005). Compartments and their boundaries in vertebrate brain development. *Nature Reviews Neuroscience* **6**, 553-564.

Kilian, B., Mansukoski, H., Barbosa, F. C., Ulrich, F., Tada, M. and Heisenberg, C. P. (2003). The role of Ppt/Wnt5 in regulating cell shape and movements during zebrafish gastrulation. *Mech Dev* **120**, 467-76.

Kobayashi, M., Toyama, R., Takeda, H., Dawid, I. B. and Kawakami, K. (1998). Overexpression of the forebrain-specific homeobox gene six3 induces rostral forebrain enlargement in zebrafish. *Development* **125**, 2973-2982.

Kourakis, M. J., Master, V. A., Lokhorst, D. K., Nardelli-Haefliger, D., Wedeen, C. J., Martindale, M. Q. and Shankland, M. (1997). Conserved anterior boundaries of Hox gene expression in the central nervous system of the leech Helobdella. *Dev Biol* **190**, 284-300.

Kumano, G. and Smith, W. C. (2002). Revisions to the Xenopus gastrula fate map: Implications for mesoderm induction and patterning. *Dev Dyn* **225**, 409-21.

Lacalli, T. C. (1981). Structure and development of the apical organ in trochophores of *Spirobranchus polycerus*, *Phyllodoce maculata*, and *Phyllodoce mucosa* (Polychaeta). *Proc. R. Soc. Lond. B* **212**, 381-402.

Lagutin, O. V., Zhu, C. C., Kobayashi, D., Topczewski, J., Shimamura, K., Puelles, L., Russell, H. R., McKinnon, P. J., Solnica-Krezel, L. and Oliver, G. (2003). Six3 repression of Wnt signaling in the anterior neuroectoderm is essential for vertebrate forebrain development. *Genes Dev* **17**, 368-79.

Lartillot, N., Le Gouar, M. and Adoutte, A. (2002). Expression patterns of fork headand goosecoid homologues in the mollusc *Patella vulgata* supports the ancestry of the anterior mesendoderm across Bilateria. *Dev Genes Evol* **212**, 551-61.

Li, J. Y. H. and Joyner, A. L. (2001). *Otx2* and *Gbx2* are required for refinement and not induction of mid-hindbrain gene expression. *Development* **128**, 4979-91.

Li, Y., Allende, M. L., Finkelstein, R. and Weinberg, E. S. (1994). Expression of two zebrafish orthodenticle-related genes in the embryonic brain. *Mechanisms of Development* **48**, 229-44.

Li, Y., Brown, S. J., Hausdorf, B., Tautz, D., Denell, R. E. and Finkelstein, R. (1996). Two orthodenticle-related genes in the short-germ beetle *Tribolium castaneum*. *Dev Genes Evol* **206**, 35-45.

Loosli, F., Köster, R. W., Carl, M., Krone, A. and Wittbrodt, J. (1998). Six3, a medaka homologue of the *Drosophila* homeobox gene sine oculis is expressed in the anterior embryonic shield and the developing eye. *Mechanisms of Development* **74**, 159-164.

Loosli, F., Winkler, S. and Wittbrodt, J. (1999). Six3 overexpression initiates the formation of ectopic retina. *Genes and Development* **13**, 649-654.

Lowe, C. J., Issel-Tarver, L. and Wray, G. A. (2002). Gene expression and larval evolution: changing roles of *distal-less* and *orthodenticle* in echinoderm larvae. *Evol Dev* **4**, 111-23.

Lowe, C. J., Wu, M., Salic, A., Evans, L., Lander, E., Stange-Thomann, N., Gruber, C. E., Gerhart, J. and Kirschner, M. (2003). Anteroposterior Patterning in Hemichordates and the Origins of the Chordate Nervous System. *Cell* **113**, 853-865.

Lufkin, T., Dierich, A., LeMeur, M., Mark, M. and Chambon, P. (1991). Disruption of the Hox-1.6 homeobox gene results in defects in a region corresponding to its rostral domain of expression. *Cell* **66**, 1105-19.

Lüter, C. (2000). The origin of the coelom in Brachiopoda and its phylogenetic significance. *Zoomorphology* **120**, 15-28.

Mallatt, J. and Winchell, C. J. (2002). Testing the new animal phylogeny: first use of combined large-subunit and small-subunit rRNA gene sequences to classify the protostomes. *Mol Biol Evol* **19**, 289-301.

Mark, M., Lufkin, T., Vonesch, J. L., Ruberte, E., Olivo, J. C., Dolle, P., Gorry, P., Lumsden, A. and Chambon, P. (1993). Two rhombomeres are altered in Hoxa-1 mutant mice. *Development* **119**, 319-38.

Marlow, F., Topczewski, J., Sepich, D. and Solnica-Krezel, L. (2002). Zebrafish Rho kinase 2 acts downstream of Wnt11 to mediate cell polarity and effective convergence and extension movements. *Curr Biol* **12**, 876-84.

Martindale, M. Q. (2005). The evolution of metazoan axial properties. *Nat Rev Genet* **6**, 917-27.

Martindale, M. Q., Finnerty, J. R. and Henry, J. Q. (2002). The Radiata and the evolutionary origins of tge bilaterian body plan. *Mol Phylogenet Evol* **24**, 358-65.

Martindale, M. Q., Pang, K. and Finnerty, J. R. (2004). Investigating the origins of triploblasty: 'mesodermal' gene expression in a diploblastic animal, the sea anemone Nematostella vectensis (phylum, Cnidaria; class, Anthozoa). *Development* **131**, 2463-74.

Matakatsu, H. and Blair, S. S. (2004). Interactions between Fat and Dachsous and the regulation of planar cell polarity in the *Drosophila* wing. *Development* **131**, 3785-94.

Matus, D. Q., Thomsen, G. H. and Martindale, M. Q. (2006). Dorso/Ventral Genes are asymmetrically expressed and involved in germ-layer demarcation during cnidarian gastrulation. *Current Biology* **16**, 499-505.

Maxmen, A., Browne, W. E., Martindale, M. Q. and Giribet, G. (2005). Neuroanatomy of sea spiders implies an appendicular origin of the protocerebral segment. *Nature (London)* **437**, 1144-1148.

McClintock, J. M., Jozefowicz, C., Assimacopoulos, S., Grove, E. A., Louvi, A. and Prince, V. E. (2003). Conserved expression of *Hoxa1* in neurons at the ventral forebrain/midbrain boundary of vertebrates. *Dev Genes Evol* **213**, 399-406.

McHugh, D. (1997). Molecular evidence that echiurans and pogonophorans are derived annelids. *Proc Natl Acad Sci U S A* **94**, 8006-8009.

Meinhardt, H. (2002). The radial-symmetric hydra and the evolution of the bilateral body plan: an old body became a young brain. *Bioessays* **24**, 185-191.

Mercier, P., Simeone, A., Cotelli, F. and Boncinelli, E. (1995). Expression pattern of two *otx* genes suggests a role in specifying anterior body structures in zebrafish. *Int J Dev Biol* **39**, 559-73.

Millet, S., Campbell, K., Epstein, D. J., Losos, K., Harris, E. and L., J. A. (1999). A role for *Gbx2* in repression of *Otx2* and positioning the mid/hindbrain organizer. *Nature (London)* **401**, 161-164.

Mittmann, B. and Scholtz, G. (2003). Development of the nervous system in the "head" of *Limulus polyphemus* (Chelicerata: Xiphosura): morphological evidence for a correspondence between the seg-

ments of the chelicerae and of the (first) antennae of Mandibulata. *Development Genes & Evolution* **213**, 9-17.

Molkentin, J. D., Black, B. L., Martin, J. F. and Olson, E. N. (1995). Cooperative activation of muscle gene expression by MEF2 and myogenic bHLH proteins. *Cell* **83**, 1125-36.

Molkentin, J. D., Black, B. L., Martin, J. F. and Olson, E. N. (1996). Mutational analysis of the DNA Binding, Dimerization, and Transcriptional Activation Domains of MEF2C. *Molecular & Cellular Biology* **16**, 2627-36.

Molkentin, J. D. and Olson, E. N. (1996). Combinatorial control of muscle development by basic helix-loop-helix and MADS-box transcription factors. *Proc Natl Acad Sci U S A* **93**, 9366-9373.

Morgan, R., Hooiveld, M. H., Pannese, M., Dati, G., Broders, F., Delarue, M., Thiery, J. P., Boncinelli, E. and Durston, A. J. (1999). Calponin modulates the exclusion of Otx-expressing cells from convergence extension movements. *Nature Cell Biology* **1**, 404-8.

Muller, P., Seipel, K., Yanze, N., Reber-Muller, S., Streitwolf-Engel, R., Stierwald, M., Spring, J. and Schmid, V. (2003). Evolutionary aspects of developmentally regulated helix-loop-helix transcription factors in striated muscle of jellyfish. *Dev Biol* **255**, 216-29.

Murphy, P., Davidson, D. R. and Hill, R. E. (1989). Segment-specific expression of a homeobox-containing gene in the mouse hindbrain. *Nature (London)* **341**, 156-9.

Naef, A. (1927). Notizen zur Morphologie und Stammesgeschichte der Wirbeltiere. 14. Über Blastoporusverschluss und Schwanzknospenanlage bei Anamniern. *Zool. Jahrb. Abt. Anat. Ontog. Tiere* **49**, 357-390.

Nederbragt, A. J., Lespinet, O., van Wageningen, S., van Loon, A. E., Adoutte, A. and Dictus, W. J. (2002a). A lophotrozoan *twist* gene is expressed in the ectomesoderm of the gastropod mollusk *Patella vulgata*. *Evol Dev* **4**, 334-343.

Nederbragt, A. J., te Welscher, P., van den Driesche, S., van Loon, A. E. and Dictus, W. J. (2002b). Novel and conserved roles for orthodenticle/ otx and orthopedia/ otp orthologs in the gastropod mollusc Patella vulgata. *Dev Genes Evol* **212**, 330-7.

Nielsen, C. (2001). Animal Evolution. Interrelationships of the Living Phyla. Oxford: Oxford University press.

Nielsen, C. (2004). Trochophora Larvae: Cell-Lineages, Ciliary Bands, and Body Regions. 1. Annelida and Mollusca. *Journal of Experimental Zoology (Mol Dev Evol)* **302B**, 35-68.

Nishida, A., Furukawa, A., Koike, C., Tano, Y., Aizawa, S., Matsuo, I. and Furukawa, T. (2003). Otx2 homeobox gene controls retinal photoreceptor cell fate and pineal gland development. *Nat Neurosci* **6**, 1255-63.

Oliver, G., Mailhos, A., Wehr, R., Copeland, N. G., Jenkins, N. A. and Gruss, P. (1995). Six3, a murine homologue of the sine oculis gene, demarcates the most anterior border of the developing neural plate and is expressed during eye development. *Development* **121**, 4045-4055.

Orrhage, L. (1993). On the Microanatomy of the Cephalic Nervous System of Nereidae (Polychaeta), with a Preliminary Discussion of Some Earlier Theories on the Segmentation of the Polychaete Brain. *Acta Zoologica (Stockholm)* **74**, 145-172.

Orrhage, L. (1995). On the Innervation and Homologues of the Anterior End Appendages of the Eunicea (Polychaeta), with the Tentative Outline of the Fundamental Constitution of the Cephalic Nervous System of the Polychaetes. *Acta Zoologica (Stockholm)* **76**, 229-248.

Pannese, M., Polo, C., Andreazzoli, M., Vignali, R., Kablar, B., Barsacchi, G. and Boncinelli, E. (1995). The Xenopus homologue of Otx2 is a maternal homeobox gene that demarcates and specifies anterior body regions. *Development* **121**, 707-20.

Papillon, D., Perez, Y., Caubit, X. and Le Parco, Y. (2004). Identification of chaetognaths as protostomes is supported by the analysis of their mitochondrial genome. *Mol Biol Evol* **21**, 2122-9.

Park, M. and Moon, R. T. (2002). The planar cell-polarity gene *stbm* regulates cell behaviour and cell fate in vertebrate embryos. *Nature Cell Biology* **4**, 20-25.

Patel, N. H., Kornberg, T. B. and Goodman, C. S. (1989a). Expression of *engrailed* during segmentation in grasshopper and crayfish. *Development* **107**, 201-12.

Patel, N. H., Martin-Blanco, E., Coleman, K. G., Poole, S. J., Ellis, M. C., Kornberg, T. B. and Goodman, C. S. (1989b). Expression of *engrailed* proteins in arthropods, annelids, and chordates. *Cell* **58**, 955-968.

Peifer, M. and McEwen, D. G. (2002). The Ballet of Morphogenesis: Unveiling the Hidden Choreographers. *Cell* **109**, 271-4.

Philippe, H., Lartillot, N. and Brinkmann, H. (2005). Multigene analyses of bilaterian animals corroborate the monophyly of Ecdysozoa, Lophotrochozoa and Protostomia. *Mol Biol Evol* **22**, 1246-53.

Primus, A. and Freeman, G. (2004). The cnidarian and the canon: the role of Wnt/b-catenin signaling in the evolution of metazoan embryos. *Bioessays* **26**, 474-78.

Prud'homme, B., de Rosa, R., Arendt, D., Julien, J. F., Pajaziti, R., Dorresteijn, A. W., Adoutte, A., Wittbrodt, J. and Balavoine, G. (2003). Arthropod-like expression patterns of engrailed and wingless in the annelid Platynereis dumerilii suggest a role in segment formation. *Curr Biol* **13**, 1876-81.

Puelles, L. and Rubenstein, J. L. (2003). Forebrain gene expression domains and the evolving prosomeric model. *Trends Neurosci* **26**, 469-76.

Puelles, L. and Rubenstein, J. L. R. (1993). Expression Patterns of Homeobox and Other Putative Regulatory Genes in the Embryonic Mouse Forebrain Suggest a Neuromeric Organization. *Trends in Neurosciences* **16**, 472-479.

Raible, F., Tessmar-Raible, K., Oseogawa, K., Wincker, P., Jubin, C., Balavoine, B., Ferrier, D. E., Benes, V., de Jong, P., Weissenbach, J. et al. (2005). Vertebrate-type intron-rich genes in the marine annelid *Platynereis dumerilii*. *Science* **310**, 1325-6.

Remane, A. (1950). Die Entstehung der Metamerie der Wirbellosen. *Vh. Dt. Zool. Ges. Mainz*, 16-23.

Rempel, J. G. (1975). The evolution of the insect head: the endless dispute. *Quaestiones Entomologicae* **11**, 7-24.

Rhinn, M., Lun, K., Amores, A., Yan, Y. L., Postlethwait, J. H. and Brand, M. (2003). Cloning, expression and relationship of zebrafish gbx1 and gbx2 genes to Fgf signaling. *Mech Dev* **120**, 919-36.

Rouse, G. W. (1999). Trochophore concepts: ciliary bands and the evolution of larva in spiralian Metazoa. *Biological Journal of the Linnean Society* **66**, 411-464.

Rouse, G. W. and Pleijel, F. (2001). Polychaetes. Oxford: Oxford University Press.

Sambrook, J., Fritsch, E. F. and Maniatis, T. (1989). Molecular Cloning, A Laboratory Manual: Cold Spring Habor Laboratory Press.

Schmidt-Ott, U., Sander, K. and Technau, G. M. (1994). Expression of *engrailed* in embryos of a beetle and five dipteran species with special reference to the terminal regions. *Roux's Arch Dev Biol* **203**, 298-303.

Schmidt-Ott, U. and Technau, G. M. (1992). Expression of *en* and *wg* in the embyronic head and brain of *Drosophila* indicates a refolded band of seven segment remnants. *Development* **116**, 111-125.

Schoenwolf, G. and Alvarez, S. (1989). Roles of epithelial cell rearrangement and division in shaping the avian neural plate. *Development* **112**, 713-722.

Scholtz, G. and Edgecombe, G. D. (2005). Heads, Hox and the phylogenetic position of trilobites. In *Crustacea and Arthropod Relationships*, vol. 16, pp. 139-165.

Schroeder, P. C. and Hermans, C. O. (1975). Annelida: Polychaeta. In *Reproduction of Marine Invertebrates*

Volume III: Annelids and Echiurans, (ed. A. C. Giese and J. S. Pearse), pp. 1-213. New York
San Francisco
London: Academic Press.

Schubert, M., Meulemans, D., Bronner-Fraser, M., Holland, L. Z. and Holland, N. D. (2003). Differential expression of two amphioxus *MyoD* family members (*AmphiMRF1* and *AmphiMRF2*). *Gene Expression Patterns* **3**, 199-202.

Schulz, R. A., Chromey, C., Lu, M. F., Zhao, B. and Olson, E. N. (1996). Expression of the D-MEF2 transcription factor in the *Drosophila* brain suggests a role in neuronal cell differentiation. *Oncogene* **12**, 1827-1831.

Seaver, E. C. (2003). Segmentation: mono- or polyphyletic? *Int J Dev Biol* **47**, 583-95.

Seaver, E. C. and Kaneshige, L. M. (2006). Expression of 'segmentation' genes during larval and juveline development in the polychaetes Capitella sp. I and H. elegans. *Dev Biol* **289**, 179-94.

Seaver, E. C., Paulson, D. A., Irvine, S. Q. and Martindale, M. Q. (2001). The spatial and temporal expression of Ch-en, the engrailed gene in the polychaete Chaetopterus, does not support a role in body axis segmentation. *Dev Biol* **236**, 195-209.

Sedgwick, A. (1884). On the origin of metameric segmentation and some other morphological questions. *Q. J. Microsc. Sci.* **24**, 43-82.

Seimiya, M. and Gehring, W. J. (2000). The Drosophila homeobox gene optix is capable of inducing ectopic eyes by an eyeless-independent mechanism. *Development* **127**, 1879-1886.

Seo, H. C., Curtiss, J., Mlodzik, M. and Fjose, A. (1999). Six class homeobox genes in Drosophila belong to three distinct families and are involved in head development. *Mech Dev* **83**, 127-39.

Seo, H. C., Drivenes, O., Ellingsen, S. and Fjose, A. (1998). Expression of two zebrafish homologues of the murine Six3 gene demarcates the initial eye primordia. *Mechanisms of Development* **73**, 45-57.

Shankland, M. and Seaver, E. C. (2000). Evolution of the bilaterian body plan: what have we learned from annelids? *Proc Natl Acad Sci U S A* **97**, 4434-7.

Shih, J. and Keller, R. (1992). Cell motility driving mediolateral intercalation in explants of *Xenopus laevis*. *Development* **116**, 901-14.

Shishido, E., Higashijima, S., Emori, Y. and K., S. (1993). Two FGF-receptor homologues of *Drosophila*: one is expressed in mesodermal primordium in early embryos. *Development* **117**, 751-761.

Siewing, R. (1963). Zum Problem der Arthropodenkopfsegmentierung. *Zoologischer Anzeiger* **170**, 429-68.

Siewing, R. (1976). Probleme und neuere Erkenntnisse in der Großsystematik der Wirbellosen. *Verh. Dtsch. Zool. Ges.*, 59-83.

Siewing, R. (1985). Lehrbuch der Zoologie. Systematik. Stuttgart, new York: Gustav Fischer Verlag.

Simeone, A., Avantaggiato, V., Moroni, M. C., Mavilio, F., Arra, C., Cotelli, F., Nigro, V. and Acampora, D. (1995). Retinoic acid induces stage-specific antero-posterior transformation of rostral central nervous system. *Mech Dev* **51**, 83-98.

Simeone, A., Puelles, E. and Acampora, D. (2002). The Otx family. *Curr Opin Genet Dev* **12**, 409-15.

Simpson, P. (1983). Maternal-zygotic gene interactions during formation of the dorsoventral pattern in *Drosophila* embryos. *Genetics* **105**, 615-32.

Spicer, D. B., Rhee, J., Cheung, W. L. and Lassar, A. B. (1996). Inhibition of myogenic bHLH and MEF2 transcription factors by the bHLH protein Twist. *Science* **272**, 1476-1480.

Spring, J., Yanze, N., Josch, C., Middel, A. M., Winninger, B. and Schmid, V. (2002). Conservation of Brachyury, Mef2, and Snail in the myogenic lineage of jellyfish: a connection to the mesoderm of bilateria. *Dev Biol* **244**, 372-84.

Starck, D. (1982). Vergleichende Anatomie der Wirbeltiere. Berlin, Heidelberg, New York: Springer.

Steinmetz, P. (2002). Identifizierung und Funktionsanalyse eines Fibroblastenwachstumsfaktor-Rezeptors (FGFR) bei der Entwicklung von *Platynereis dumerilii* (Polychaeta). In *Fakultät der Biologie*, (ed. Heidelberg: Ruprecht-Karls-Universität Heidelberg.

Strausfeld, N. J., Hansen, L., Li, Y., Gomez, R. S. and Ito, K. (1998). Evolution, discovery, and interpretations of arthropod mushroom bodies. *Learn Mem* **5**, 11-37.

Strutt, D. (2003). Frizzled signalling and cell polarisation in *Drosophila* and vertebrates. *Development* **130**, 4501-13.

Strutt, H., Mundy, J., Hofstra, K. and Strutt, D. (2004). Cleavage and secretion is not required for Four-jointed function in *Drosophila* patterning. *Development* **131**, 881-90.

Strutt, H. and Strutt, D. (2002). Planar Polarity: Photoreceptors on a High Fat Diet. *Curr Biol* **12**, R384-5.

Strutt, H. and Strutt, D. (2005). Long-range coordination of planar polarity in *Drosophila*. *Bioessays* **27**, 1218-27.

Studer, M., Lumsden, A., Ariza-McNaughton, L., Rijli, F. M., Chambon, P. and Krumlauf, R. (1998). Genetic interactions between *Hoxa1* and *Hoxb1* reveal new roles in regulation of early hindbrain patterning. *Development* **125**, 1025-36.

Tautz, D. (2004). Segmentation. *Developmental Cell* **7**, 301-312.

Taylor, M. V., Beatty, K. E., Hunter, H. K. and Baylies, M. K. (1995). Drosophila MEF2 is regulated by *twist* and is expressed in both the primordia and differentiated cells of the embryonic somatic, visceral and heart musculature. *Mech Dev* **50**, 29-41.

Technau, U. (2001). *Brachyury*, the blastopore and the evolution of the mesoderm. *Bioessays* **23**, 788-794.

Telford, M. J. and Thomas, R. H. (1998). Expression of homeobox genes shows chelicerate arthropods retain their deutocerebral segment. *Proc Natl Acad Sci U S A* **95**, 10671-5.

Tessmar-Raible, K. and Arendt, D. (2003). Emerging systems: between vertebrates and arthropods, the Lophotrochozoa. *Curr Opin Genet Dev* **13**, 331-40.

Tessmar-Raible, K., Steinmetz, P. R. H., Snyman, H., Hassel, M. and Arendt, D. (2005). Fluorescent two color whole-mount in situ hybridization in Platynereis dumerilii (Polychaeta, Annelida), an emerging marine molecular model for evolution and development. *Biotechniques*.

Thompson, J. D., Gibson, T. J., Plewniak, F., Jeanmougin, F. and Higgins, D. G. (1997). The ClustalX windows interface: flexible strategiesfor multiple sequence alignment aided by quality analysis tools. *Nucleic Acids Research* **24**, 4876-4882.

Ticho, B. S., Stainier, D. Y. R., Fishman, M. C. and Breitbart, R. E. (1996). Three zebrafish MEF2 genes delineate somitic and cardiac muscle development in wild-type and mutant embryos. *Mech Dev* **59**, 205-218.

Tour, E., Pillemer, G., Gruenbaum, Y. and Fainsod, A. (2002). Gbx2 interacts with Otx2 and patterns the anterior-posterior axis during gastrulation in Xenopus. *Mech Dev* **112**, 141-51.

Toy, J., Yang, J.-M., Leppert, G. and Sundin, O. H. (1998). The Optx2 homeobox gene is expressed in early precursors of the eye and activates retina-specific genes. *Proceedings of the National Academy of Sciences USA* **95**, 10643-10648.

Urano, A., Suzuki, M. M., Zhang, P., Satoh, N. and Satoh, G. (2003). Expression of muscle-related genes and two *MyoD* genes during amphioxus notochord development. *Evol Dev* **5**, 447-58.

Urbach, R. and Technau, G. M. (2003a). Early steps in building the insect brain: neuroblast formation and segmental pattern in the developing brain of different insect species. *Arthropod Structure & Development* **32**, 103-123.

Urbach, R. and Technau, G. M. (2003b). Molecular markers for identified neuroblasts in the developing brain of Drosophila. *Development* **130**, 3621-37.

Urbach, R. and Technau, G. M. (2003c). Segment polarity and DV patterning gene expression reveals segmental organization of the Drosophila brain. *Development* **130**, 3607-20.

Vandendries, E. R., Johnson, D. and Reinke, R. (1996). orthodenticle is required for photoreceptor cell development in the Drosophila eye. *Dev Biol* **173**, 243-55.

von Bubnoff, A., Schmidt, J. E. and Kimelman, D. (1996). The Xenopus laevis homeobox gene Xgbx-2 is an early marker of anteroposterior patterning in the ectoderm. *Mech Dev* **54**, 149-60.

Wallingford, J. B., Fraser, S. E. and Harland, R. M. (2002). Convergent extension: the molecular control of polarized cell movement during embryonic development. *Dev Cell* **2**, 695-706.

Wallingford, J. B., Rowning, B. A., Vogeli, K. M., Rothbächer, U., Fraser, S. E. and Harland, R. M. (2000). Dishevelled controls cell polarity during Xenopus gastrulation. *Nature (London)* **405**, 81-85.

Warga, R. M. and Kimmel, C. B. (1990). Cell movements during epiboly and gastrulation in zebrafish. *Development* **108**, 569-80.

Wassarman, K. M., Lewandoski, M., Campbell, K., Joyner, A. L., Rubenstein, J. L. R., Martinez, S. and Martin, G. R. (1997). Specification of the anterior hindbrain and establishment of a normal mid/hindbrain organizer is dependent on *Gbx2* gene function. *Development* **124**, 2923-34.

Weber, H. (1952). Morphologie, Histologie und Entwicklungsgeschichte der Articulaten. *Fortschritte der Zoologie* **9**, 18-231.

Weber, U., Paricio, N. and Mlodzik, M. (2000). Jun mediates Frizzled-induced R3/R4 cell fate distinction and planar polarity determination in the Drosophila eye. *Development* **127**, 3619-29.

Wedeen, C. J. and Weisblat, D. A. (1991). Segmental expression of an *engrailed*-class gene during early development and neurogenesis in an annelid. *Development* **113**, 805-814.

Westheide, W. and Rieger, R. (1996). Spezielle Zoologie Erster Teil: Einzeller und Wirbellose Tiere. Stuttgart: Gustav Fischer Verlag.

Weygoldt, P. (1979). Significance of Later Embryonic Stages and Head Development in Arthropod Phylogeny. In *Arthropod Phylogeny*, (ed. A. P. Gupta), pp. 107-135. New York: Van Nostrand Reinhold.

Wilkinson, D. G., Bhatt, S., Cook, M., Boncinelli, E. and Krumlauf, R. (1989). Segmental expression of *Hox-2* homeobox genes in the developing mouse hindbrain. *Nature (London)* **341**, 405-409.

Williams, N. A. and Holland, P. W. H. (1996). Old head on young shoulders. *Nature (London)* **383**, 490.

Wilson, D. P. (1932). On the Mitraria Larva of *Owenia fusiformis* Delle Chiaje. *Philos Trans R Soc Lond B Biol Sci* **221**, 231-334.

Wilson, E. B. (1892). The cell-lineage of *Nereis*. A contribution to the cytogeny of the annelid body. *J. Morphol.* **6**, 361-480.

Wilson, E. B. (1898). Considerations on cell-lineage and ancestral reminiscence, based on a re-examination of some points in the early development of annelids and polyclades . *Annals of the New York Academy of Sciences* **11**, 1-27.

Wolf, C., Thisse, C., Stoetzel, C., Thisse, B., Gerlinger, P. and Perrin-Schmitt, F. (1991). The M-twist gene of Mus is expressed in subsets of mesodermal cells and is closely related to the Xenopus X-twi and the Drosophila twist genes. *Dev Biol* **143**, 363-73.

Woltereck, R. (1904). Beiträge zur praktischen Analyse der Polygordius-Entwicklung n ach dem »Nordsee-« und dem »Mittelmeertypus«. *Arch. Entwicklungsmech. Org.* **18**, 377-403.

Yamanaka, H., Moriguchi, T., Masuyama, N., Kusakabe, M., Hanafusa, H., Takada, R., Takada, S. and Nishida, E. (2002). JNK functions in the non-canonical Wnt pathway to regulate convergent extension movements in vertebrates. *EMBO Rep* **3**, 69-75.

Yang, J., Mani, S. A., Donaher, J. L., Ramaswamy, S., Itzykson, R. A., Come, C., Savagner, P., Gitelman, I., Richardson, A. and Weinberg, R. A. (2004). Twist, a master regulator of morphogenesis, plays an essential role in tumor metastasis. *Cell* **117**, 927-39.

Yasui, K., Zhang, S., Uemura, M., Aizawa, S. and Ueki, T. (1998). Expression of a *twist*-related gene, *Bbtwist*, during the development of a lancelet species and its relation to the cephalochordate anterior structures. *Dev Biol* **195**, 49-59.

Zeidler, M. P., Perrimon, N. and Strutt, D. I. (2000). Multiple roles for *four-jointed* in planar polarity and limb patterning. *Dev Biol* **228**, 181-96.

Zhou, X., Hollemann, T., Pieler, T. and Gruss, P. (2000). Cloning and expression of *xSix3*, the *Xenopus* homologue of murine *Six3*. *Mechanisms of Development* **91**, 327-330.

Zuber, M. E., Gestri, G., Viczian, A. S., Barsacchi, G. and Harris, W. A. (2003). Specification of the vertebrate eye by a network of eye field transcription factors. *Development* **130**, 5155-67.

Zuniga, A., Quillet, R., Perrin-Smith, F. and Zeller, R. (2002). Mouse *Twist* is reuired for fibroblast growth factor-mediated epithelial-mesenchymal signalling and cell survival during limb morphogenesis. *Mechanisms of Development* **114**, 51-59.

6 Summary

The aim of this thesis was the molecular and morphogenetic characterisation of the larval body regions of the polychaete *Platynereis dumerilii* for evolutionary comparison with the body regions of other protostome and deuterostome model species.

I have described the expression of several conserved homeobox transcription factors that broadly mark the neuroectoderm of the different larval body regions and can therefore be used as regionalisation markers in the trochophore larva of *Platynereis dumerilii*. A *six3* orthologue is a marker gene for the prostomium, the most anterior region of the trochophore larva. The peristomium that harbours the mouth region and the prototroch ciliary band expresses an *otx* orthologue as regionalisation marker in *Platynereis*. The subdivision of the metastomium into larval segments has been analysed by *Pdu-engrailed* expression. It is found to give rise to four larval segments, of which the first one is reduced and bears the first tentacular cirri. It is furthermore characterised as the most anterior *gbx*-expressing segment and is innervated by axons that connect to the circumoesophageal connectives left and right of the mouth opening. The second larval segment develops into the first chaetiferous segment and is characterised by the anterior-most *hox1* expression. The molecular and morphological comparison of the *Platynereis* anterior CNS with arthropods brains has allowed homologisation of the polychaete prostomial ganglia to the “archicerebrum” (putative most anterior part of the protocerebrum of arthropods), the peristomial ganglia with the “prosocerebrum” (putative posterior part of the protocerebrum), the ganglia of the first larval segment with the deutocerebrum and the second larval segment (first chaetiferous) ganglia with the tritocerebrum.

Comparison with enteropneust (basal deuterostomes) larvae suggests homology and evolutionary conservation in Bilateria of the following larval body regions: prostomium/prosoma (*six3*), peristomium/mesosoma (*otx*) and metastomium/metasoma (*gbx* and *hox1*). This is supported by the origin and localisation of the different mesodermal populations in *Platynereis* that I have characterised by the expression of *six3*, *fgfr*, *myoD*, *twist*, *mef2* and *troponin I*. I have found that the *Platynereis* “brain mesoderm” expresses *six3* as does the enteropneust prosoma. The

mesodermal sheath around the stomodaeum in *Platynereis* has morphological similarities to the enteropneust mesosomal coelomic pouches and expresses *fgfr* and *twist* in *Platynereis*. The trunk mesoderm in *Platynereis* dynamically expresses *myoD*, *twist*, and *mef2*, forms differentiated muscles cells as described by *troponin I* expression and originates from a similar position as the enteropneust metasomal mesoderm.

The molecular comparison of *Platynereis* neuroectodermal regions with lower vertebrates' brain regions suggests homology of prostomium/forebrain (*six3*), peristomium/midbrain (*otx*) and trunk CNS/hindbrain (*gbx* and *hox1*). In vertebrates, the midbrain-hindbrain boundary (positioned at the *otx*/*gbx* boundary) is a morphogenetic boundary between the posterior hindbrain/spinal chord region that undergoes convergent extension and the anterior forebrain-/midbrain regions that do not extend. I have found that reminiscent to vertebrate convergent extension in the hindbrain, the *gbx*-/*hox1*-expressing neural plate in *Platynereis* undergoes convergent extension by mediolateral cell intercalation that is possibly controlled by the non-canonical Wnt pathway. Similar to the vertebrate midbrain, the *otx*-expressing peristomium does not extend.

Yet, these movements take place along a slit-like blastopore that develops into both mouth and anus in *Platynereis*, but occur in front of the blastopore that develops exclusively into the anus in vertebrates. This suggests that convergent extension movements are ancestral in Bilateria and have evolved in early bilaterians to relocate the blastopore-derived mouth and anus to opposite ends of the elongating body axis.

7 Zusammenfassung

Ziel dieser Arbeit ist die molekulare und morphogenetische Analyse der larvalen Körperregionen des Polychaeten *Platynereis dumerilii*. Die Charakterisierung der Larvalregionen durch Analyse der Expressionsdomänen konservierter Markergene ermöglicht den Vergleich mit Körper- und Hirnabschnitten von Arthropoden und Deuterostomier.

Die Arbeit beschreibt die Expression mehrerer Homöobox-Transkriptionsfaktoren, die als ideale Marker für die Larvalregionen von *Platynereis dumerilii* genutzt werden können. Beinahe jede Zelle im Prostomium, dem anteriorsten Bereich der Trochophoralarve, exprimiert ein Ortholog des *six3*-Gens. Die mittlere Region, die die Mundregion und das Prototroch-Cilienband einschließt, ist durch die Expression von *otx* gekennzeichnet. Die Unterteilung des Metastomiums in Larvalsegmente wurde durch den Vergleich der *engrailed*-Expression mit der der Regionalisierungsgene untersucht. Bei *Platynereis* wird *engrailed* an der anterioren Segmentgrenze – vergleichbar mit der Expression an der anterioren Parasegmentgrenze in Arthropoden – exprimiert. Die Expression von *engrailed* macht die Unterteilung des Metastomiums von *Platynereis* in vier Larvalsegment sichtbar, von denen das erste Larvalsegment unvollständig bleibt und sich durch die Expression des *Platynereis gbx*-Gens und durch die axonale Verbindung mit den circumoesophagealen Konnektiven beidseitig der Mundöffnung charakterisieren lässt. Das zweite Larvalsegment hingegen exprimiert *hox1* und ist das erste borstentragende Segment.

Damit wird ein Vergleich der Polychaetensegmente und –ganglien mit den parasegmentalen Anteilen und den zugehörigen Ganglien der Arthropodensegmente möglich. Der molekulare Vergleich ermöglicht folgende Homologisierung: die Ganglien des Polychaeten-Prostomiums entsprechen dem Archicerebrum (dem anterioren Teil des Protocerebrum) der Arthropoden, die Ganglien des Peristomium dem Prosocerebrum (dem posterioren Teil des Protocerebrums), das Ganglion der ersten Tentakularcirren entspricht dem Deutocerebrum, und die Ganglien des zweiten Larvalsegments dem Tritocerebrum. Folglich umfasst das Protocerebrum der Arthropoden (wie das Cerebralganglion in Polychaeten) zwei ontogenetisch verschiedene Anteile – wie u.a.

bereits 1963 von Siewing erörtert. Kein Hinweis findet sich jedoch für eine Metamerie dieser Anteile. Weiterhin ist der parasegmentale Teil des Antennal-/Chelicerensegments homolog zum ersten, Tentakularcirren-tragenden Larvalsegment in *Platynereis*. Die Antennen der Polychaeten sind somit nicht zu den Antennen der Arthropoden homolog. Der parasegmentale Anteil des Interkalar-/2.Antennal-/Pedipalpensegments der Arthropoden entspricht schließlich dem zweiten Larvalsegment von *Platynereis*.

Der Vergleich der molekularen Spezifizierung der larvalen Körperregionen zwischen Polychaeten und Enteropneusten (einer Gruppe basaler Deuterostomier) bringt unerwartete und erhebliche Ähnlichkeiten zum Vorschein. Sowohl das Prostomium von *Platynereis* als auch das Prosoma der Enteropneusten ist durch die Expression von orthologen *six3*-Genen charakterisiert. Die mittlere larvale Körperregion, das Peristomium von *Platynereis* und das Mesosoma von Enteropneusten, trägt die Mundöffnung und zeichnet sich durch die Expression von *otx*-Genen im Ektoderm aus. Das Ektoderm des hinteren Körperabschnitts exprimiert sowohl bei *Platynereis* (im Metastomium mit Larvalsegmenten) als auch bei Enteropneusten (im unsegmentierten Metasoma) orthologe *gbx*- und *hox1*-Gene. Die Homologie von Körperregionen bei Polychaeten und Enteropneusten wird auch durch die ontogenetische Herkunft und Lage des Mesoderms gestützt, deren Entwicklung in *Platynereis* mit Hilfe der Expressionsmuster der Gene *six3*, *fgfr*, *myoD*, *twist*, *mef2* und *troponin I* untersucht wurde. Das “Hirnmesoderm”, das direkt an das Neuropil der Cerebralganglien im Prostomium angrenzt, exprimiert *six3*, genauso wie das Coelom des Prosoma in Enteropneusten. Das Lage der Mesodermhülle des Stomodaeums im Peristomium, das in *Platynereis* die Gene *twist* und *fgf-Rezeptor* exprimiert, ist vergleichbar mit dem mesosomalen Coelom, das ebenso wie bei Enteropneusten den Pharynx umschließt. Das Rumpfmesoderm im Metastomium von *Platynereis* zeigt dynamische Expression von *twist*-, *myoD*-, *mef2*- und *troponin I*-Genen. Es hat einen mit dem Metasoma-Coelom in Enteropneusten vergleichbaren Ursprung am posterioren Ende des Blastoporus. Somit ergeben sich molekulare und morphologische Ähnlichkeiten zwischen den drei Larvalregionen von Polychaeten und Enteropneusten, was die These stützt, dass die dreigliedrigen Primärlarven der Proto- und Deuterostomier homolog und somit ancestral für Bilaterier sind.

Der molekulare Vergleich zwischen den neuroektodermalen Regionen der Polychaeten und den Abschnitten des Wirbeltiergehirns macht des weiteren folgende Homologien wahrscheinlich: der prostomiale Anteil des Polychaeten-Neuroektoderm entspricht dem Vorderhirn (als *six3*-Region), der peristomiale Anteil dem Mittelhirn (als *otx*-Region) und die Ganglien der Larvalsegmente dem Hinterhirn (als *gbx*- und *hox1*-Regionen). Die Grenze zwischen Mittel- und Hinterhirn ist eine molekulare Grenze mit Organisatorfunktion zwischen *otx*- und *gbx*-exprimierenden Regionen. Sie bildet jedoch auch eine morphogenetische Grenze zwischen der Hinterhirn-Rückenmark-Region, die sich durch Konvergenz- und Extensionsbewegungen verlängert, und der Vorderhirn-Mittelhirn-Region, die sich nicht streckt. Auch bei *Platynereis* unterscheiden sich das *otx*-exprimierende Peristomium und das *gbx*/*hox1*-exprimierende Metastomium hinsichtlich ihrer Morphogenese. Durch Zeitrafferaufnahmen der Neuralplatte der sich streckenden *Platynereis*-Larve konnte gezeigt werden, dass während der Elongation Konvergenz- und Extensionsbewegungen in der Neuralplatte des Metastomiums stattfinden. Diese sind sowohl in zellulärer als auch in molekularer Hinsicht den morphogenetischen Gastrulationsbewegungen in Wirbeltieren sehr ähnlich. In beiden Fällen beruht die Konvergenz und Extension des Neuroektoderms auf mediolateraler Zellinterkalation, die bei Wirbeltieren durch den nicht-kanonischen Wnt-Signalweg gesteuert werden. Letzteres erscheint aufgrund der spezifischen Expression des *strabismus*-Gens im Neuroektoderm von *Platynereis* zum Zeitpunkt der Elongation ebenfalls möglich. Unterstützt wird diese Hypothese durch das Faktum, dass ein chemischer Inhibitor (SP600125) der Jun N-terminalen Kinase (JNK), die im nicht-kanonischen Wnt-Signalweg eine Schlüsselrolle spielt, die Elongation des Embryos blockiert. Zellteilungen spielen hingegen keine maßgebliche Rolle bei der Elongation.

Es verbleibt ein grundlegender Unterschied zu Wirbeltieren, nämlich dass die Konvergenz- und Extensionsbewegungen bei *Platynereis* entlang des schlitzförmigen Blastoporus (der Mund und After hervorbringt) stattfinden. Bei Wirbeltieren hingegen erfolgen diese morphogenetischen Bewegungen vor dem Blastoporus, der ausschließlich den After hervorbringt. Unter der Voraussetzung dass die amphistome Gastrulation ursprünglich für Bilaterier ist, schlage ich vor dass Konvergenz- und Extensionsbewegungen während der Gastrulation ursprünglich entstanden sind, um Mund und

After auseinanderzubewegen. Diese Bewegung bleibt jedoch auf die Region hinter der *otx*-exprimierenden Mundöffnung beschränkt, womit die Mundöffnung im anterioren Bereich verbleibt (und sich nicht schlitzförmig verlängert). Bei Wirbeltieren sind sowohl die morphogenetischen Bewegungen als auch die anteriore morphogenetische Grenze erhalten geblieben, der schlitzförmige Blastoporus und die anteriore Mundöffnung jedoch sind im Laufe der Evolution der deuterostomen Gastrulation verloren gegangen. Damit ermöglicht der Vergleich der morphogenetischen Bewegungen während der Gastrulation bei Wirbeltieren und Polychaeten auch neue Einblicke in die Evolution der Körperachsen der Bilaterier von den Körperachsen Cnidarier-ähnlicher Vorfahren wie ich im Schluss meiner Diskussion näher erläutere.